Modelling the effects of IL-1β – mediated inflammation during ex vivo lung perfusion

Thomas L. Pither

NIHR Blood and Transplant Research Unit in Organ Donation and Transplantation – Research Student

Submitted as a Thesis for the Degree of

Doctor of Philosophy

2020

NIHR | Blood and Transplant Research Unit in Organ Donation and Transplantation at Cambridge and Newcastle Universities

Newcastle University

Abstract

Introduction

Ex vivo lung perfusion (EVLP) provides a potential means of increasing the number of donor-lungs suitable for transplantation. The concentration of IL-1β during EVLP has been previously identified as being predictive of 1-year transplant survival. We sought to develop a model of lung reperfusion to assess the impact of IL-1β on neutrophil adhesion and physiological function during EVLP.

Methods

An *ex vivo* model for assessing neutrophil adhesion was developed with lung pairs and then applied to a split lung model of perfusion, whereby lung pairs (N=4) were dissected into individual lungs and perfused simultaneously, with one receiving a bolus of exogenous IL-1β. Perfusates were collected at regular time points and measured for a markers of endothelial dysfunction well as being used in a variety of functional *in vitro* assays. Tissues were assessed for differences in transcriptomic profile via Nanostring.

Results

Labelled neutrophils were successfully identified in both perfusate and tissue biopsies from lungs perfused using a split-lung model. Lungs treated with IL-1β had significantly lower levels of circulating neutrophils in perfusate at regular time points and at the end of EVLP (p = 0.042), exhibited greater oedema formation (p = 0.065) and increased pCO_2/lactate. Perfusates from lungs treated with IL-1β facilitated greater E-selectin expression and neutrophil adhesion *in vitro*. Reduction in adhesion marker expression (p = 0.067) and neutrophil adhesion (p = 0.025) occurred when perfusates were pre-incubated with an IL-1β neutralizing antibody (NAb). Tissues from IL-1β-stimulated lungs had an enhanced inflammatory RNA profile.

Discussion

These data suggest that blockade of IL-1β during EVLP could produce a less inflammatory micro-environment via decreasing endothelial activation and neutrophil adhesion, increasing the number of lungs available for transplant whilst improving post-transplant outcomes.

Statement of originality

I confirm that the information depicted in this thesis is my original work, unless specifically acknowledged in the text. The planning, design and execution of assays and subsequent analysis of results was performed by me, with supervision and guidance from Professors Andrew Fisher and Simi Ali and Dr William Scott. I have been a PhD student at Newcastle University since September 2016 within the Translational and Clinical Research Institute (formerly the Institute of Cellular Medicine) and a BTRU-sponsored Research Technician at Newcastle University since September 2019.

This project has utilised donor lungs as part of NHS-BT RINTAG-approved Study 66 entitled 'Further Evaluation of Ex Vivo Lung Perfusion to Improve Transplantation Outcomes,' REC approval number 16/NE/0230. Donor organs have been accepted under both generic and specific consent pathways. The work has been generously funded by the National Institute for Health Research (NIHR) Blood and Transplant Research Group in Organ Donation and Transplantation (BTRU ODT).

The funding organisation has had no direct role in the planning, collection and interrogation of data and has had no major involvement in the preparation of this manuscript. I have no conflict of interest to declare between the funding body and myself for the work depicted in this thesis.

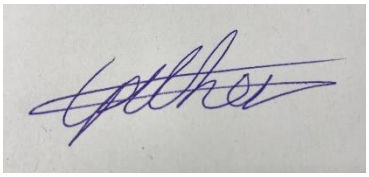

Thomas L. Pither

Acknowledgements

Firstly, a simple thank you does not seem to do this justice, but I would like to extend my immense gratitude to every one of the organ donors and their families who have made the ultimate contribution to this work. I will never be able to personally acknowledge any of you, but not once have I ever taken your immense generosity for granted. Thank you.

I would like to thank my supervisors Professors Andrew Fisher, Simi Ali and Dr William Scott. None of the work here would have been possible without your guidance and expertise and it has truly been a privilege to learn from you all. I could not have asked for better people to prepare me for my future career and I truly feel I have progressed on so much from the person who you took a chance on all those years ago.

Ex vivo perfusion is technically challenging and time-consuming work. With this in mind, I would like to thank Lucy Bates, Morvern Morrison, Lu Wang, John Dark, Catriona Charlton, Emily Thompson, Chelsea Griffiths, Sam Tingle, Jennifer Doyle and Gill Hardman for helping day or night with whatever challenges have been thrown my way, as well as being on hand to offer advice whenever needed.

I would like to show my gratitude towards members of the JK/Ali research group; Georgie Wilkins, Laura Ferreras, Nina Jordan, Katie Cooke, Irene del Molino del Barrio, Sarah Thompson, Barbara Innes and Ben Millar. Thank you for teaching me so much and for generally being so lovely to work with.

A great deal of thanks must go to Dr Anders Andreasson who performed such brilliant research prior to starting my own project. The work here would not have been possible without your achievements and I have no doubt that you will continue to have a fantastic career in clinical research.

I would also like to extend my thanks to Dr Lee Borthwick, who has always been on hand to assist me with experiments, offer advice for my research and generally provide support.

I would like to recognise the Blood and Transplant Research Unit in Organ Donation and Transplantation (BTRU ODT) for generously funding this work. Moreover, I feel incredibly fortunate to have been able to rub shoulders with some of the greats in the world of transplantation and have learnt so much from my time spent working with such brilliant scientists and clinicians.

Thank you to Minna Honkanen-Scott and the other staff at the NHS-BT laboratory at Barrack Road for assisting me with EVLP work.

I am also extremely grateful to Pauline Cogan and the other members of the clinical academic office for their administrative support and more importantly for being supportive whenever I needed assistance with anything.

On a more personal note, I would like to thank Medicals Rugby Club, for providing me with many (usually) welcome distractions at the weekends. The club has introduced me to a number of people who I now consider myself lucky to count amongst my truly great friends.

Lastly, I would like to thank Richard, Kathryn and Joseph Pither for being the best family that anyone could ever ask for. Your unwavering support, encouragement and love has always given more meaning to anything that I accomplish in life and I would not be where I am right now today without you all.

Contents

List of abbreviations

ALI	Acute lung injury
ARDS	Acute respiratory distress syndrome
ATG	Anti-thymocyte globulin
ATP	Adenosine triphosphate
BAL	Bronchoalveolar lavage
BOS	Bronchiolitis obliterans
CF	Cystic fibrosis
CFSE	Carboxyfluorescein diacetate succinimidyl ester
CLAD	Chronic lung allograft dysfunction
CLES	Centralized lung evaluation system
CNI	Calcineurin inhibitor
CO	Cardiac output
COPD	Chronic obstructive pulmonary disease
DAMP	Damage-associated molecular pattern
DBD	Donation after brainstem death
DCD	Donation after circulatory death
EC	Extended criteria
ECM	Extracellular matrix
ECMO	Extracorporeal membrane oxygenation
ETC	Electron transport chain
EVLP	Ex-vivo lung perfusion
FDA	Food and drug administration
g-CSF	Granulocyte colony-stimulating factor
gm-CSF	Granulocyte-macrophage colony-stimulating factor
GSEA	Gene set enrichment analysis
HMEC-1	Human microvascular endothelial cell line 1
HMGB1	High-mobility group box 1
HPMEC	Human pulmonary microvascular endothelial cell
HRP	Horseradish peroxidase
IBW	Ideal bodyweight
ICAM	Intercellular adhesion molecule
ICU	Intensive care unit
IFN	Interferon

IL	Interleukin
IPF	Idiopathic pulmonary fibrosis
IRI	Ischaemia-reperfusion injury
ISHLT	International Society of Heart and Lung Transplantation
LA	Left atrium
LDH	Lactate dehydrogenase
LLOD	Lower limit of detection
LPS	Lipopolysaccharide
mAb	Monoclonal antibody
MAPK	Mitogen-activated protein kinase
MFI	Median fluorescence intensity
MHC	Major histocompatibility complex
MMP	Matrix metalloproteinase
mPAP	Mean pulmonary arterial pressure
MPO	Myeloperoxidase
MSD	Mesoscale discovery
NAb	Neutralizing antibody
NADPH	Nicotinamide adenine dinucleotide phosphate (reduced)
NE	Neutrophil elastase
NET	Neutrophil extracellular trap
NF-κβ	Nuclear factor-κβ
NHS-BT	National Health Service - Blood and Transplant
NO	Nitric oxide
OCS	Organ Care System
ONOO-	Peroxynitrite
P/F ratio	Ratio of partial pressure of oxygen / fraction of expired oxygen
PA	Pulmonary artery
PAI-1	Plasminogen activator inhibitor-1
PAP	Pulmonary artery pressure
PaO2	Partial pressure of oxygen
PEEP	Peak end expiratory pressure
PGD	Primary graft dysfunction
PRR	Pattern recognition receptor
RAGE	Receptor for advanced glycation end products

ROC	Receiver operating characteristic
ROS	Reactive oxygen species
RR	Respiratory rate
SC	Standard criteria
SD	Standard deviation
SOP	Standard operating procedure
SEM	Standard error of mean
THAM	Tromethamine
TLR	Toll-like receptor
TNF	Tumour necrosis factor
TV	Tidal volume
VCAM-1	Vascular cell adhesion molecule 1
VILI	Ventilator-induced lung injury
vWF	von-Willebrand factor
XPS	XVIVO Perfusion System

List of figures

List of tables

CHAPTER 1

-

INTRODUCTION

Chapter 1 – Introduction

Section 1 – Lung Transplantation

History and overview

The first single lung transplant took place in 1963, being performed by Dr James Hardy and his colleagues at the University of Mississippi [1]. A 58-year old male patient with left lung bronchial carcinoma was the recipient of a lung from a patient admitted with shock. The lung functioned for 18 days post-transplant before the recipient died due to renal failure, with the autopsy showing no signs of rejection. The 1960s and 70s thereafter proved difficult for lung transplantation, as all attempts resulted in no real long-term success. Not until the advent of cyclosporine and revisions to surgical protocol, did success begin to become widespread in a number of transplant centres around the world [2-4]. Research highlighted the detrimental effects of previous immunosuppressive drugs on aspects of physiology such as bronchial healing, which was a process unaffected by cyclosporine [5]. Development and refinement of elaborate immunosuppressive therapies and surgical protocol enables patients to live far longer and with an improved quality of life. Individuals that receive new lungs are often extremely unwell, meaning a life of extreme tiredness and the need for constant oxygen therapy. Lung transplantation is transformative in the lives of these people, often with dire consequences if a suitable graft cannot be found.

Lung donation

Lung donation occurs in two main forms – donation after brainstem death (DBD) and donation after circulatory death (DCD). The manner of donation has profound effects on the overall health and function of an organ. Ischaemia – which will be elaborated on more in due course, begins at different times of the retrieval process for DBD and DCD lungs. NHS Blood and Transplant (NHS-BT) defines DBD as “irreversible loss of the capacity for consciousness and irreversible loss of the capacity for respiration before terminal apnoea has resulted in hypoxic cardiac arrest and circulatory standstill [6].” This means that cessation of circulation to the lungs will occur during the retrieval process. In the case of DCD, death is pronounced using cardio-respiratory criteria and in a controlled setting, involving the gradual withdrawal of life support. DCD lungs have usually experienced a longer period of ischaemia, including warm ischaemia prior to retrieval, and these are generally considered to be of a higher risk for use in transplantation [7]. However, greater use of these lungs has also been investigated more in recent years [8].

Immunosuppression following organ transplantation

Induction therapy

The immunosuppressive drugs prescribed to a lung recipient immediately before, during or straight after transplantation is known as 'induction' therapy. High doses of drugs alone or in combination are given to ensure that a wide range of immunological mechanisms are dampened down. These include but are not limited to: Alemtuzumab; a CD52-binding antibody, Basiliximab; a CD25 antibody and Anti-thymocyte globulin (ATG) which is an infusion of antibodies directed against CD3 positive leukocytes [9, 10]. Survival and incidence of Chronic Lung Allograft Dysfunction (CLAD), inflammation and obstruction of the airways and a significant cause of long-term survival, reduces when induction immunosuppression is used following lung transplantation [11, 12]. The therapeutics used today have largely superseded steroids. Although these are still used, doses are now reduced much more quickly, as long-term treatment with these has been linked to improper bronchial recovery post-surgery [5, 13].

Maintenance

After a period of a few weeks, the potency of this immunosuppressive cocktail is often reduced, with the patient continued on 'maintenance' immunosuppressive therapy. The widespread implementation of Cyclosporine A in the 1980s as a calcineurin inhibitor (CNI) provided surgical teams with a powerful means of increasing the lifespan of implanted allografts, thus beginning what is now deemed the 'modern immunosuppressive era.' Nowadays, tacrolimus has largely superseded cyclosporine as the CNI of choice, due to increased efficacy and generally lower rates of acute rejection when utilised clinically [14, 15]. However, both continue to be used clinically today, with the discovery of calcineurin inhibitors being one of the most significant ever in transplantation. Typically, individuals will receive a triple drug approach consisting of a CNI, corticosteroids and a cell cycle inhibitor [10].

Rate and outcomes of lung transplantation

In the UK, lung transplant activity is currently very low when compared to other organs. NHS Blood and Transplant (NHS-BT) highlight that utilisation rates of DBD and DCD lungs in 2019 was just 13% and 6%, respectively [16]. In the case of the former of these, around 60% of lungs were consented and offered for transplant, with fewer than 20% of these retrieved for use [17]. Less than 40% of DCD lungs were offered, as these are generally considered higher risk candidates for use in transplant surgeries. Many data show however, that outcomes between DCD and DBD donation are comparable, highlighting that this is currently an under-utilised resource for increasing the size of the donor pool [8, 18-21].

The data from NHS-BT shown in Fig. 1.1 illustrates survival rates for lung transplantation within the UK. 3-year survival from DBD donation is between 50-60%, which is broadly comparable to survival from DCD donation. Both of these however, compare very poorly to survival rates following transplantation of other solid organs such as kidney and liver, both of which are around 90% at 3 years [16]. Whilst lung transplant is life-changing for individuals with chronic lung disease, the poor longer-term outcomes remain a challenge.

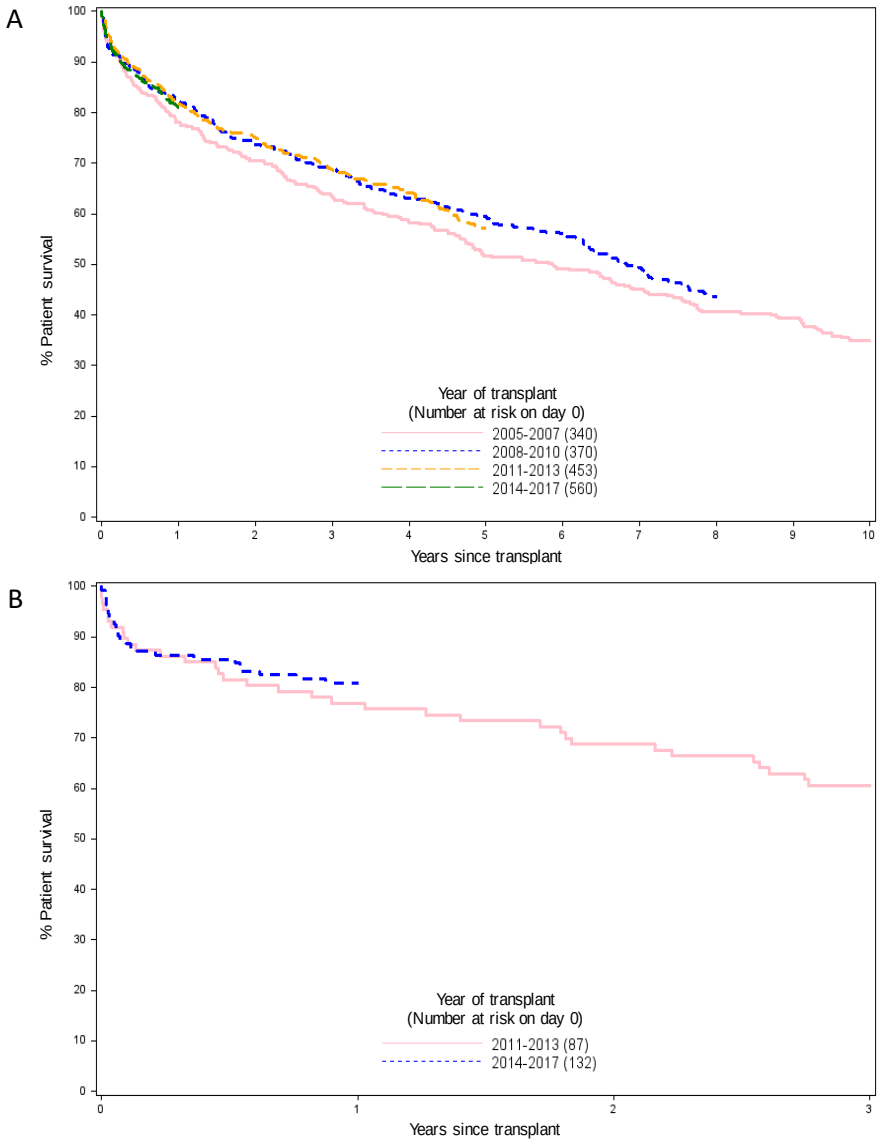

Fig. 1.1 – Survival rates for recipients of lungs from DBD and DCD donors. DCD recipient survival (A) at 3 years is comparable to survival rates of lungs used from DBD recipient survival (B). Lung transplant survival time overall is relatively poor compared to most other solid organ transplants. Data from NHS-BT Annual Transplant Report [16].

Shortage of suitable organ donors

Currently, the number of surgeries performed annually remains significantly below the number of patients that remain on the waiting list for a lung transplant. This pattern is highlighted by Fig. 1.2 shown below. The number of individuals currently on the transplant waiting list in the UK has continued to rise over the last decade, whilst the number of suitable donors and surgeries has largely remained static. As previously mentioned, 14% and 6% of DBD and DCD lungs are utilised for transplant in the UK, respectively, meaning that an enormous potential resource of organs is unutilised. Waiting list mortality for individuals on the waiting list is around 10%, meaning that increasing the number of lungs available for transplant is of paramount importance [17].

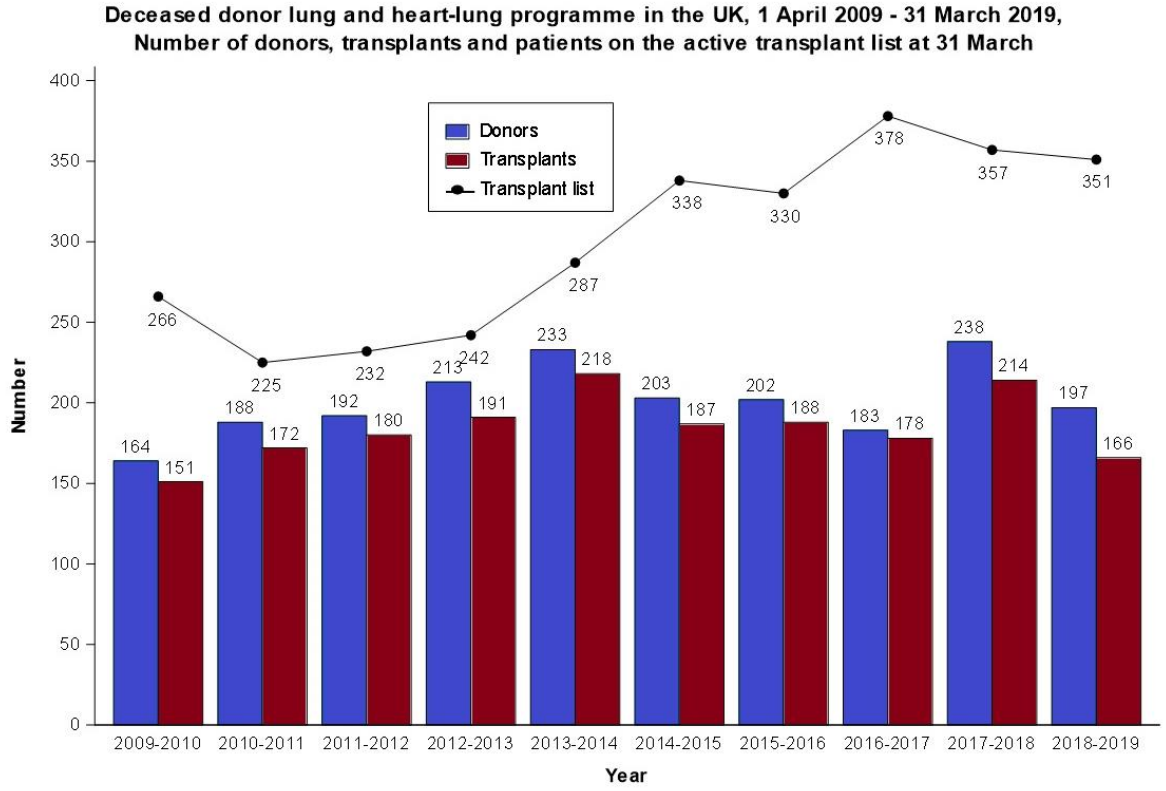

Fig. 1.2 – Deceased organ donation in the UK from 2008-2019. Depicted are the number of annual deceased organ donors (blue), number of transplant surgeries performed annually (red) and number of individuals on the transplant waiting list (black). This data highlights the disparity between the numbers of surgeries performed annually and the number of individuals remaining on the waiting list for an organ in 2019. Adapted from Transplant Activity in the UK, 2017-2018 NHS Blood and Transplant [accessed on 31/12/18 from https://www.odt.nhs.uk/statistics-and-reports/annual-activity-report/]

Use of extended criteria lung donors

Clinical staff will refer to standardised criteria when judging the suitability of a lung for use in transplant surgery. Fig. 1.3 displays the typical measures for donors deemed 'extended [22].' Numerous factors may all contribute towards the viability of a particular organ and include, but are not limited to donor health, warm/cold ischaemic times, and whether the donor is categorised as deceased due to brain death (DBD) or circulatory death (DCD). Use of organs from the latter of these two groups is generally considered much higher risk, as there is a warm ischaemic period and potentially more severe incidence of subsequent ischaemia-reperfusion injury (IRI). An ideal donor is young and has no co-morbidities, though in reality this is rare.

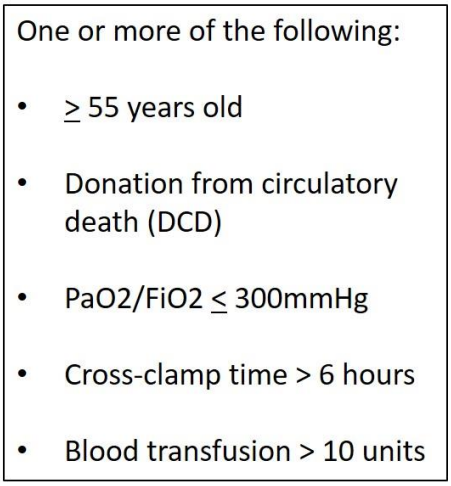

Fig. 1.3 – Criteria for designation of lungs as extended or marginal donors. If one or more of the criteria listed is/are present in the case of a potential lung donor, this is designated as 'extended.' [Information adapted from CLES trial donor inclusion criteria [22]]

The practice of using these extended criteria lungs in transplant is considered more of a risk than standard criteria. However, the initial measures for classifying EC have come under criticism at times, with many studies showing comparable outcomes compared to standard criteria lungs [23]. This highlights the potential for use of these lungs in expanding the donor pool, particularly given that post-transplant outcomes remain more favourable for an individual receiving an extended criteria lung than remaining on the transplant waiting list, despite the presence of donor risk factors such as smoking [24].

Clearly, the priority for treatment of end-stage lung disease is to increase the rate of lung transplantation. Utilisation rate of donor-lungs in the UK remains low, meaning that this represents an enormous potential resource. If these lungs could be used whilst negating unfavourable outcomes to the recipient, then this donor shortfall would be addressed, decreasing waiting list mortality.

Section 2 – Ex vivo lung perfusion

Introduction and overview

As previously highlighted, there is a disparity between the number of lungs available for transplant and the number of individuals currently placed on the transplant waiting list. Ex-vivo lung perfusion represents a potential means to increase the number of lung transplants via reconditioning of donor-lungs previously considered unsuitable due to injury or other risk factors. This idea has progressed on from initially being considered an assessment tool to enable more precise judgement of organ suitability [25]. A typical EVLP circuit is outlined in Fig. 1.4. A pump will drive perfusate into the pulmonary artery which is cannulated directly to the circuit. Perfusate is collected in a reservoir either by an open or cannulated left atrium (LA) according to perfusion protocol. All circuits will have a pressure line to monitor pulmonary arterial pressure (PAP), as this must be strictly regulated in order to prevent mechanical damage to lung tissue. The key differences in philosophy for EVLP will be discussed in greater depth later on.

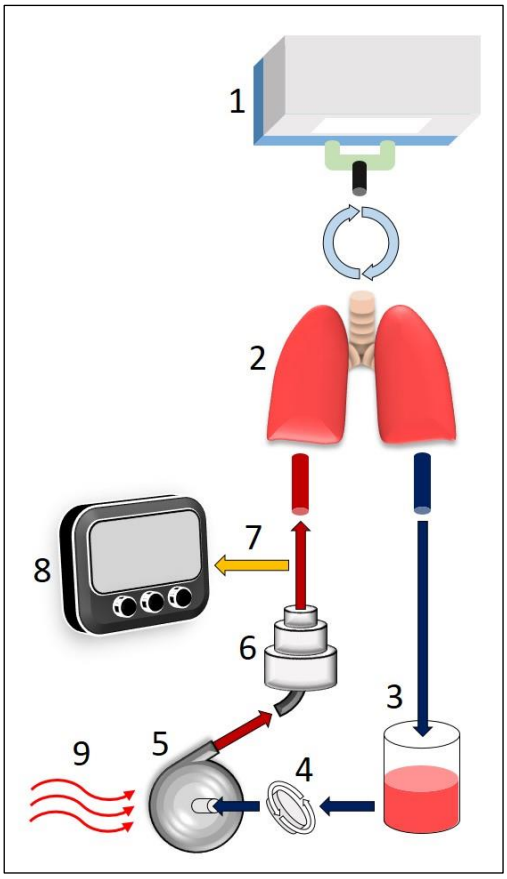

Fig. 1.4 – EVLP circuit outline. Lungs (2) are perfused and simultaneously ventilated (1). Perfusate enters the pulmonary artery (red) and either leaves via a cannulated pulmonary vein (blue) (Toronto protocol) or free drains into the reservoir (3) (Lund and OCS™ protocols). The pump (4) drives perfusate through the arterial into a hollow fibre membrane oxygenator (5) which adds CO_2 into the perfusate and then through the leukocyte filter (6). A pressure line (7) feeds into the console (8) which can be used to adjust temperature, flow rate and other aspects of perfusion. The heater-cooler (9) circulates heated water around the oxygenator which in turn heats the perfusate solution.

History of EVLP

Steen and colleagues first pioneered EVLP clinically in 2001, where the group reported successful transplantation of a single right lung from a DCD donor. The recipient was a 54-year old woman with chronic obstructive pulmonary disease (COPD), the authors reported good function in the lung during the first 5 months post-surgery [25]. This group had originally considered EVLP as an assessment tool to allow for more precise decision-making prior to transplantation. However, in 2007 this research group reported the successful transplantation of a lung initially declined for surgery into a 70-year old male with COPD [26] The lung showed good short-term function and postoperative management of the recipient was uneventful [26]. EVLP was then adopted by a number of transplant centres globally, including Toronto, Manchester and Newcastle, where many groups reported comparable or improved

outcomes to standard lung transplantation [27-29]. Today, a multitude of research groups globally all perform pre-clinical and clinical research centred on EVLP, which has now been established in two FDA-approved devices.

EVLP allows controlled lung reperfusion

As previously highlighted, perfusion of lungs prior to transplant was initially pioneered as an evaluation platform. Today, EVLP is postulated to be actively beneficial to the organ in question. Given that the donor microenvironment is far from optimal in terms of sustainment of organ viability, removal of the lungs from this into a comparatively less inflammatory one is likely inherently beneficial. Placing these donor-lungs in an *ex vivo* setting following ischaemia allows for controlled and gradual reperfusion of the organ, reducing the risk of mechanical damage sustained from high flow rate [30, 31]. The same can be applied to ventilation, as excessively high airway pressures can exacerbate the pathology of acute lung injury (ALI) [32, 33]. Protective ventilation strategies are often difficult to implement post-transplant, meaning that EVLP represents an ideal way to increase aspects of ventilation such as tidal volume (TV) and respiratory rate (RR) in a more gradual and less damaging manner.

Perfusion strategies

EVLP was first championed by Steen and colleagues in Lund, Sweden. Since then, three differing philosophies have emerged, each with variable aspects of perfusion such as perfusate components, flow rates and target pressures. These have arisen due to the different approaches that researchers have taken towards EVLP utilisation of donor-lungs, with the aspects compared in Table 1.1.

	LUND	TORONTO	OCS
PERFUSION			
Target flow	40% of cardiac output	40% of cardiac output	2.5 L/min
Pulmonary arterial pressure (mmHg)	<20	<15	<20
Left atrial pressure (mmHg)	0 (open LA)	3-5	0 (open LA)
Pump	Roller	Centrifugal	Pulsatile
Perfusate	2L Steen Solution™ with red cell concentrates (Haematocrit 10-15%)	2L Steen Solution™	1.5 L "OCS Lung solution" with red cell concentrates (Haematocrit 15-25%)
VENTILATION			
Tidal volume (ml/kg)	6-8	7	6
Frequency (bpm)	10-15	7	10
PEEP (cm H_2O)	5	5	5
FiO_2	0.5	0.21	0.21
TEMPERATURE			
Start of ventilation (o^c)	32	32	32
Start of perfusion (o^c)	15	15	32
Start of evaluation (o^c)	37	37	37

Table 1.1 – Perfusion strategy parameters [adapted from Andreasson et al (2014) [34].

The Lund group aims to keep perfusion as *in vivo*-like as possible, with a prolonged period of stable perfusion necessary in order to fully assess and recondition perfused lungs. As such, lungs perfuse at 100% of calculated CO, have an open LA and use perfusate solution containing packed red cells [25, 35]. By contrast, the Toronto protocol perfuses at a flow rate of 40% of cardiac output in order to reduce reperfusion injury to the lungs, with an absence of red cells so as to negate any potential, detrimental haemolysis. The primary focus of this research has been to establish longer perfusion times of lungs prior to transplantation in order to enable lengthier periods in which to recondition and potentially supplement the lungs therapeutically, whilst also facilitating added logistical flexibility for the transplant procedure. The Toronto protocol details are listed in Table 1.1, with the group having success using this technique to prolong examination time as early as 2008 [36]. Toronto therefore places emphasis on ensuring that any damage to declined lungs is not exacerbated, with the key aim of extending preservation time prior to transplant. This protocol utilises the XVIVO Perfusion System (XPS), an in-house, static perfusion device. By contrast, the Organ Care System (OCS) was developed

in order to realise the idea of portable EVLP. Data comparing 12 EVLPs using the OCS system was released in 2012 by Warnecke et al, showing a comparative safety profile to controls and thus enabling the INSPIRE and EXPAND trials [37]. The differing strategies that have emerged all have inherent strengths and weaknesses, which will be expanded upon later.

EVLP devices

As highlighted in the previous section, differing philosophies of EVLP have emerged, which is in turn reflected in the systems developed by manufacturers. Systems such as XPS and Organ Assist (Lung Assist) are static devices, whilst others such as OCS and the Tevosol Ex-vivo Organ Support system (EVOSS) favour portability. At the time of writing, two systems have commercial approval from the FDA – XPS and OCS. The trials involving these systems will be discussed in more detail, with their protocols outlined in Table 1.2.

XPS - Operational on-site EVLP

One perfusion strategy for clinical use is the XPS (XVIVO Perfusion). This static device comprises a system with an integrated Hamilton intensive care unit (ICU) ventilator, centrifugal pump, oxygenator and heater/cooler, with facilitation of X-ray also possible. A 2011 report by Cypel et al demonstrated that 20 lungs subjected to 4 hours of EVLP had comparable rates of PGD to 116 standard lung transplants [38]. This landmark publication spawned the NOVEL trial. This began in 2011 and is set to conclude in December 2020, with final reports for this yet to be released. However, data published in 2014 reported 42 out of 76 extended donor lungs that underwent EVLP were successfully transplanted, giving a utilisation rate of 55% [39]. Donor inclusion criteria for this study includes multiple blood transfusions, pulmonary oedema, DCD and PaO_2/FiO_2 $\leq$300mmHg. Short-term outcomes were not significantly different between the two groups, despite donors in the EVLP group having a significantly lower P/F ratio (p=0.001) [39]. Static EVLP performed by the XPS platform with Steen solution offers a safe way of preserving lungs prior to transplantation.

OCS - Portable EVLP

The OCS platform from TransMedics attempts to move EVLP from an evaluation to an intervention-focused platform in the form of a portable perfusion circuit. Lungs are attached to the device immediately following retrieval and then transported during the EVLP process. This completely negates any necessity for storage of organs on ice, eliminating cold ischaemia. Two seminal research efforts utilising the OCS of the last few years are the INSPIRE and EXPAND trials. Both of these are

multi-centre trials based within the US and have utilised the OCS lung system. INSPIRE enrolled 370 suitable lung transplant recipients, with 320 undergoing transplantation (n=151 OCS / n=169 control). The INSPIRE trial reported no improvement in short-term outcomes compared to standard transplantation, however, was deemed comparable in terms of safety, thereby showing the OCS as a safe means of performing EVLP [40]. This landmark research effort gave weight to the idea of portable perfusion, demonstrating excellent utilisation rates of lungs for transplant.

EXPAND recruited 91 extended donor lungs, of which 79 were subsequently transplanted, giving a utilisation rate of 87%. Primary graft dysfunction (PGD) grade 3 at 72 hours was 6.4% and 30-day, 6-month and 1-year survival were 99%, 93% and 91% respectively. The EXPAND results therefore show exceptional short-term and 1-year outcomes, particularly given the utilisation rate, championing the OCS system as a viable option for safe expansion of the lung donor pool [41]. An element of the trial that has faced criticism is the designation of 'extended criteria,' as a number of centres would likely use many lungs from donors regardless of EVLP involvement prior to transplant. This idea of extended criteria lungs has been discussed prior.

OCS™ **XPS™**

Perfusate	OCS solution + red cell concentrate	Steen solution™
Flow rate	2-2.5l/min	40% of cardiac output
PA pressure (mmHg)	<20	<15
LA pressure (mmHg)	Open LA cuff	3-5
Pump type	Piston	Centrifugal
Perfusion temperature (^{O}C)	32	25
Ventilation temperature (^{O}C)	32	32
Final temperature (^{O}C)	37	37
Tidal volume	6	7
Fraction of inspired oxygen (%)	21	21
Breaths per minute (bpm)	10	7
FDA approval for SC donors	Yes	Yes
FDA approval for EC donors	Yes	Yes

Table. 1.2 – Comparison of OCS and XPS systems for EVLP. Different philosophies of the optimal way to roll out EVLP as a technology have provoked the development of two different perfusion systems. The OCS is designed to facilitate perfusion in transit, with the philosophy behind development of the XPS being that specialised EVLP centres provide the most effective means of perfusion. Other fundamental variations in flow rate, perfusate and desired pressures also mean that the overall approaches to perfusion differ.

OCS: Organ Care System™, XPS: XVIVO Perfusion System™, PA: Pulmonary Artery, LA: Left Atrium, FDA: U.S. Food and Drug Administration, SC: Standard Criteria, EC: Extended Criteria

Protocol questions remaining for clinical EVLP

Whilst both the XPS™ and OCS™ have shown comparative outcomes to cold storage of lungs, there remain a number of key unaddressed points regarding the optimum EVLP strategy.

Flow rate

Of the three EVLP protocols developed, Lund perfuses with a cardiac flow rate of 100%, whereas the Toronto and OCS protocols do so with this significantly reduced. As previously mentioned, the latter two have more recently shifted emphasis away from assessment towards reconditioning, thus a lower flow rate likely reduces risk of unwanted physiological damage to the endothelium. Both have recorded 12 hours of perfusion and therefore can effectively preserve tissue integrity. However, the argument in favour of Lund is that subjecting lungs to 100% CO provides a more accurate assessment of viability and thus gives the surgical team more confidence in how the lungs will tolerate transplantation, even with a shorter EVLP time. Flow rate during EVLP is an important factor which is decided primarily by the end goal of the perfusion team.

Fig. 1.5 – Lungs perfused on a Medtronic circuit according to the Toronto protocol. This is a bespoke perfusion circuit adapted for EVLP as part of our research cohort. The LA is cannulated, generating positive pressure. The Toronto protocol for EVLP aims for a cardiac output of 40% in order to ensure that PAP does not become excessively high and cause trauma to the graft.

Cellular vs acellular perfusate solution

As highlighted in the various different protocols – EVLP platforms continue to both utilise cellular- and acellular-based perfusates. The Toronto protocol places emphasis on preservation of lungs and argues

that avoiding haemolysis is more beneficial to lung viability, whilst this is of course further away from the more *in vivo*-like solution than the Lund and OCS protocols advocate. Pre-clinical comparisons on perfusate solution have been made by various research groups, with evidence pointing towards greater oedema formation with use of acellular perfusate solution [42, 43]. However, the clinical significance of this is unknown. To the knowledge of the author, only one study by Yeung et al (2012) has looked at directly comparing cellular additions into the perfusate within the same model [44]. Addition and then removal of erythrocytes into the perfusate over 12 hours of EVLP correlated with enhanced PaO_2, which raises questions over the accuracy of crucial blood gas measurements of acellular EVLP, though the small study number should be considered. As all previous large-scale trials have compared one form of EVLP against cold storage, perhaps the lack of a clear comparison now gives weight to the argument for a wide-scale clinical trial that directly assesses cellular and acellular EVLP.

Ventilation strategy

Current commercially available EVLP systems utilise positive pressure ventilation systems; they force air into the lungs, as in much the same way as an ICU ventilator. Whilst these systems have various logistical advantages over negative pressure systems such as an iron lung, *in vitro* data gathered by a number of groups has shown superiority of negative over positive pressure in lung function [42, 45, 46]. It is well known that in critical care, even appropriate ventilation of patients may induce lung damage, termed ventilator-induced lung injury (VILI), thus logically this is likely to be the case when applied to EVLP [47]. One trial currently running at the University of Alberta is using a custom-built negative pressure ventilation system, so as to more accurately mimic *in vivo* conditions [48]. The results of this trial are due to be released later in 2020, with the company Tevosol recently announcing the Ex-Vivo Organ Support System (EVOSS) system which is based around negative pressure ventilation. 12 transplants have already been performed using this system, which will likely move into an FDA trial soon [49]. Whilst many data suggest that negative pressure ventilation could be advantageous therefore, it remains to be seen if this benefit is of clinical significance.

Duration of EVLP

Whilst the prevailing thought is that EVLP can be used to safely assess and recondition lungs prior to transplant, there remains the question of how long this should ideally be performed for. As previously alluded to, the Toronto protocol places emphasis on elongating perfusion duration, with the group having done so for 12 hours prior to transplant with good clinical outcomes [36]. This could enable

more a more efficient means of coordinating the persons involved in the transplant, ensuring that a higher number of surgeries are performed during normal working hours. The other factor that comes into consideration is the aim of perfusion – to assess or recondition the lung? The early emphasis of the Lund protocol was very much aimed towards EVLP as an assessment method and therefore used a single time point [50], whereas the Toronto protocol aims to extend preservation times so that opportunity for reconditioning is maximised. Therefore, the duration of EVLP is likely to centre on the fundamental aim of perfusion.

Mechanisms of EVLP reconditioning

Leukocyte migration

EVLP has been observed to facilitate the migration of donor leukocytes out of the graft and into the perfusate, enabling depletion of these by utilisation of a leukocyte filter within the perfusion circuit [51]. This effect has also been observed during perfusion of kidneys prior to transplantation [52]. Donor leukocytes are involved in initiating immune responses prior to and following transplant; hence, these findings suggest that EVLP may reduce the recipient immune response and rate of PGD via this mechanism of leukocyte depletion.

Drug delivery platform

The idea of EVLP being an ideal platform to deliver therapies has been well established. Cypel et al published a study utilising human donor lungs which investigated the effect of adding an adenoviral gene vector for IL-10 into an EVLP circuit. The authors noted that human lungs which received intra-airway supplementation of IL-10 demonstrated higher PaO_2, lower pulmonary vascular resistance and showed lower expression of inflammatory cytokines [53]. A 2018 study performed by Weathington et al utilised EVLP as a platform for testing the effects of a small molecule BC1215 on conferred lung injury, which is postulated to have anti-inflammatory effects via targeting of a pro-inflammatory E3 ligase-associated protein [54]. The data showed that compared to lungs treated with LPS, those additionally administered with BC1215 showed a reduced inflammatory profile as measured in the bronchoalveolar lavage (BAL) fluid. Moreover, RNA sequencing showed that BC1215 down-regulated NF-κβ activity initially provoked via administration of LPS. Human lungs can therefore be treated during perfusion to enhance the reconditioning process.

EVLP may also be used to reduce microbial loads prior to transplantation. Whilst postulated prior to the study that this was possible, it had not been directly assessed. Andreasson et al (2014) treated lungs that underwent EVLP with high doses of anti-microbial drugs over 3-6 hours. The authors saw

significant reductions in bacterial and fungal cultures during EVLP as a result of these treatments [55]. Prevention of respiratory infections following lung transplantation is of utmost importance, as this is a major contributory factor towards patient mortality [56, 57]. This study therefore showed the feasibility of antimicrobial administration *ex vivo*.

An exciting development in transplant research is the development and utilisation of models using animals. This can include a real-time transplant procedure, meaning that additional information on graft health, tolerance and immunological response is provided by modelling in this format [58]. Yeung et al (2012) used a porcine transplant model to assess the impact of IL-10 delivery during EVLP. The authors noted improved function in lungs that received the adenoviral vector containing IL-10, with effectiveness of this delivery being enhanced compared to intra-tracheal, *in vivo* delivery [59]. Another group looked at targeting the adenosine 2A (A2A) receptor in EVLP of porcine lungs. The researchers observed that lungs supplemented with CGS21680; a selective inhibitor of A2A, showed improved oxygenation and airway pressures compared to the controls, indicating enhanced lung function [60]. These data provided by porcine and human EVLPs as well as porcine transplant models show that perfusion *ex vivo* can be used to deliver novel therapies and provide accurate readouts for lung function and viability prior to use in human models.

Practical questions for EVLP moving forwards

Logistics of EVLP deployment

Logistically, how best to deploy EVLP technology remains disputed – static or portable? If static – to distribute to every cardiothoracic transplant centre or to house the systems in specialised perfusion hubs? The latter of these would of course enable dedicated staff exclusively trained in EVLP to a higher standard and perhaps enable easier set-up of custom-designed laboratory spaces to facilitate perfusion, with the counter being that this will incur greater costs around transportation and potentially extend ischaemic times. A trial being coordinated by Lung Bioengineering Inc is examining the feasibility of using a centralized lung evaluation system (CLES) to acquire lungs, perfuse them and then transport these to the transplant centre as required [61]. To the knowledge of the author, no direct comparison between the different prospective logistical arrangements for EVLP has been conducted thus far.

Financing lung perfusion

Transplant surgery is an expensive procedure, with EVLP involvement only serving to further increase these costs. The DEVELOP-UK study published in 2016 calculated that the mean cost of a standard

lung transplant procedure was £59,608, whilst the cost of involving EVLP increased this to a mean of £139,081, when all elements such as transportation, pre-operative and post-operative care are all factored in [62]. The CLES trial aims to use a specialised perfusion hub [61], which of course requires further transportation of organs. The other consideration is the conversion rate of perfusions into transplanted lungs, as for every lung not utilised, this results in money wasted. If EVLP was to undergo widespread implementation, the issue of funding implementation of this technology would therefore need to be addressed, particularly in developing nations with less financial resources than other well-established transplant centres.

Should all organs be perfused prior to transplantation?

As perfusion is postulated to reduce the impact of IRI, a valid consideration is whether application of this technique to all organs acquired for transplant is warranted. As previously mentioned, EVLP is expensive to utilise and therefore requires justification to do so. The EXPAND and NOVEL trials have shown comparable safety profiles of extended criteria lungs that underwent EVLP and standard lung transplants [39, 41]. This results in larger numbers of lungs for transplant, but no discernible reason as to why perfusion of all lungs is necessary. Therefore, whilst EVLP undoubtedly offers a way to assess and recondition lungs deemed unsuitable for transplant, the immense costs and additional time taken to perform EVLP mean that most centres will remain likely to use it exclusively for extended criteria lung donors. This viewpoint could change if newer perfusion strategies began to show improvements in post-transplant outcome however.

Trial name	Aims	Primary outcome(s)	EVLP system / protocol	Completed
CLES	Observe effectiveness of centralized lung evaluation system in evaluating donor lungs deemed unsuitable for transplantation	6-month survival	XPS™ / Toronto	No
DEVELOP-UK	Assess clinical and cost-effectiveness of EVLP in increasing lung transplant activity in the UK	1-year patient survival	Vivoline® / Lund/hybrid	Yes
EVLP-CHUM	Evaluate EVLP effectiveness in increasing lung transplant activity and investigate biomarkers of interest	1-year patient survival	Lund	No
EXPAND	USE OCS™ to recruit, preserve and assess extended criteria lungs for use in transplantation	30-day survival, donor lung utilisation rate	OCS™ lung / OCS	No
INSPIRE	Assess effectiveness of OCS™ system in physiological preservation of lungs for transplant compared to cold storage	3-year survival/PGD grade 3 <72 hours	OCS™ lung / OCS	Yes
NOVEL	Use normothermic EVLP to assess extended/marginal donor lungs	3-year survival/PGD grade 3 <72 hours	XPS™ / Toronto	No
NPV-EVLP	Observe effect of negative pressure ventilation on lungs perfused ex vivo	30-day survival, PGD grade 3 <72 hours	NPV EVLP device / protocol	No
Toronto	Use Toronto EVLP protocol to increase the preservation time of lungs prior to use in clinical transplantation	30-day survival, PGD grade 3 <72 hours	XPS™ / Toronto	No

Table 1.3 – Clinical trials centred on EVLP. Adapted from Gilmour et al, 2020 [63].

Concluding remarks

Since the first case of clinical use in 2001, multiple philosophies of EVLP have emerged, potentially enabling not only an increase in the rate at which lung transplants can be performed, but also improving the logistical and technical challenges associated with transplantation as a whole. The current devices have shown comparable safety profiles compared to standard transplantation, though a lack of agreed, standardised criteria for trials means that results are somewhat difficult to directly compare. Differences in method of perfusion but also in how optimally implement the technology still require addressing. The advent of EVLP means that it is truly an exciting time for transplant research, with the possibility of more life-changing surgeries than ever before.

Section 3 – Primary graft dysfunction and ischaemia-reperfusion injury

Primary graft dysfunction

The most significant short-term cause of morbidity and mortality following lung transplantation is primary graft dysfunction (PGD). This term refers to incidence of ALI within 72 hours of lung transplantation and encompasses a spectrum of disease which is clinically graded from 3 (significant PGD) through to 0 (absence of PGD). The features of this are displayed in Table 1.4. The pathology of the disease follows one of severe IRI and involves a combination of physiological and immunological responses to transplantation. Incidence of PGD is negatively associated with long-term survival, incidence of Bronchiolitis Obliterans (BOS) and pulmonary function [64, 65]. Clearly, reducing incidence and severity of PGD is a priority with regard to increasing the success rates of lung transplantation, as the short-term outcomes are inextricably linked with the longer-term. Understanding the mechanisms behind PGD are therefore of paramount importance.

PGD grade	PaO_2/FiO_2 ratio (mmHg)	Chest radiography
0	>300	Normal
1	>300	Diffuse allograft infiltration/pulmonary oedema
2	200-300	Diffuse allograft infiltration/pulmonary oedema
3	<200	Diffuse allograft infiltration/pulmonary oedema

Table 1.4 – Classification of PGD following lung transplantation. Adapted from Morrison et al (2017) [66].

Pathology of PGD – Ischaemia-reperfusion injury

Ischaemia-reperfusion injury (IRI) is the cessation of normal blood flow to tissues for an extended period, then followed by a return of normal flow. This culminates in significant tissue and organ damage, facilitated by widespread release of reactive oxygen species (ROS), endothelial dysfunction/disruption and leukocyte recruitment. The pattern of damage is bi-phasic, with factors that prolong or enhance the ischaemic period prior to reperfusion serving to worsen the overall pathology observed. IRI pathology is observed in many diseases such as a stroke or recovery of myocardial infarction.

In the context of a potentially transplantable organ, the ischaemic period begins depending on the manner of donor death. Ischaemia for DBD lungs begins during retrieval when the pulmonary artery is clamped. In the case of DCD lungs, this commences upon withdrawal of life support and the resulting decline in blood pressure. Termination of normal blood flow upon circulatory death serves to abolish the delivery of key metabolic components to the tissues. The oxygen deprivation associated with

ischaemia prior to organ transplantation does not affect the lungs as significantly, due to air oxygen stored within the alveolar spaces during the pre-transplantation period [67]. However, ischaemia still provokes dysfunction of immune pathways, triggering release of pro-inflammatory cytokines and reactive oxygen species (ROS). Cell apoptosis and necrosis both follow, whereby damage-associated molecular patterns (DAMPs) are in turn released into the local microenvironment, along with pro-inflammatory mediators from tissue-resident macrophages. This pro-inflammatory environment adversely affects a number of different types of cell within the newly engrafted tissue, often manifesting in a number of clinically significant short- and long-term complications. Fig. 1.6 illustrates key hallmarks that constitute IRI following transplantation.

Cellular and molecular contributions towards ischaemia-reperfusion injury

Whilst the following section highlights the contributions that key individual cell lineages make towards IRI pathology, one should remember not to consider the disease in this manner. Acute injury following transplantation is a multi-factorial, multi-cellular mass immune response that likely involves contribution from all the major cell types within the newly engrafted tissues. A multitude of models exist utilising animal ex vivo systems that highlight how reduction of removal of one cell type usually has a resultant down-regulatory effect on others. Several of these highlight how knockdown of macrophages completely abolishes the ability of neutrophils to then enter the tissues upon reperfusion, for example, thus highlighting the bi-phasic nature of IRI [68].

Professor Jason D Christie founded the lung transplant outcomes group (LTOG), which was a multi-centre study that aimed to dissect and interrogate a number of the mechanisms involved in mediating and exacerbating PGD [69-72]. Numerous data have been published because of this, with examples of the research discussed in due course.

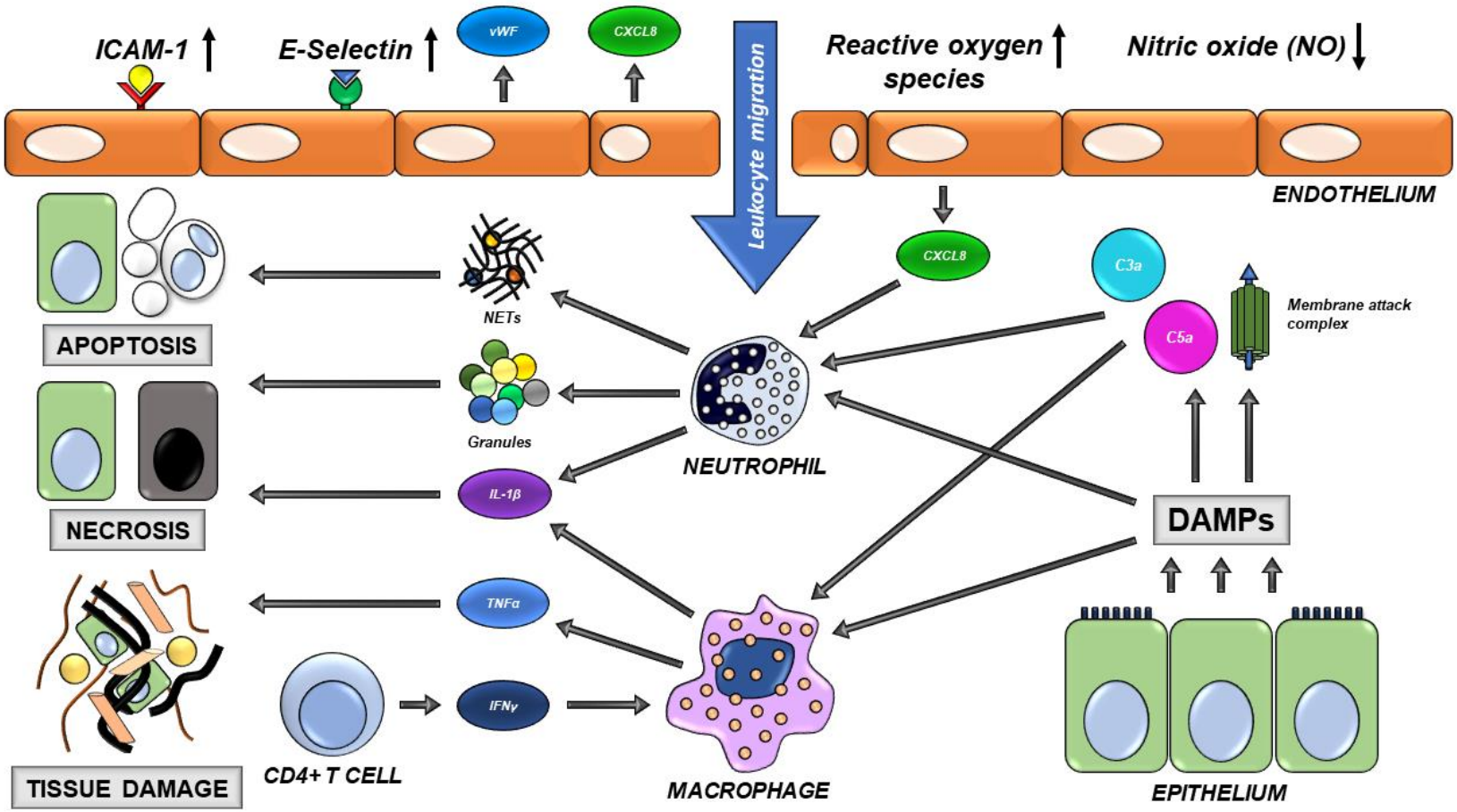

Fig. 1.6 – Mechanisms of ischaemia-reperfusion injury (IRI) in the tissues of transplanted organs. During the ischaemic or oxygen-deficient phase; localised production of DAMPs such as reactive oxygen species (ROS) increases whilst concurrently production of anti-inflammatory compounds such as nitric oxide (NO) decrease, resulting in an anti-inflammatory environment. Upon reperfusion of the vasculature, the resulting endothelial dysfunction causes up-regulation of surface adhesion receptors such as ICAM-1, enabling binding and transmigration across the endothelial layer for neutrophils and other circulating leukocytes. Once present, production of cytokines and other inflammatory mediators by immune cells facilitates widespread and potentially graft-threatening tissue damage.

Polymorphonuclear neutrophils

Perhaps the most significant contribution to the progression and pathology of IRI is that made by recipient neutrophils. Upon reperfusion of the organ post-transplant, neutrophils are drawn along a chemoattractant gradient consisting of both pro-inflammatory cytokines and chemokines, as well as DAMPs released by the apoptosis and necrosis initiated in ischaemia. Localisation to the tissues is accomplished through transmigration across the dysfunctional endothelium the via adhesion markers expressed on the surface of these cells, such as ICAM-1 and E-Selectin [73]. Once bound, neutrophils translocate through the endothelial barrier to the newly engrafted tissues. Here, a wide range of immunological functions become dysregulated due to high concentrations of pro-inflammatory cytokines and DAMPs, provoking widespread tissue and organ damage [74]. Influx of these cells is only facilitated by the preceding events that occur during ischaemia, as the local microenvironment is effectively 'primed' by macrophages, the epithelium, the endothelium and other contributory cell types to enable neutrophil migration out of the vasculature.

As previously outlined, the first component of the neutrophil contribution to IRI revolves around these cells being 'pulled' out of the circulation and into the tissues of the newly engrafted organ. IL-8 is a chemotactic protein that acts predominantly on granulocytes such as neutrophils. IL-8 released during early reperfusion of the graft following transplantation is predictive of lung function assessed by factors such as FiO_2/PaO_2 ratio and airway pressure [75]. Fisher et al showed in a 2001 study that the IL-8 signal in the donor-lung before transplantation was indicative of graft failure [76]. These observations have been confirmed during EVLP, as one research group measured perfusate levels of IL-8 in and established that increased levels were predictive of PGD following transplant of these lungs [77]. Chemotaxis of neutrophils and other granulocytes is a key process in mediating tissue damage following transplantation.

Cytokines released by neutrophils include pro-inflammatory factors such as IL-1β, chemokines such as CXCL8, CXCL10 and CCL10, colony-stimulating factors such as granulocyte (g-CSF), granulocyte-macrophage (gm-CSF) and TNF-superfamily members such as TNFα [78] (other reference). This wide-ranging cytokine profile expressed by neutrophils enables them to influence a wide-ranging array of immunologically significant cell types. In abundance, these signals cooperate to further facilitate leukocyte localisation to the inflamed tissue(s), initiate cell apoptosis, secondary necrosis and promote leukocyte survival and persistence.

The consequence of neutrophil infiltration into the site of a newly engrafted organ is widespread tissue damage and disruption. Fig. 1.7 highlights a number of neutrophil secretions, which range in function but facilitate targeting of a plethora of structural components. Release of cytokines, chemokines, neutrophil extracellular traps (NETs) and other highly damaging reactive intermediates

occurs, directly targeting the structures of the tissues in acute lung injury [74, 79-82]. These data show clearly that mediating and controlling the neutrophil response following lung transplantation is of utmost importance with regard to improving graft function and survival.

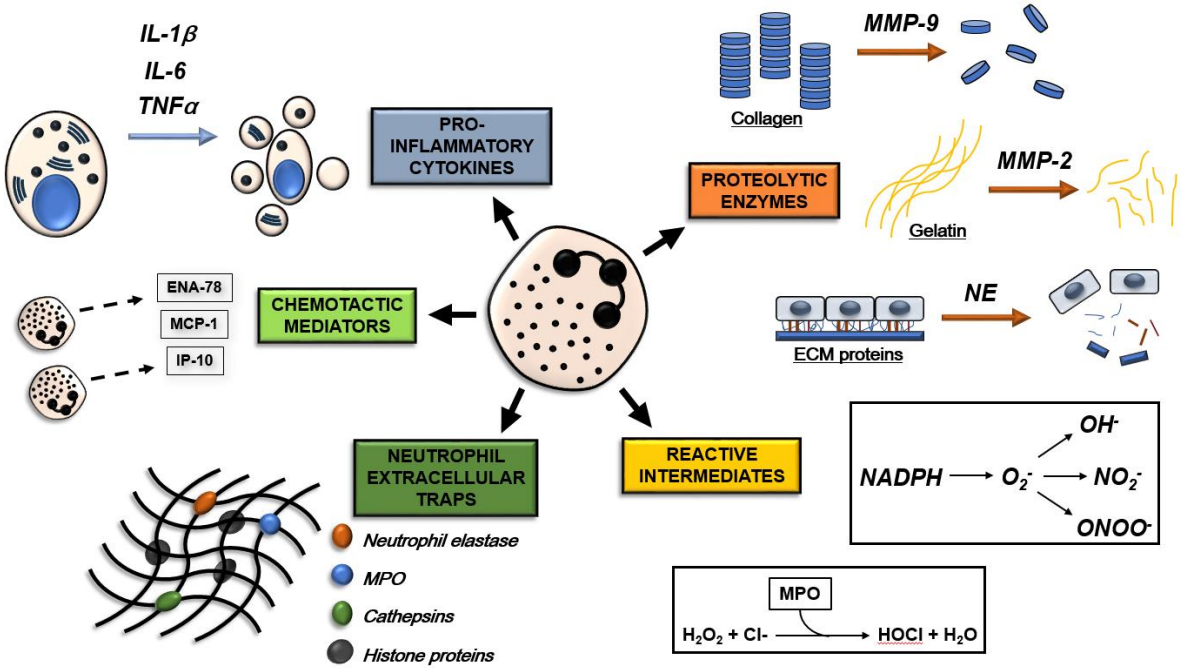

Fig. 1.7 – Mechanisms of neutrophil inflammatory responses to stimuli. Upon recruitment out of circulation and into the tissues of the newly engrafted organ, neutrophils release their highly damaging payload of inflammatory mediators. Cytokines and chemokines serve to recruit leukocytes to the site of inflammation, whilst NETs, ROS and enzymes such as MMPs catalyse the disruption and breakdown of tissues at the site of inflammation.

Endothelial cell dysfunction

During brainstem death, rises in hydrostatic pressure and vasoconstriction initiate damage to the pulmonary endothelial layer, resulting in oedema formation, which is indicative of injury to these cells [83]. The subsequent cessation of blood flow during ischaemia is mechanically sensed by endothelial cells and has significant resulting effects on gene expression, provoking even greater dysfunction [31]. Reductions in blood flow then begin reducing oxygen concentration, producing subsequent reductions in oxidative phosphorylation. Availability of ROS such as peroxynitrite ($ONOO^-$) and superoxide (O_2^-) then subsequently begin to increase, which can be damaging to both nucleic acids as well as proteins in cells . Nitric oxide (NO) secretion via endothelial cells is reliant on activity of the electron transport chain (ETC), thus severance of this provokes a decrease in localised NO concentration [84]. This reduces vasodilation, increasing intravascular pressure whilst concomitantly promoting circulatory arrest of leukocytes and up-regulating adhesion markers on the surface of the endothelium [85]. The

result of these processes is to effectively prime the microenvironment to induce widespread leukocyte recruitment following reperfusion of the graft.

Following reperfusion injury, a number of factors contribute towards further dysfunction of the endothelium, which are summarised in Table 1.5. Mean pulmonary arterial pressure (mPAP) is significantly higher in IPF patients that develop higher grades of PGD following transplantation, likely due to the effect of shear stress on the endothelium [86]. Production of pro-inflammatory cytokines such as IL-8 can induce further inflammatory responses from the endothelial layer, as well as help to disrupt its integrity [87].

The net result of these contributory stimuli during the transplant process is abnormal endothelial cell function, which is a hallmark of reperfusion injury following transplantation. Covarrubias et al (2007) measured ICAM-1 in blood specimens taken from 128 idiopathic pulmonary fibrosis (IPF) patients following lung transplantation and found that levels were significantly associated with PGD ($p = 0.002$), with levels in PGD patients higher after only 2 hours post-transplant [72]. Expression of ICAM-1 is up regulated on the surface of the endothelium in a number of acute pulmonary diseases [88-90]. A wide range of clinical pulmonary diseases have also shown associations with levels of von-Willebrand factor (vWF), another marker of endothelial activation [91].

The inflammatory pathways and interactions with other cells promoted during reperfusion injury result in further damage to the endothelium. Several models of acute lung injury have examined the role of neutrophil-endothelial interactions in mediating endothelial disruption [80]. Another study that used a mouse model of lung injury highlighted that increased NET production *in vivo* correlated with an increase in extravascular water, indicative of oedema formation and endothelial barrier disruption [74]. These data highlight that reducing endothelial activation and subsequent injury is key to inhibition of PGD development.

PATHOLOGICAL STIMULUS	EXAMPLE(S)
Hypertension	Angiotensin-II, ROS
Oxidative stress	Multi-factorial
Pro-inflammatory cytokines/chemokines	IL-1α/β, IL-8, TNFα
Infectious agents	Bacterial endotoxin, viruses (various)
Hypercholesterolemia	Lipoproteins with oxidative modifications
Haemodynamic forces	Disturbed blood flow

Table 1.5 – Stimuli of endothelial dysfunction. Numerous chemical and physical stimuli may provoke endothelial dysfunction, which is a key component of IRI. Upon becoming dysfunctional, endothelial cells then participate in and actively contribute towards inflammation. Table adapted from Gimbrone, M. A., García-Cardeña, G. (2016).

Tissue resident macrophages initiate IRI with subsequent participation from inflammatory monocyte subsets

As previously alluded to, IRI occurs in a bi-phasic pattern. Macrophages resident to the local microenvironment play an essential role in this initial establishment of IRI and there are numerous examples of this highlighted in small animal models. A commonly used method for selective knockdown of macrophages is via application of liposome-encapsulated clondronate (LC) [92, 93]. These models have often utilised both mice and rats, with macrophage knockdown generally being associated with improved tissue histology, a reduction in release of pro-inflammatory cytokines and improved organ function. A study by Tsushima et al (2014) used a lung transplant model with this technique to selectively knock out macrophages in a mouse model of lung transplantation. The researchers note improved histology as well as a significantly impaired inflammatory response relative to an empty liposome control [94]. Dhaliwal et al (2012) used a selection of methods to abolish monocytes from a murine model of ALI and highlighted that these negated the subsequent influx of neutrophils and associated injury [95]. These and numerous other examples of data in animal models collectively suggest that the macrophage contribution in this context is essential in initiating the early inflammatory cascades involved in IRI.

Animal models centred on the role of macrophages are corroborated by IRI-related studies in humans. Number and activation status of macrophages in the lungs of patients following transplantation is inextricably linked to lung function and outcomes [96]. Shah et al (2012) examined a cohort of patients that received a lung transplantation. Levels of the inflammatory macrophage protein MCP-1 (CCL2) at 24 hours were found to be a predictive biomarker for subsequent development of Primary Graft Dysfunction (PGD), suggesting an involvement for monocyte/macrophage chemotaxis in IRI [97]. A

more recent 2020 study retrospectively examined a panel of 30 protein biomarkers in BALF samples from 80 double lung transplant patients. 8 biomarkers showed ability to differentiate between mild grades (0-1) and more severe grades (2-3) of PGD, one of which was macrophage inflammatory protein 1α (MIP-1α) which can result in the downstream activation of granulocytes and other immune cells via the activity of monocytes and macrophages [98]. The roles of macrophage activation and polarisation in disease is well defined, highlighting that an aberrant, pro-inflammatory response from these cells following transplant will likely result in poorer graft function.

CD4+ T lymphocytes

CD4+ T helper cells play key roles in both mediating and maintaining inflammation in newly transplanted grafts. As previously mentioned, the early stages of IRI pathology involve predominantly macrophage-driven events, which generates a large influx of circulating leukocytes; chiefly among which are neutrophils and lymphocytes including T helper cells. Yang, Z. et al (2009) depleted CD4+ T lymphocytes from a murine model of ALI and observed that this had the dual effect of reducing levels of cytokines as well as influx of circulating neutrophils into the tissue. The authors note that degree of dysfunction was proportionate to the numbers of neutrophils that infiltrated into the tissues [99]. Hoffman et al (2008) showed that PGD patients had increased plasma levels of IL-2R, which is essential in mediating and stimulating T cell activity [100].

Another key pathway of PGD and unfavourable long-term outcomes following transplantation is the presence of pre-formed anti-Collagen V (Col (V) antibodies. These have been highlighted in both animal and human studies as highly pathogenic and indicative of PGD, facilitated by a Th17-driven response [101, 102]. This has been further linked with incidence of BOS development [103]. T lymphocytes are highly pathogenic in the underlying mechanisms of PGD, with their activation and persistence indicative of graft failure following lung transplantation.

Natural Killer T cells

Natural Killer T (NKT) cells are a unique subset of T lymphocytes that possess phenotypic characteristics of both T and Natural Killer (NK) cells. Research performed by Li, L et al (2007) highlights that in a mouse model of renal IRI, NKT cell blockade noticeably diminished the severity of IRI. By administering an anti-CD1d antibody directed against the NKT cell population, the authors noted an overall reduction in degree of kidney IRI, a reduction in the number of infiltrating CD4+ T cells and a lower number of neutrophils within the tissues, all of which served to protect the kidney from IRI-associated damage[104]. Another study that inhibited the actions of the Soluble Receptor for

Advanced Glycation End Products (RAGE) receptor on NKT cells found similarly, that this attenuated lung injury [105]. These data suggest a critical role for NKT cells in mediating inflammatory processes communicated across a variety of immune cell types.

Reactive oxygen species cause widespread tissue damage and provoke leukocyte migration

Logically, one may assume reperfusion of ischaemic organs to be beneficial, as provision of oxygen and other compounds would plausibly restore metabolic balance within the tissues. In practice, a markedly different pathology is observed. Re-introduction of oxygen results in a widespread production of ROS catalysed through a number of reactions. The overall progression of ROS production is shown in Fig. 1.8. Xanthine oxidase and NADPH oxidase are two prominent examples of enzymes that become overexpressed in cells of tissues affected by IRI and catalyse ROS generation [106, 107]. This is a key process in a number of cellular signalling events, including those that play a key role in immunological responses to pathogens, normally forming a crucial part of the intracellular signalling network within human tissues and organ systems. However, compartmentalisation is a key factor in ensuring protection from other cellular components from the reactiveness of ROS [108]. When this compartmentalising of ROS and their various targets breaks down, widespread and catastrophic damage can result from this.

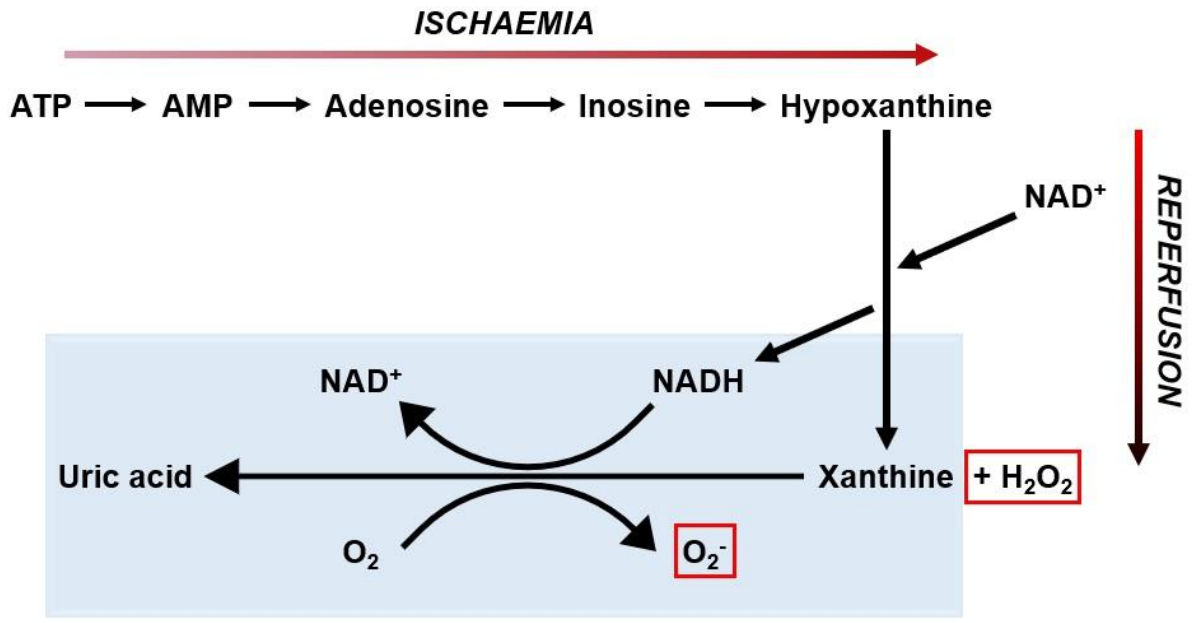

Fig. 1.8 – ROS generation by cells in IRI. Lack of oxygen during ischaemia provokes anaerobic respiration to become the dominant pathway for oxygen consumption within the tissues of the newly engrafted organ. Reperfusion of the organ then provides an abundance of oxygen molecules that can be utilised by cells to produce copious amounts of ROS.

This catastrophic release of ROS has the potential to damage all the major structural components that comprise mammalian cells. The primary pathogenic functions of ROS are two-fold: to damage structural components and integrity of cells and to attract circulating leukocytes by acting as DAMPs. Endothelial cells are provoked to increase expression of adhesion markers by H_2O_2 *in vitro*, for example [109].

Biomarkers of PGD

As previously highlighted, many of the biomarkers and related studies of PGD have emerged from work performed as part of the LTOG, which enrolled 10 transplant centres within the U.S. as part of a concerted research effort. Current findings suggest that pathways such as toll- and NOD-like receptors are involved, along with the up-regulation of cytokines such as IL-1β and IL-8. Many of these results remain epidemiological; however, recent studies have begun to flesh out the mechanisms behind provocation of PGD.

Shah et al (2012) looked at a panel of biomarkers in the plasma of 315 lung transplant patients and correlated these with PGD. Soluble RAGE (sRAGE), plasminogen activator inhibitor-1 (PAI-1) and surfactant-D (SF-D) all showed a strong relationship with higher grades of graft dysfunction, whilst sRAGE, PAI-1 and ICAM-1 also significantly improved the prediction of 90-day patient mortality [71]. Another group used gene set enrichment analysis (GSEA) of BAL fluid from 23 patients with PGD matched with valid controls. NLR, TLR and IL-1 pathways were significantly up-regulated in these patients, with transcript levels of IL-1β the highest individual transcript [110]. These data implicate inflammasome and acute inflammatory pathways in mediating damage to the lungs following transplantation and suggest that these would be susceptible to therapeutic modulation.

The IL-1 pathway in acute lung injury

IL-1β signalling has many well-documented effects in regard to provocation of immune pathway signalling and inflammatory disease progression. This is also the case in pulmonary disease, with alveolar macrophages among the cell types shown to have capacity to produce IL-1β, with this exacerbated in the case of pulmonary disease, such as IPF [111, 112]. IPF patients have been shown to have a pre-disposition towards overzealous IL-1β signalling [113]. The authors note a decrease in IL-1Ra/IL-1β ratio, indicating increased cytokine activity in these individuals. Patella et al (2015) correlated IL-1β level in BAL fluid with acute rejection following lung transplantation, with this also

increasing in the case of infection [114]. An acute response mediated by IL-1β following graft reperfusion appears to be detrimental to a successful post-transplant outcome.

Animal models of ALI have highlighted that expression and activity of IL-1β promotes tissue damage centred on endothelial disruption and leukocyte adhesion characteristic of PGD [115, 116]. One study by Gasse et al that utilised a mouse model of ALI highlighted that application of Anakinra, an anti-IL-1R1 monoclonal antibody (mAb), significantly down-regulated Bleomycin-induced inflammation within their model [117]. What is clear from both of these clinical studies and animal models of lung disease, is that IL-1β and its associated inflammatory signalling pathways are of immense importance in promotion and progression of respiratory disease. The other finding from this study was the key role of the inflammasome within mediating this lung damage. Knockout mice for ASC, a key mediator of inflammasome activity, showed significantly reduced IL-1β level in the lung, reduced neutrophil number in the BALF and reduced MPO activity. This highlights the key role the inflammasome has in mediating the inflammatory effects of IL-1β [117].

Section 4 – Concluding remarks

Lung transplantation has the possibility of reaching further than ever before, thanks to the implementation of EVLP worldwide. Clinical trials involving EVLP have so far shown comparable outcomes to standard transplantation, which highlights that EVLP could provide a means of safely increasing the lung donor pool. The optimum protocols and strategies for perfusion may yet remain some way off however, as refinements to not only perfusion but also the logistics of implementing the technology continue even today.

Acute graft dysfunction after transplantation remains clouded in doubt and dubiousness even today. Whilst ongoing research into this area continues to unearth new and novel findings, it is certain that numerous pathways and thus potential therapeutic targets are yet to be unveiled. IRI can be considered a 'non-specific inflammatory event' by the sheer number of signalling cascades and pathways involved in establishing and maintaining pathology. PGD following transplantation shapes the short- and long-term outcomes of graft function for the recipient, meaning that any attempt to increase the lung donor pool with EVLP must be done so with utmost care.

Study background

Previous work conducted by the Newcastle group examined a cohort of perfusates taken from 53 lung perfusions performed as part of DEVELOP-UK, a multi-centre UK trial [62]. Levels of 40 inflammatory mediators were measured in these perfusates, with level of the pro-inflammatory cytokine IL-1β at 30 minutes of perfusion proving to be predictive of 1-year patient survival (shown in Fig. 1.9) [118]. The researchers then went on to confirm that IL-1β in the perfusate correlated with propensity to provoke endothelial activation *in vitro* through flow cytometry, neutrophil adhesion and other assay formats. Due to the compelling observations made over the course of this work, it was felt further exploration of the mechanisms of IL-1β in lung perfusion was warranted.

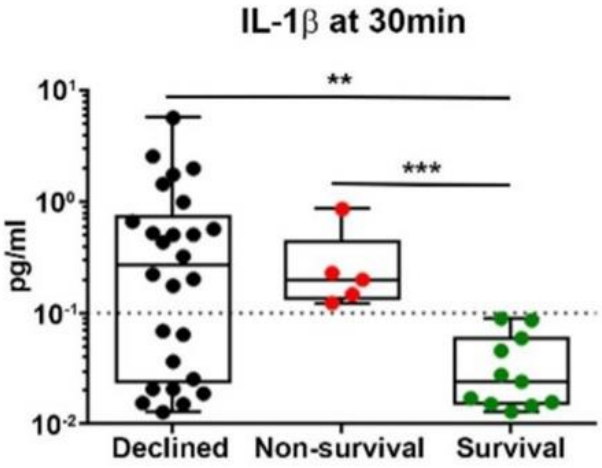

Fig. 1.9 – IL-1β level in EVLP perfusate is predictive of 1-year patient survival post-transplantation. Patients were able to be stratified into 3 groups according to concentration. 'Declined,' whereupon lungs were not accepted for transplant following EVLP, 'non-survival' and 'survival' where recipients of a lung did not or did survive for 1 year or more following transplant, respectively [118].

Section 6 – Hypothesis and aims

Hypothesis of work

Increasing levels of IL-1β cause endothelial activation, subsequently increasing adhesion molecule expression and facilitating neutrophil adhesion during EVLP. This compromises endothelial integrity, promotes immunological dysfunction and results in increased ALI following reperfusion.

Aims

Aim 1

Develop a working model of neutrophil migration through the vasculature of lungs in an *ex vivo* setting which can be used to test efficacy of interventions

Objectives

1) Develop a system to monitor real-time levels of neutrophils in the perfusate
2) Develop a split lung model of perfusion to compare lungs from the same donor

Aim 2

Use model developed previously to assess the impact of IL-1β supplementation on endothelial interactions with circulating neutrophils and overall lung function

Objectives

1) Assess impact of IL-1β on circulating neutrophil numbers and lung damage *ex vivo*
2) Establish effect of IL-1β supplementation on endothelial activation *in vitro*

Aim 3

Assess impact of IL-1β supplementation on transcriptomic profile of lungs perfused *ex vivo*

Objectives

1) Interrogate the RNA profile of biopsies acquired following EVLP
2) Validate observations made by RNA profiling

CHAPTER 2

-

METHODS

Chapter 2 – Methods

Ethical approval and containment level

This project has utilised donor lungs as part of NHSBT Study 66 entitled 'Further Evaluation of Ex Vivo Lung Perfusion to Improve Transplantation Outcomes,' accepted under both generic and specific consent pathways. REC approval number 16/NE/0230. *Ex vivo* work was performed in a controlled access laboratory within the NHS Blood and Transplant building at Barrack Road, Newcastle upon Tyne.

The laboratories of the William Leech building within the Medical School, Newcastle University, for *in vitro* assays, EVLP sample processing and long-term storage of material. All *in vitro* activation work was performed within class II biosafety cabinets unless stated otherwise.

Methods – *Ex vivo*

A detailed standard operating procedure (SOP) for all *ex vivo* work can be found in Appendix 2.

Preparation of Steen solution

Bovine serum albumin (BSA), Dextran 40, sodium bicarbonate and calcium chloride were added to 1600ml ultra-pure water. All components were fully dissolved and then the mixture was made up to 2000ml with more water. The solution was then transferred to a sterile 2L glass bottle via a 0.22µm sterile Ultra Cruz filter, sealed and stored at 4^{o}C prior to use.

Ex-vivo lung perfusion for whole lung pair

Priming of circuit

Medtronic circuits were set-up (as seen in Fig. 2.1) and primed with 1.5L Steen solution containing 7500 units of heparin. Air was completely cleared from the arterial line prior and perfusate was left circulating between 0.5-1L/min. The temperature of the heater-cooler was initially set to 20^{o}C.

Fig. 2.1 – Dual Medtronic perfusion circuits for split lung perfusion model.

Preparation of lungs for split perfusion model

(For whole lung perfusions, skip to bronchial and tracheal cannulation steps)

Lungs were gently taken out of the ice box and placed in a dissection bowl in solution at 4°C. The pulmonary artery (PA) branch was located and cut down the back and front, with enough PA left to cannulate for each lung. Yellow XVIVO cannulae were inserted into the left and right lung PA and secured with a 1usp tie. The left pulmonary vein (PV) was located before a green cannula was inserted inside the left atrium (LA). This was cut down to an appropriate size and then secured using a 4-0 Prolene with a 20mm needle. This step was repeated for the right half of the LA. Following this, the trachea was dissected down to the carina, whereby the left bifurcation was clamped, and the trachea cut just below, resulting in deflation of the left lung. The left and right main bronchi were then cannulated in place with a 1usp tie.

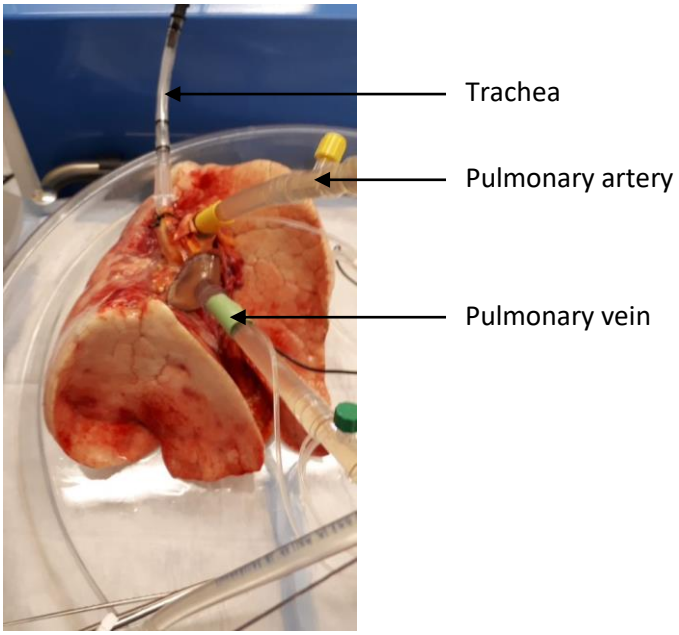

Fig. 2.2 – Example of lung cannulation to circuit. Here, a single lung is cannulated to the trachea (black), pulmonary artery (yellow) and pulmonary vein (green).

Perfusion procedure

The starting weights of both lungs were recorded, and this information was then used to calculate flow rate at 20% CO. Flow rates on the perfusion circuits were adjusted accordingly before the arterial tubing was attached to the PA cannula for each lung. The venous cuff cannula was attached once return was visible from the PV. The position of the tubing and lungs were adjusted to achieve an appropriate arterial pressure, as shown below on Fig. 2.3. The CO_2 tubing was attached to the oxygenator and infusion of gas into the circuit was started. Flow rate was gradually increased to 40% CO, along with temperature to 32°C in line with this.

1. Check Ideal body weight (IBW) as per formula and note maximum minute volume

Donor Ideal Body Weight / kg	40	45	50	55	60	65	70	75	80	85	90	95	100
Maximum Minute Volume L/min	4	4.5	5	5.5	6	6.5	7	7.5	8	8.5	9	9.5	10
Maximum Perfusate Flow L/min	2.8	3.15	3.5	3.85	4.2	4.55	4.9	5.2	5.6	5.95	6.3	6.65	7

Note minute volume must not exceed 1.5X the perfusate flow

2. Dial tidal volume and respiratory rate to achieve the target minute volume and target V_T/kg for the appropriate donor IBW

If Donor IBW 60kg or greater increase minute volume by 1L/min for each degree from 32 to 37 degrees keeping Peak airway Pressure less than 20cmsH_2O

If Donor IBW 59kg or less increase minute volume by 1L/min for each 2 degrees from 32 to 37 degrees keeping Peak Airway Pressure less than 20cmsH_2O

Target Minute Volume	Breaths/min	Tidal volume (ml) for given donor ideal body weight													Target V_T ml/kg
		40kg	45kg	50kg	55kg	60kg	65kg	70kg	75kg	80kg	85kg	90kg	95kg	100kg	
1L/min	5						200	200	200	200	200	200	200	200	2-3 ml/kg
32°C	8	120	120	120	120	120									
2L/min	8								300	300	300	300	300	300	3-4 ml/kg
33°C	10			200	200	200	200	200							
34°C	12	170	170	170	170										
3L/min	10					300	300	300	300	300	300	300	300	300	3-5 ml/kg
34°C	12			250	250	250	250	250	250	250					
36°C	15	200	200	200	200	200	200								
4L/min	10								400	400	400	400	400	400	3-5 ml/kg
35°C	12						330	330	330	330	330	330	330	330	
37°C	15	260	260	260	260	260	260	260	260	260	260				
		MAX	MAX												
5L/min	10										500	500	500	500	4-6 ml/kg
36°C	12							420	420	420	420	420	420	420	
37°C	15			330	330	330	330	330	330	330					
				MAX	MAX										
6L/min	10										600	600	600	600	5-7 ml/kg
37°C	12								500	500	500	500	500	500	
	15					400	400	400	400	400					
						MAX	MAX								
7L/min	12										580	580	580	580	6-7 ml/kg
37°C	15							470	470	470	470				
								MAX	MAX						
8L/min	12												670	670	6-7ml/kg
37°C	15									530	530	530	530		
										MAX	MAX				

Fig. 2.3 – Ventilator value calculation based on ideal body weight (IBW) – Ventilator values are calculated according to ideal body weight (IBW) of the lung donor. Tidal volume and breaths per minute are gradually increased in line with flow rate and temperature of the perfusate [119].

At a perfusate temperature of 32°C, ventilation of lungs was initiated. This was done for split lung perfusions using a custom-made bronchial tree from a single ventilator. The tidal volume and respiratory rate were calculated based on the temperature and ideal bodyweight (IBW) of the donor, which are shown in Fig. 2.3. Once the perfusate temperature reached 37°C, regular blood gas measurements were acquired to ensure measurements remained within normal range throughout EVLP. pH was adjusted with addition of Tromethamine (THAM) solution if required.

Fig. 2.4 – Whole lung perfusion. Image representative of whole lung perfusions performed as part of the work in Chapter 3.

Sample acquisition and storage

Perfusate

5ml of perfusates were acquired from the venous line at the specified time points (as can be seen in Fig. 2.4) and centrifuged at 200xg for 5 minutes. 1ml aliquots were made up for each sample and then remaining cell pellets were re-suspended in 1ml of FACS buffer (PBS, 2% BSA) and stored on ice prior to flow cytometry. All perfusates were stored at -80^{o}C long-term.

Tissue

An initial biopsy was acquired during the warming phase of EVLP with a TLC 75 tissue stapler. This was dissected into two samples and stored in Formalin and RNAlater. Upon completion of EVLP, lungs were weighed and then lobes were dissected down the centre, with biopsies then acquired from the centre. For samples placed in Formalin, these were left at room temperature for 48 hours before embedding in paraffin. Samples placed in RNAlater were stored at 4^{o}C for 24 hours and then transferred to -80^{o}C for long-term storage. Fig. 2.5 shows an example of a post-EVLP biopsy.

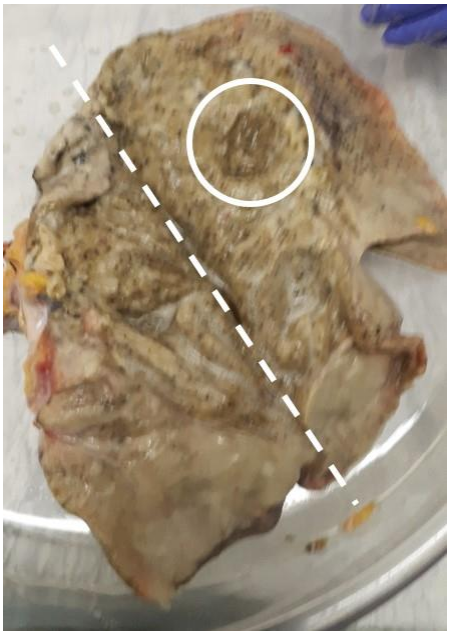

Fig. 2.5 – Example biopsy method. Upon completion of EVLP and having been weighed, lungs were dissected in order to retrieve tissue from the centre of the lower lobe. The white dashed line represents the dissection, the encircled area has just been removed. This was replicated for all biopsies obtained for our split lung perfusions.

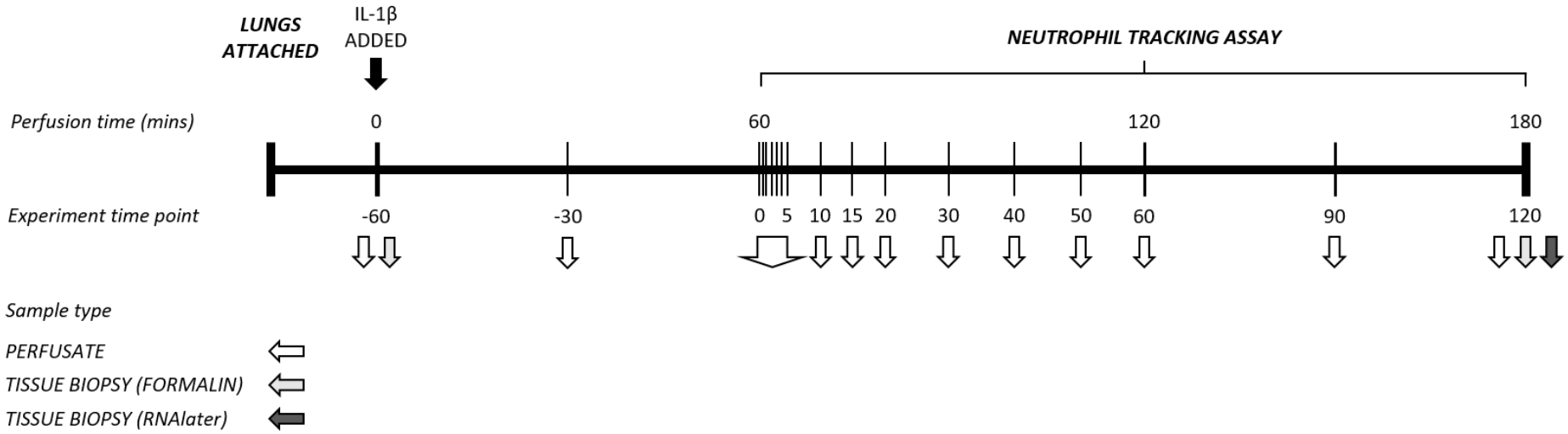

Fig. 2.6 – Timeline of EVLP tracking model stimulation and sample acquisition for split lung perfusions. Arrows under the timeline represent perfusate (white), tissue biopsies placed in Formalin (grey) and tissue biopsies stored in RNAlater solution (dark grey). The total perfusion time upon infusion of IL-1β into the circuit is 180 minutes. After 60 minutes, neutrophils are infused and perfusates are acquired for both neutrophil tracking and future analysis of proteins.

Methods – *In vitro* for EVLP experiments

IL-1β addition

Sufficient human, recombinant IL-1β to achieve a 'free circuit' concentration of 1ng/ml (for 1.5L of Steen use 1500ul of 1ng/µl IL-1β) was made up into 5ml of sterile Steen solution™. This was infused as a bolus into one of the perfusion circuits at 'T-60m,' with the other receiving no IL-1β to act as a control. A sample of perfusate from the circuit was acquired and stored on ice immediately prior to infusion of the IL-1β as 'T-60m.' Further perfusate samples were acquired at '-30m,' and '-15m' prior to beginning the neutrophil tracking model.

Neutrophil isolation

8ml of blood was collected from a healthy donor into an EDTA tube. Neutrophils were then isolated from whole blood using a MACSXpress® Neutrophil isolation kit (Miltenyi Biotec) according to the manufacturer's instructions.

Neutrophil labelling

Neutrophils at a density of $5x10^6$ cells/ml were labelled with 5µM Carboxyfluorescein succinimidyl ester (CFSE) at 4°C in the dark for 10 minutes. Cells were then washed two times in PBS before being re-suspended in HBSS prior to infusion.

Neutrophil tracking assay

$4x10^7$ neutrophils were simultaneously infused into each perfusion circuit gradually over 1 minute through the arterial inlet line in the perfusion circuits. This was done by attaching the syringe of neutrophils and drawing up a small amount of perfusate before then infusing into the circuit, to ensure no air was pushed into the perfusate entering the lungs. Infusion took place at 'T0,' exactly 60 minutes after infusion of IL-1β into the circuit. Perfusates were acquired at the appropriate time points as outlined in Fig. 2.6.

Following EVLP, lungs were detached from the perfusion circuit and a leukocyte filter was attached to the PA and PV. The pump was then left on for 5 minutes. Filters were then washed with PBS in an anterograde direction to clear remaining red cells before a series of retrograde washes were performed to remove any captured leukocytes.

Fig. 2.7 – Haemonetics leukocyte filter for salvaged blood – Upon completion of EVLP, lungs were detached from the circuits and remaining perfusate was run through a leukocyte filter for 5 minutes. Cells were washed out of this with PBS and then analysed by flow cytometry in the same manner as detailed for perfusates taken during the EVLP.

Regular perfusate samples were acquired from EVLPs at regular time points (Fig. 2.6). These were centrifuged at 200xg for 5 minutes, with 4ml of each sample aliquoted into cryovials which were then frozen at -80^{o}C for subsequent biomarker analysis. The cell pellet was then washed in FACS buffer (PBS, 2% FBS) before being re-suspended in 1ml of FACS buffer. 10µl of the re-suspended cells was then run through a FACS Accurri™ C6 flow cytometer and multiplied up to give a total cell count for each perfusate sample taken. Results were then plotted using Prism software (GraphPad©). All final counts were adjusted to total lung capacity using the following formula:

Male donor - (7.99 x height (m)) - 7.08

Female donor - (6.60 x height (m)) - 5.79

This was done in order to account for the inherent variability in donor-lung size.

Methods – *In vitro*

Cell Culture

Human dermal endothelial microvascular cells (HMEC-1) were obtained from American Type Culture Collection (ATCC©) (Middlesex, UK). These cells were cultured in MCDB131 media (Thermofisher Scientific) supplemented with 10% foetal bovine serum (Gibco), penicillin-streptomycin (10ml/l), l-glutamine, epidermal growth factor (10ng/ml) and hydrocortisone (1µg/ml) (all Sigma).

Human pulmonary microvascular endothelial cells (HPMECs) were obtained from PromoCell (Heidelburg, Germany). These were grown in endothelial cell growth medium MV2 (PromoCell) that included supplementation with 10% foetal calf serum, epidermal growth factor (5ng/ml), basic fibroblast growth factor (10ng/ml), insulin-like growth factor (20ng/ml), vascular endothelial growth factor (0.5ng/ml), ascorbic acid (1µg/ml) and hydrocortisone (0.2µg/ml).

All cells were grown in T75 tissue culture flasks at 37°C, 5% CO_2 in a humidified incubator. These were passaged when confluent (usually every 2-3 days).

Passaging cells

In preparation for *in vitro* assays, cells were removed from the T75 flasks through application of HEPES solution (Lonza) before being incubated with Accutase® solution (Biolegend®) for 10 minutes at 5%CO_2/37°C. Visualisation through a light microscope was used to verify that they had detached before being transferred to a Corning® 50ml tube (Sigma-Aldrich©) and washed twice with the appropriate complete culture media. Cells were then counted using a haemocytometer (Sigma-Aldrich©) and re-suspended in the correct volume of media prior to passaging, freezing or use in an *in vitro* assay.

IL-1β activation

Cells were re-suspended to an appropriate density as previously detailed. For 6-well and 12-well plate assays, a cell density of $2x10^5$/ml and $1x10^5$/ml was used with 2ml and 1ml being added to each well respectively. Cells were left to adhere overnight, with half of the media being replaced the next day. This was repeated daily until cells became confluent. Completed media with IL-1β at 2x the working concentration was made up. The assay was begun when half of the media in the first well was replaced with the media/2x IL-1β mixture.

Enzyme-linked immunosorbent assay (ELISA)

An ELISA was used in order to measure the concentration of soluble ICAM-1 (sICAM-1) (cat. no DY720-05) and von-Willebrand factor (vWF) (cat. no DY2764-05) from perfusate samples (R&D Systems). Standards for each plate were used to generate a curve. In the case of sICAM-1, standards were diluted through 2-fold serial dilutions from 2000pg/mL to 31.3pg/mL, for vWF this was from 3000pg/ml to 46.9pg/ml. Perfusates were diluted to 1:1000 for sICAM-1 and used neat for vWF. Standards and perfusate samples were applied in technical duplicate. Optical density of plates were assessed through the Synergy™ spectrophotometer and Gen5™ plate reading software (BioTek) at 450nm. Final concentration values were adjusted to total lung capacity (TLC). The mechanism for ELISA is shown in Fig. 2.8.

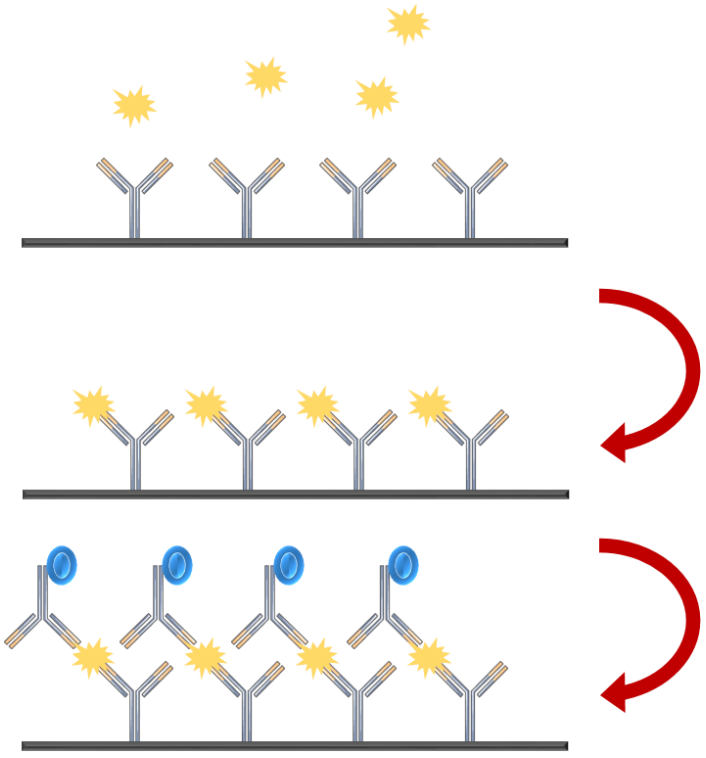

Fig. 2.8 – ELISA mechanism diagram. Plates are coated with capture antibodies specific to the target substrate. Once bound, the substrate is then incubated on the plate and binds to the capture antibodies. Detection antibodies specific for the capture-substrate complex are then bound, with the relative fluorescence of the signal being used to determine the amount of bound substrate.

IL-1β MSD perfusate analysis

The plates used for research were single analyte U-plex plates obtained from Mesoscale Discovery© (MSD). In summary, the wells in each plate are coated with electrochemiluminescent labels known as 'SULFO-TAGS.' These are conjugated to detection antibodies that are specific for the

cytokine/chemokine of interest. Upon binding, this generates light from the tag when an electrical current is applied to the plate via the specialised plate reader. The light intensity is then used to quantify the amount of bound substrate. The MSD assay format was chosen here because it allows far greater sensitivity, having a lower limit of detection (LLOD) of 0.15pg/ml, as well as a greater dynamic range compared to a traditional ELISA. Perfusate samples had previously been recorded by our group and had been below the minimum concentration required for ELISA detection.

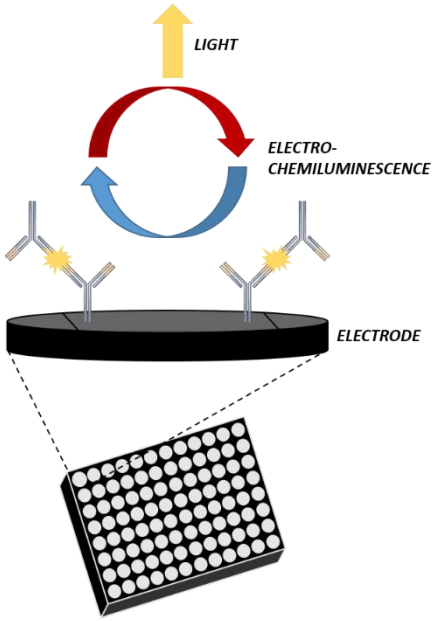

Fig. 2.9 – MSD plate technology. Capture antibodies bind to the target substrate, which are then in turn bound by detection antibodies with an electrochemiluminescent tag attached. Electricity is then applied to the electrode which emits light via the tags on the detection antibodies. The light intensity is then measured to quantify the amount of substrate present.

IL-1β U-plex plates were prepared for the work according to the manufacturer's instructions. Perfusates and standards were diluted with diluent buffer in a 1:1 ratio. Values were adjusted to total lung capacity (TLC).

Neutrophil isolation

Neutrophils were isolated using a MACSXpress® Whole Blood Isolation Kit (Miltenyi Biotec©) as per the manufacturer's instructions, as described in detail previously (*in vitro* methods for EVLP). Neutrophils were made up to 50ml in Hank's balanced salt solution (HBSS) and then centrifuged at 200xg for 5 minutes before being re-suspended to a density of $5x10^6$ cells/ml.

Cytospin and Giemsa stain

A slide for the cytospin chamber was pre-prepared before being loaded with 150µl of cell suspension (at a density of around $5x10^5$ cells/ml). This was then centrifuged at 300xg for 3 minutes before being allowed to air dry. Cells were then fixed in acetone for 10 minutes, allowed to dry once more and then stained with Giemsa solution (diluted 1/10 from stock in PBS-Tween) for 10 minutes. Excess Giemsa was then washed off with cold water. One drop of DPX mountant (Sigma-aldrich©) was added and then the cells were covered with a coverslip. These were then analysed under the microscope to determine purity of the isolated cell population.

Microfluidic flow assay - Cellix

The propensity of perfusates to facilitate neutrophil adhesion to a confluent endothelial monolayer was assessed using a microfluidic platform (Cellix Ltd). Vena8 Endothelial+ Biochips were coated with 8-10µl of fibronectin (100µg/ml) and incubated overnight at 4°C. HPMECs were cultured as previously detailed before and then seeded onto the chips at a density of $1.5x10^7$/ml and left to attach for 15 minutes. 40µl of treatments were then added to each well per channel and the cells were incubated at 37°C/5%CO_2 for 4 hours. In the case of blocking experiments, perfusates were pre-incubated with an IL-1β NAb at 4µg/ml for 30 minutes before stimulating.

Fig. 2.10 – Mirus™ Evo Nanopump connected to MultiFlow8. This system facilitates equal splitting of flow into 8 individual channels. This in turn connects directly to a Vena8 Endothelial+ biochip (Cellix© Ltd) which has been pre-coated with human primary endothelial cells. These can then be either unstimulated or stimulated with cytokines or patient samples prior to commencing the flow assay. Image from Cellix©.

Human primary neutrophils were isolated from healthy volunteers as previously detailed. $1x10^7$ cells were collected in hank's balanced salt solution (HBSS) and left at room temperature for 20 minutes. These were then washed and re-suspended in 2ml of cold PBS (no Ca^{2+}, no Mg^{2+}) containing Celltracker™ CFSE (Biolegend®) at a concentration of 20µM. These were then incubated at 4°C in the dark for 10 minutes and then 8ml of complete RPMI media was added to quench the reaction. Cells were washed twice in complete RPMI and then counted before being washed a final time and re-suspended to a density of $1x10^6$/ml, in order to account for any cells lost during the labelling process.

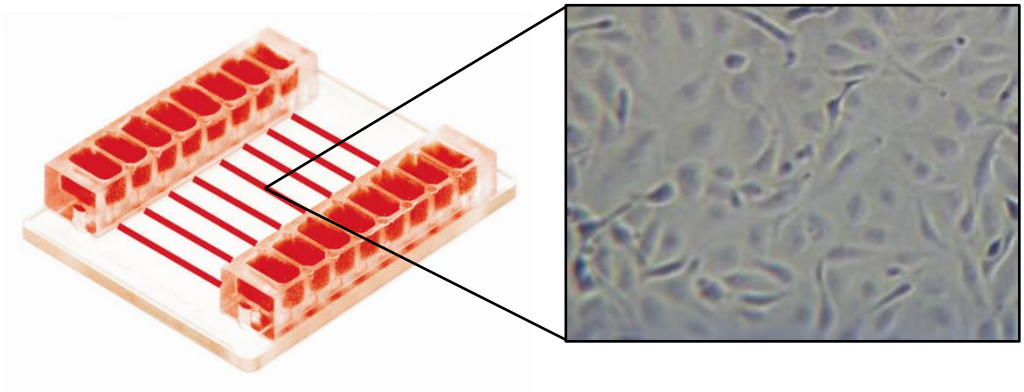

Fig. 2.11 – Vena8 endothelial+ biochip – Each of the 8 channels is evenly coated with a confluent layer of endothelial cells before the treatments are added. There are 5 evenly spaced fields of view along each channel, so that each series of images are directly comparable.

The microfluidic assay was run with a Mirus™ Evo Nanopump controlled via PC link with VenaFluxAssay™ software (Cellix© Ltd). A detailed protocol of the microfluidic platform can be found in Appendix 4. For the experimental runs, flow was initially set up for -10 dyne for 5 seconds before being maintained at -0.5 dyne for the remainder of the assay. Labelled neutrophils were allowed to flow over the endothelial layer for 3.5 minutes before images were acquired at points 2, 3, 4, 5 and 6 on the biochip, with an image of each channel also taken prior to the assay beginning. Images were then analysed and quantified for neutrophil adhesion via DucoCell™ software, as demonstrated in Fig. 2.12. Results were plotted on excel and then presented using Prism 8 software (GraphPad).

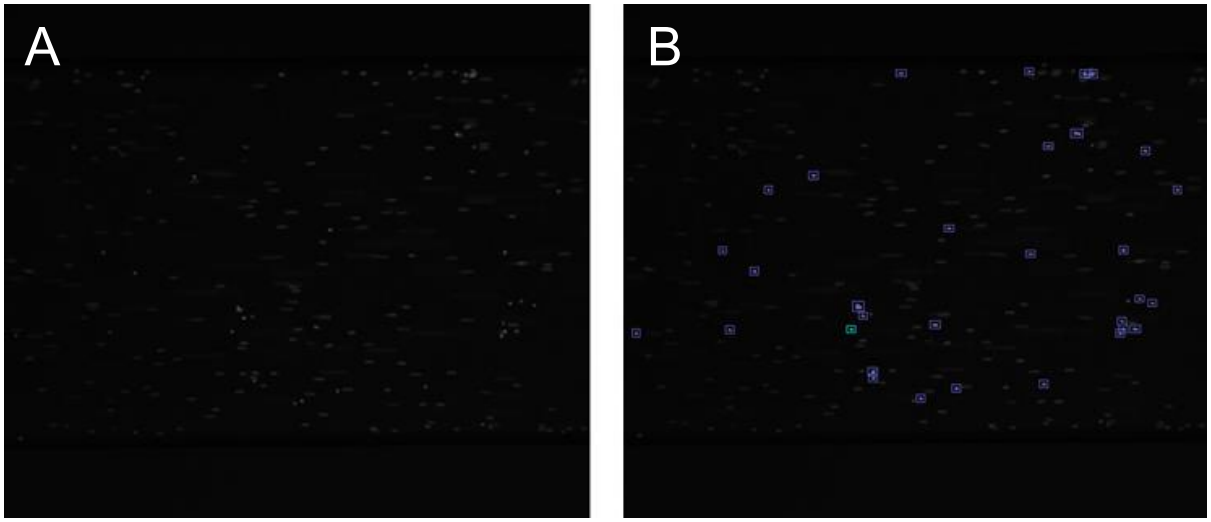

Fig. 2.12 – DucoCell™ software images of adhered cells. Neutrophils labelled with CFSE under flow with HPMECs shown before (A) and after (B) cell image capture. Software calibration ensures that only adhered cells are captured, with cells still flowing over not included in the final figure for a particular field of view.

Prior to using samples from perfusions in the flow system, varying concentrations of IL-1β were used to stimulate HPMECs in order to establish the optimum concentration to use. The results of this are shown in Fig. 2.13.

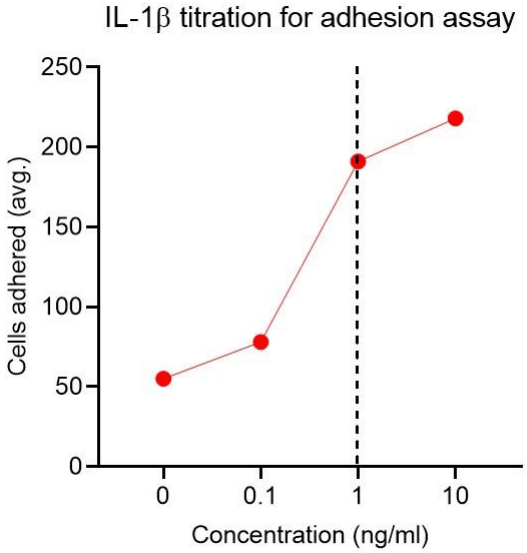

Fig. 2.13 – Optimisations for quantifying neutrophil adhesion under flow. Primary human pulmonary endothelial cells (HPMECs) were stimulated with IL-1β for 4 hours at varying concentrations before CFSE-labelled primary neutrophils were passed over as per the experimental design. The sigmoidal curve seemed to begin plateauing at 1ng/ml, which was chosen as the concentration to use for assays using perfusates. Representative of n=2 experiments.

Flow cytometry

In vitro activation

HPMECs were seeded onto 24-well plates, left to adhere and then stimulated with perfusates obtained from EVLP for 4 hours. In the case of blocking experiments, these were pre-incubated with an IL-1β NAb (R&D Systems) at 4μg/ml for 30 minutes before the stimulation step.

Antigen	Fluorophore	Manufacturer	Clone	Assay
CD106	PE-Cy7	Biolegend	STA	Endothelial activation
CD14	Pacific Blue	BD Biosciences	M5E2	Neutrophil characterisation
CD15	AF700	Biolegend	W6D3	Neutrophil characterisation
CD16	FITC	Biolegend	3G8	Neutrophil characterisation
CD31	APC	Biolegend	WM59	Endothelial activation
CD54	PE	eBioscience	HA58	Endothelial activation
CD62E	FITC	eBioscience	CL2	Endothelial activation
Mouse IgG1	PE-Cy7	Biolegend	MOPC-21	Endothelial activation
Mouse IgG1	APC	Biolegend	MOPC-21	Endothelial activation
Mouse IgG1	PE	eBioscience	P3.6.2.8.1	Endothelial activation
Mouse IgG2a	FITC	eBioscience	eBM2a	Endothelial activation

Table 2.1 – Antibody information for all *in vitro* staining work

Cells were removed from the plates with Accutase® as previously detailed before being washed twice in cold PBS. These were then re-suspended in cold FACS buffer (PBS, 2% FBS) with the appropriate concentration of antibodies for 30 minutes at 4^{o}C. This panel chosen consisted of directly conjugated antibodies specific for PECAM-1, ICAM-1, VCAM-1 and E-Selectin. These were then washed twice more in cold FACS buffer before being run on a BD FACSCanto™ II using FACSDiva software. Compensation was performed using OneComp eBeads™ (eBioscience™). Gating is shown in Fig. 2.14.

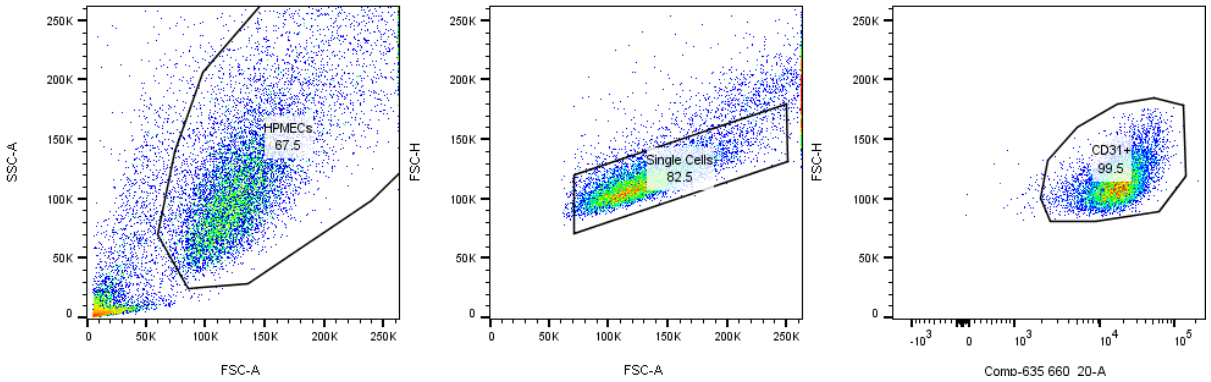

Fig. 2.14 – Gating strategy for human pulmonary microvascular endothelial cells (HPMECs) – Cells are gated on Forward and side scatter, doublets are excluded and then finally all $CD31^-$ cells are excluded.

Analysis was performed using FlowJo software (FlowJo®). Optimisations using titrations of recombinant human IL-1β at varying times and concentrations were done prior to perfusate assays. These are shown in Fig. 2.15.

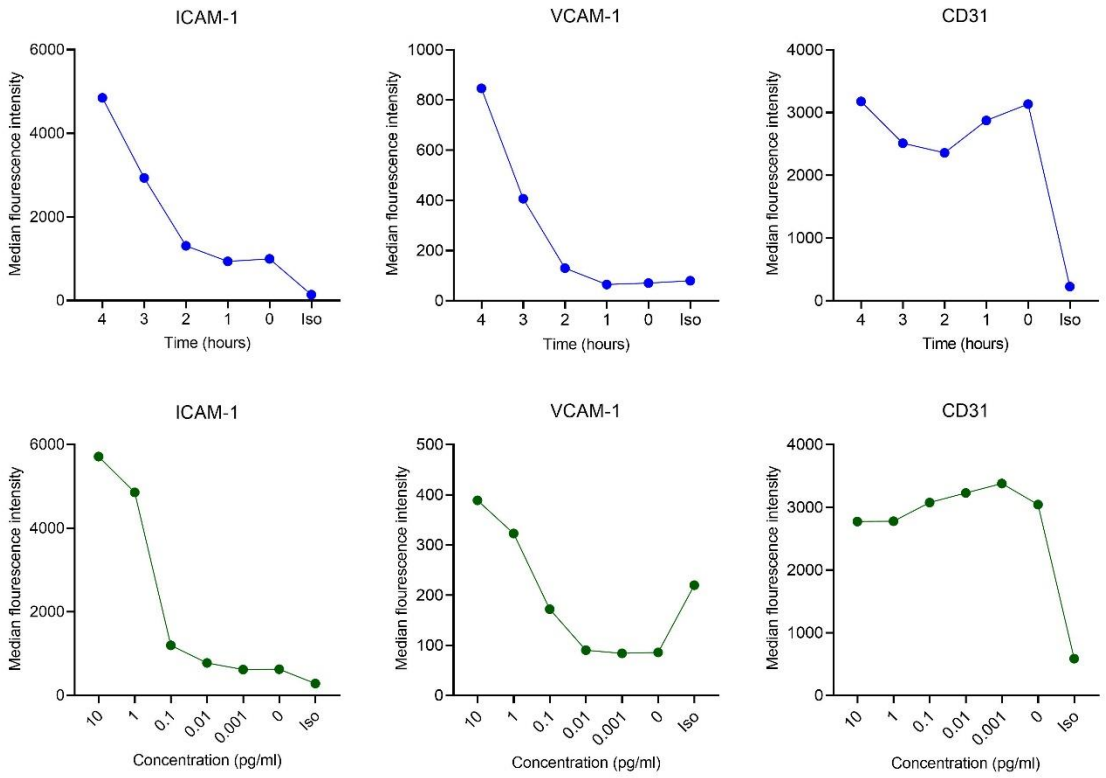

Fig. 2.15 – Optimisations of flow cytometry for ICAM-1, VCAM-1 and CD31 surface expression with HPMECs. HMEC-1 cells were seeded onto 6-well plates, adhered overnight and stimulated with IL-1β to optimise the concentration and duration of stimulation for later assays utilising experimental perfusates. For time course assays, a concentration of 1ng/ml was used. Representative of n=2 experiments.

Multi-photon imaging

Sections of tissue were acquired from perfused lungs as outlined in the *ex vivo* methodology section. PFA-fixed lung tissue was imaged using a Zeiss LSM880 on an AxioObserver inverted stand with a motorised stage and Z drive. The filters used ranged from blue to red (380-710nm) with additional second harmonic generation (SHG) imaging. The multiphoton laser used was a Coherent Chameleon Discovery. Image analysis was performed using Fiji imaging software [120]. This work was performed in collaboration with Glyn Nelson (Newcastle University bioimaging unit).

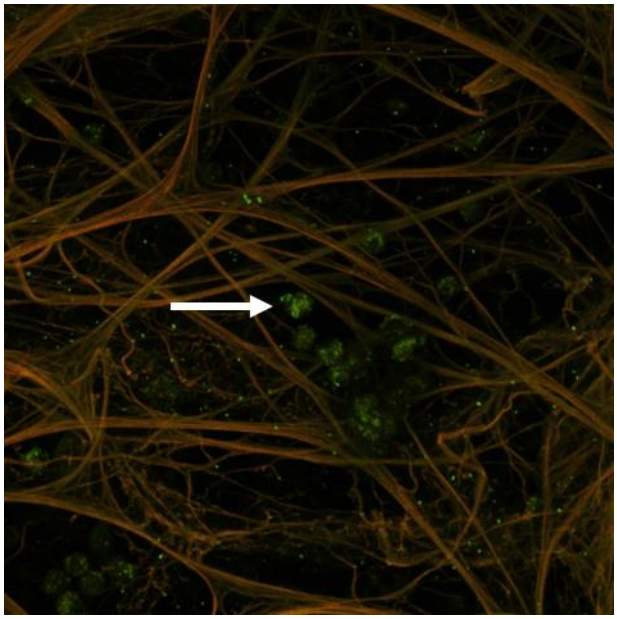

Fig. 2.16 – Imaged lung tissue with CFSE+ neutrophils. Precision cut slices of lung tissue were generated from biopsies acquired post-EVLP of a single human lung. The image shows the architecture of an alveolar space, with CFSE-neutrophils in green (indicated by the white arrow).

RNA isolation from lung tissue

All equipment and laboratory spaces were treated with RNaseZap prior to use.

Tissue samples collected from EVLP were stored in RNAlater© at -80°C until required for analysis. 20µg sections were dissected and then homogenised using a Tissue Lyser II for 2 minutes in RLT Plus buffer with stainless steel beads (Qiagen). RNA was isolated using the RNeasy Mini Plus Kit (Qiagen) as per the manufacturer's instructions. Purified RNA was analysed using a Nanodrop One for A280/260 and A260/230 ratios before being quantified for RNA concentration precisely using a Qubit high sensitivity RNA assay.

The RNA obtained from the IL-1β-stimulated lung from donor 1 required concentrating prior to Nanostring. Upon thawing of the RNA, 2µl of RNaseOUT recombinant ribonuclease inhibitor (40U/µl, Invitrogen) was added to prevent degradation and concentrated using the DNA 120 SpeedVac system (ThermoFisher Scientific) for 20 minutes. The pellet was then re-suspended in RNase Free water as per the other samples prior to analysis.

RNA profiling

In order to ascertain changes to the RNA profile of lungs perfused *ex vivo*, we utilised a targeted approach to screening genes that we hypothesised would be altered. We felt that this approach would

give a wealth of information whilst remaining streamlined to immunological pathways affected by IL-1β.

Nanostring technology was chosen as the methodology to perform our targeted RNA investigation. Analysis of homogenised tissue was performed using an nCounter® FLEX analysis system (Newcastle Human Dendritic Cell Laboratory) with the nCounter® Human immunology v2 Panel. Accessed with the following link: https://www.nanostring.com/products/gene-expression-panels/gene-expression-panels-overview/ncounter-inflammation-panels?jumpto=SUPPORT

The first stage in the process consists of a hybridisation step within a thermo-cycler, shown in Fig. 2.17. Within the mixture are capture and reporter probes, both of which contain a target 50 base region. The capture probe is bound to a biotin molecule, with the reporter probe consisting of a unique, fluorescent 'barcode.' At the conclusion of this stage, a target RNA sequence is bound to both the capture and reporter probe.

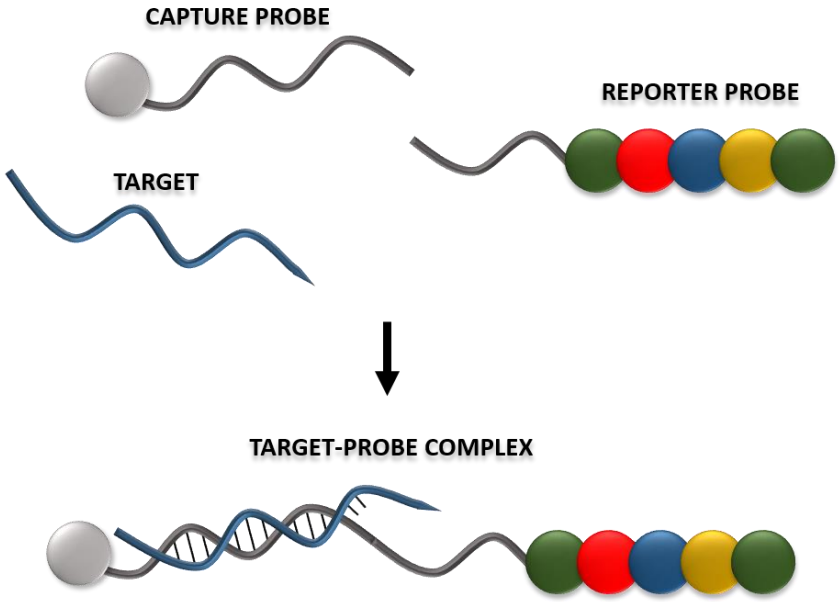

Fig. 2.17 – Target-probe complex formation. Nanostring technology uses a specific capture and reporter probe, which form a complex with the target RNA. The capture probe enables immobilisation in the subsequent stages, with the reporter probe containing a specific fluorescent signal corresponding to a particular gene.

Once formed, the target-probe complexes in solution are then transferred to the prep station. Here, they are immobilised on a streptavidin cartridge in a uniform arrangement, displayed in Fig. 2.18. Simultaneously, probes that have not bound any target mRNA are removed from the sample.

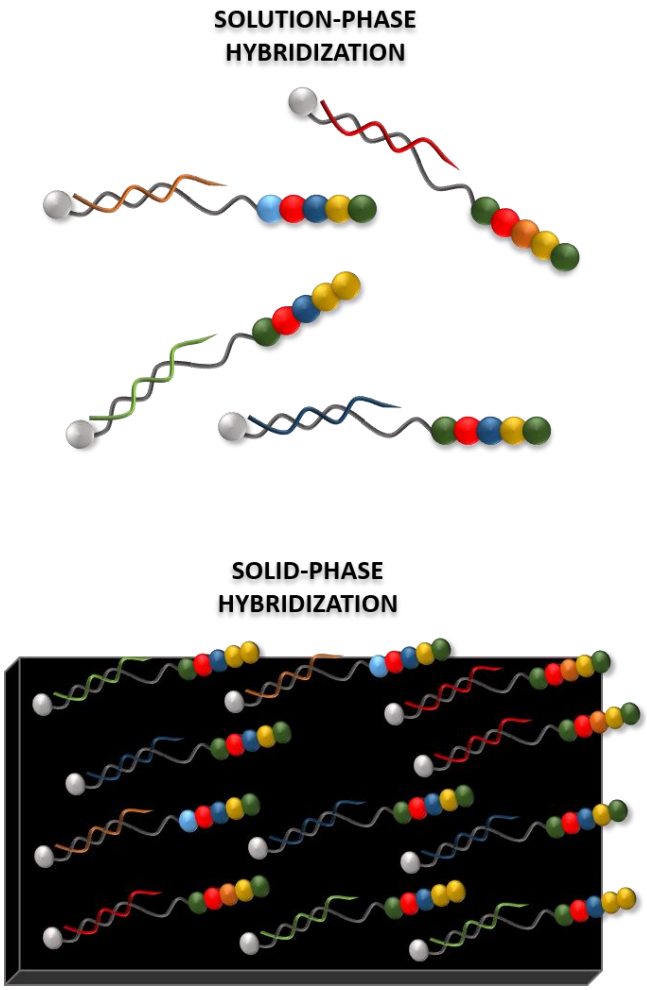

Fig. 2.18 – The hybridisation stage in Nanostring. Target-probe complexes are formed via hybridisation, as shown in Fig. 2.17. These complexes are then annealed to a streptavidin cartridge and the relative quantities of each barcode are used to determine gene counts.

Once all complexes have been immobilised, the cartridge is transferred across to the digital analyser. Multiple images of the cartridge surface are acquired in order to accurately quantify the number of unique barcodes present. Counting results are then analysed using nSolver analysis software. In the case of the work here, the Immunology panel containing target/reporter probes for 594 immunologically associated genes was selected. The pathways interrogated are shown in Table 5.1.

Annotation	Gene number
Adaptive Immune System	141
Apoptosis	54
Autophagy	11
B cell Receptor Signalling	35
Cell Adhesion	60
Chemokine Signalling	63
Complement System	39
Cytokine Signalling	259
Haemostasis	73
Host-pathogen Interaction	252
Immunometabolism	32
Inflammasomes	8
Innate Immune System	201
Lymphocyte Activation	245
Lymphocyte Trafficking	21
MHC Class I Antigen Presentation	39
MHC Class II Antigen Presentation	14
NF-kB signalling	62
NLR signalling	64
Oxidative Stress	36
Phagocytosis and Degradation	48
T Cell Receptor signalling	61
TGF-b Signalling	9
Th1 Differentiation	14
Th17 Differentiation	31
Th2 Differentiation	17
TNF Family signalling	49
TLR signalling	73
Transcriptional Regulation	53
Treg Differentiation	10
Type I Interferon signalling	28
Type II Interferon signalling	36

Table 2.2 – Gene pathway(s) investigated by the Immunology v2 panel. The panel we used within our analysis covers a wide range of cellular and immunological functions, providing significant insight into the changes to gene transcription provoked by IL-1β.

Results from the Nanostring were collated and processed using nSolver software (NanoString). The immunology panel contained 6 positive controls, 8 negative controls and 15 internal reference genes. Counts of RNA from each stimulated lung was compared to the corresponding control lung from each pair before relative changes were then compared between different lung pairs.

Statistical analysis

All error bars on graphs are representative of standard error of mean (SEM). For comparison of control and treatment groups, such as in the case of *in vitro* functional assays, paired t-tests were used. For the RNA profiling work, ratio paired t-tests were chosen, due to donors often having very different levels of RNA for some of the genes assessed in our panel. It was therefore felt that using the ratio of difference offered more of a valid comparison when using different lung donors.

For statistical tests, *p* values below 0.05 were considered statistically significant. * denotes values as follows:

* = $p < 0.05$
** = $p < 0.01$
*** = $p < 0.001$
**** = $p < 0.0001$

CHAPTER 3

-

DEVELOPING A MODEL OF REPERFUSION INJURY USING EX VIVO LUNG PERFUSION

Chapter 3 – Developing a model of reperfusion injury using ex vivo lung perfusion

Introduction

Lung transplantation is now an acceptable standard of care for many end-stage pulmonary diseases. Success rates of transplant are compromised largely by the occurrence of primary graft dysfunction (PGD), which serves to increase short-term mortality, lengthen hospital stays and reduce long-term survival following transplantation [66]. The term 'PGD' refers to a spectrum of disease that is associated with a severe incidence of ischaemia-reperfusion injury following lung transplantation. Efforts must be made to minimise severity of PGD in order to improve patient survival and quality of life.

Current research efforts are focused on elucidating the mechanisms of PGD, so that more effective treatment strategies can be implemented prior to and following successful transplantation. Many of the data that have contributed to our understanding of PGD come from animal models of transplantation. These have highlighted aspects of pulmonary IRI including the roles of crucial cell types such as macrophages and T-cells in disease progression [121-123].

There are also examples of human studies that have looked into correlating levels of biomarkers with severity and prevalence of PGD. Fisher et al (2001) identified that higher levels of IL-8 in BAL fluid in donor lungs was indicative of primary graft dysfunction and early recipient mortality after lung transplantation [76]. ICAM-1 has also been identified at higher levels in the plasma of individuals with PGD following transplantation [71, 72], suggesting a key role for endothelial dysfunction within the pathology of graft dysfunction following transplantation. Covarrubias et al (2012) identified a panel of biomarker including soluble ICAM-1 (sICAM-1), soluble receptor for advance glycation end products (sRAGE) and surfactant protein-D (SF-D) that were predictive of 90-day mortality following transplant [71, 72]. Lastly, gene set enrichment analysis performed as part of the Clinical Trials in Organ Transplantation study in the US identified key immune genes involved in the toll-like receptor pathway, NOD-signalling pathway and the IL-1 pathway were up-regulated in patients with higher grades of PGD [124].

These clinical and pre-clinical studies all highlight the diverse range of cell types and key pathways involved in mediating detrimental post-transplant outcomes. Leukocytes, epithelial cells and the endothelium all play key roles in promoting inflammation and subsequent tissue damage. This suggests that complex multi-cellular mechanisms dominate the pathology of ischaemia-reperfusion injury (IRI) which leads to PGD post-transplantation, meaning that simple, *in vitro* modelling is unlikely to effectively map out pathways of this disease.

Study background

Ex-vivo lung perfusion (EVLP) offers a potential means to address the crucial shortfall of suitable donor-lungs for transplantation, via reconditioning of marginal organs. There is concern however, over use of these lungs in transplant due to increased risk of PGD and worsening post-transplant outcomes. Previous data gathered by Newcastle University highlighted that neutrophil adhesion *in vitro* is mediated by the presence of pro-inflammatory cytokines, namely IL-1β, within the perfusate [118]. Leukocyte infiltration and the subsequent inflammatory processes exacerbated by the presence of activated leukocytes is a hallmark of reperfusion injury following transplantation. These observations suggested that a pro-inflammatory profile during EVLP is indicative of future reperfusion injury-based events.

These observations prompted us to develop an *ex vivo* model of neutrophil adhesion using EVLP and use this as an output to test interventions, such as cytokine addition to a perfusion circuit, in the future. This model aimed to assess whether neutrophil numbers could be used as an output to assess donor-lung quality. This could provide additional information on the mechanisms that can ultimately 'set the scene' for reperfusion injury and PGD.

Hypothesis and aims

Hypothesis

Neutrophil trapping in the vasculature of lungs perfused *ex vivo* can be used as an output to assess differences in donor-lung quality. This output can be used to inform efficacy/effect of interventions during EVLP moving forward.

Aims

1) Develop and validate a working model of neutrophil adhesion within the tissues of perfused lungs *ex vivo*
2) Develop a split lung perfusion system in order to test interventions *ex vivo* and use neutrophil adhesion as an output

In order to achieve these aims, this work will consist of the following objectives: -

1) Infuse neutrophils labelled with a fluorescent dye directly into a perfusion circuit with human lungs and measure numbers of these during EVLP
2) Assess the relationship of inflammatory markers and neutrophil numbers with oedema
3) Develop a split lung model that incorporates neutrophil tracking assay

Methods

Ex vivo lung perfusion

Briefly, lungs declined for transplantation underwent EVLP on Medtronic circuits, shown in Fig. 3.1. These were perfused as whole lung pairs (Donors 1-4, 6) or as single lungs (Donors 5 and 7). Lungs were perfused on custom-made Medtronic circuits. This system operated as a closed perfusion system, with lungs connected via the pulmonary artery (PA) and pulmonary vein (PV). Lungs were gradually warmed from cold storage temperature (4°C) to sub-normothermia (32°C) over 20 minutes, with cardiac output (CO) gradually increased from 20-40% over this period. Ventilation was started at 32°C, with respiratory rate (RR) and tidal volume gradually increased in line with temperature. Lungs were perfused at normothermia for the duration of EVLP thereafter. Tromethamine (THAM) was used to maintain a pH between 7.3 and 7.5 during EVLP.

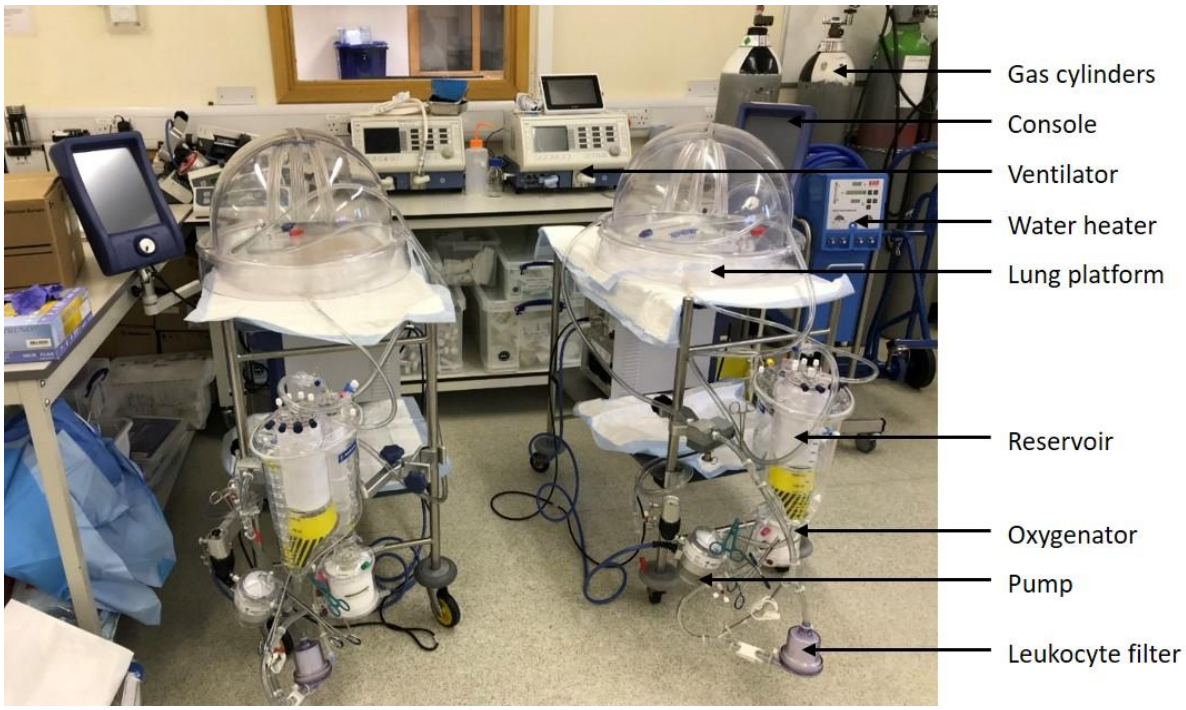

Fig. 3.1. – Dual Medtronic© EVLP circuits. Perfusate exits the reservoir at the bottom and moves through the circuit by means of pressure created by the centrifugal pump. The perfusate then receives CO_2 and heat as it moves through the oxygenator, which connects to a gas cylinder containing (BOC Ltd) as well as a heater/cooler (Hico-Varitherm) before passing through a leukocyte filter. Perfusate will then move up towards the perfusion chamber™ (XVIVO), via the flow probe, which monitors flow rate in the circuit. Finally, fluid then travels back into the reservoir through the pulmonary vein and the outflow tubing at the bottom of the dome. An ICU ventilator (Hamilton) supplied with medical grade air and oxygen facilitates ventilation of lungs whilst on the perfusion chamber™.

For Donor 7, perfusion was performed in the same manner, however this pair was dissected into individual lungs prior to undergoing EVLP. Fig 3.2 shows this approach, the rationale of which was a design by which to develop a paired-lung method to test the efficacy and effect(s) of interventions added into the perfusion circuit. The dissection strategy is fully described in the Appendix 2.

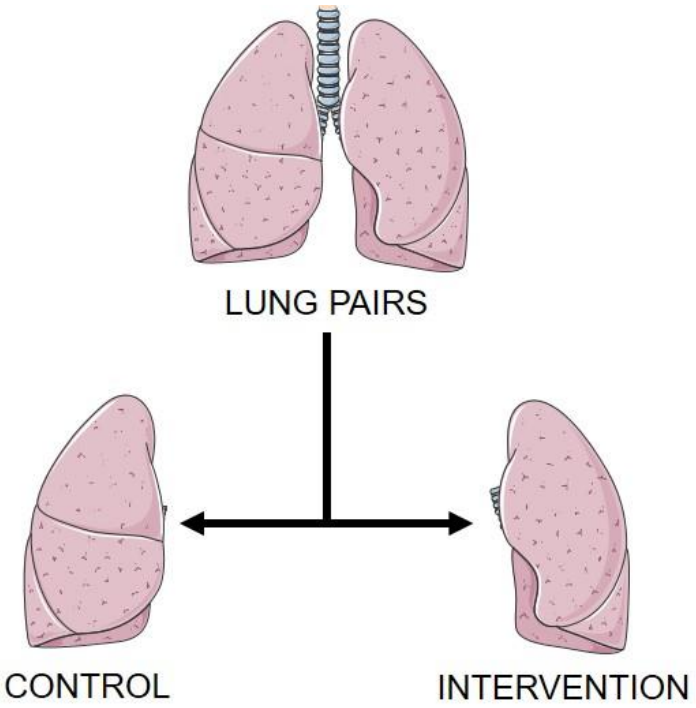

Fig. 3.2. – Split lung model. A lung pair declined for transplantation were dissected into individual lungs and perfused simultaneously, on separate perfusion circuits. This approach was developed in order to provide an internal control for comparison of interventions during EVLP.

Sample acquisition

Perfusates were acquired at regular time points throughout the duration of EVLP, centrifuged and stored at -80^{o}C in aliquots for later analysis. A tissue biopsy was acquired at the start of EVLP using a TLC 75 stapler and then upon completion of EVLP. Samples were fixed in 4% paraformaldehyde (PFA) for 24 hours before being imaged using two-photon microscopy.

Neutrophil isolation

Whole blood was obtained from healthy volunteers before being isolated through use of Miltenyi Biotec© MACSXpress whole blood neutrophil isolation kit. This was performed according to the

manufacturer's instructions. Neutrophil-rich plasma was collected from a 15ml falcon tube, made up to 50ml in Hank's balanced salt solution (HBSS) and centrifuged at 200xg for 5 minutes.

CFSE labelling of neutrophils

Cells were re-suspended at a density of $5x10^6$ cells/ml in PBS containing 5µM CFSE. The cell prep was incubated in the dark at 4°C for 10 minutes and then washed 3 times in HBSS. A final volume of $1x10^7$ and $4x10^7$ cells was re-suspended in 10ml Steen solution taken from the perfusion circuit prior to infusion into the EVLP circuit for whole lung pairs and single lungs, respectively.

Neutrophil tracking assay

A bolus of $1x10^7$ CFSE+ neutrophils was gradually infused into the arterial line of the perfusion circuits over 1 minute. 5ml of perfusate was collected from the venous outflow from the lungs at the appropriate time points, as detailed in Chapter 2. These perfusates were centrifuged and stored as aliquots for later analysis, with cell pellets re-suspended in 1ml of FACS buffer (PBS, 2% BSA). These samples were then analysed for neutrophils with a FACS Accurri flow cytometer.

Flow cytometry

The antibodies chosen for human neutrophils were specific for CD14, CD15 and CD16 all at 1:20 dilutions. Cells were stained with these antibodies for 30 minutes in the dark on ice before being washed twice at 200xg and re-suspended in FACS buffer (PBS, 2% BSA). These were then analysed using a FACS Fortessa flow cytometer, via single cell sorting and then gating on CFSE+ events. A population of cells were taken and then centrifuged onto a glass slide before being fixed in ethanol.

Giemsa stain

A Giemsa stain was performed on isolated human neutrophils in order to assess morphology and purity. Briefly, neutrophils were centrifuged onto a glass slide, fixed in ice cold methanol for 5 minutes and then stained with 1/10 Giemsa solution for 5 minutes. Slides were dried, mounted with DPX and then imaged using a light microscope.

Enzyme-linked immunosorbent assay (ELISA)

An ELISA was used in order to measure the concentration of von-Willebrand factor (vWF) and neutrophil elastase (NE) from perfusate samples (R&D Systems). Standards ranging from 3,000pg/ml to 46.9pg/ml were used to generate a curve to read concentration values. Perfusates were run neat for vWF and at 1:256 for NE. Standards and perfusate samples were applied in technical duplicate. Optical density of plates were assessed through the Synergy™ spectrophotometer and Gen5™ plate reading software (BioTek) at 450nm. Final concentration values were then adjusted to total lung capacity (TLC) and plotted against values for percentage weight gain in a model of linear regression.

Multi-photon imaging

This work was performed in collaboration with the Newcastle University bio imaging unit (www.ncl.ac.uk/bioimaging). Sections of tissue were acquired from perfused lungs as outlined in the *ex vivo* methodology section. PFA-fixed lung tissue was imaged using a Zeiss LSM880. The multiphoton laser used was a Coherent Chameleon Discovery, which enabled high resolution images to be taken at a depth of up to 1mm into tissue biopsies. Image analysis was performed using Fiji imaging software.

Statistical analysis

Raw counts for cell tracking were calculated using Accuri C6 Plus software and then normalised to cells/ml using Microsoft Excel. Paired t-tests and linear regression modelling were performed using Prism 8 software (GraphPad). P values were plotted as follows:

* = $p < 0.05$

** = $p < 0.01$

*** = $p < 0.001$

**** = $p < 0.0001$

Results

Donor and perfusion information

Lungs declined for transplantation were accepted under NHS-BT RINTAG-approved Study 66 entitled 'Further Evaluation of Ex Vivo Lung Perfusion to Improve Transplantation Outcomes' with REC approval number 16/NE/0230. This occurred through both generic and specific consent pathways, with the latter of these referring to hospital trusts within the North East of England. Table 3.1 highlights key donor information. Lungs used for this study were declined on the basis of poor function or bi-lateral consolidation prior to retrieval. Table 3.2 shows the key perfusion parameters that were assessed during EVLP.

Perfusion	Donor age	Sex	Bodyweight (kg)	Height (cm)	Donation	Smoker? (Y/N)
Donor 1	58	Male	88	180	DCD	Y
Donor 2	66	Female	64	157	DCD	N
Donor 3	52	Female	75	168	DCD	Y
Donor 4	61	Female	80	163	DCD	Y
Donor 5	52	Female	60	160	DBD	N
Donor 6	64	Male	90	188	DBD	N
Donor 7	63	Female	85	161	DBD	Y

Table 3.1. – Donor data for lungs in the development cohort

DCD – Deceased from circulatory death; DBD – Deceased from brain death

Perfusion	Type of perfusion	CIT (h, min)	Weight pre	Weight post	% weight gain
Donor 1	Double EVLP	16, 44	798.5	1258	57.7
Donor 2	Double EVLP	13, 22	606	711	17.3
Donor 3	Double EVLP	12, 37	1112	1215	9.3
Donor 4	Double EVLP	9, 55	746	1685	125.9
Donor 5	Single EVLP	24, 10	234.5	689.5	194
Donor 6	Double EVLP	3, 33	1035	1269	22.6
Donor 7	Single EVLP	5, 16	435.5	776	78
Donor 7	Single EVLP	5, 20	383.5	615.5	60

Table 3.2. – Perfusion data for lungs in the development cohort

CIT – cold ischaemic time

Pure preparations of neutrophils can be performed for EVLP tracking models

Neutrophils were isolated from whole blood using a MACSXpress isolation kit. These were then stained with a cocktail of antibodies for CD14, CD15 and CD16, whilst also being assessed for purity with a Geimsa stain. Fig. 3.3 shows the flow cytometry positive staining for CD15 and CD16, whilst being negative for CD14. The image acquired from a cytospin of Giemsa-stained cells shows a high purity of cells confirmed by the presence of multi-lobed nuclei (>95%).

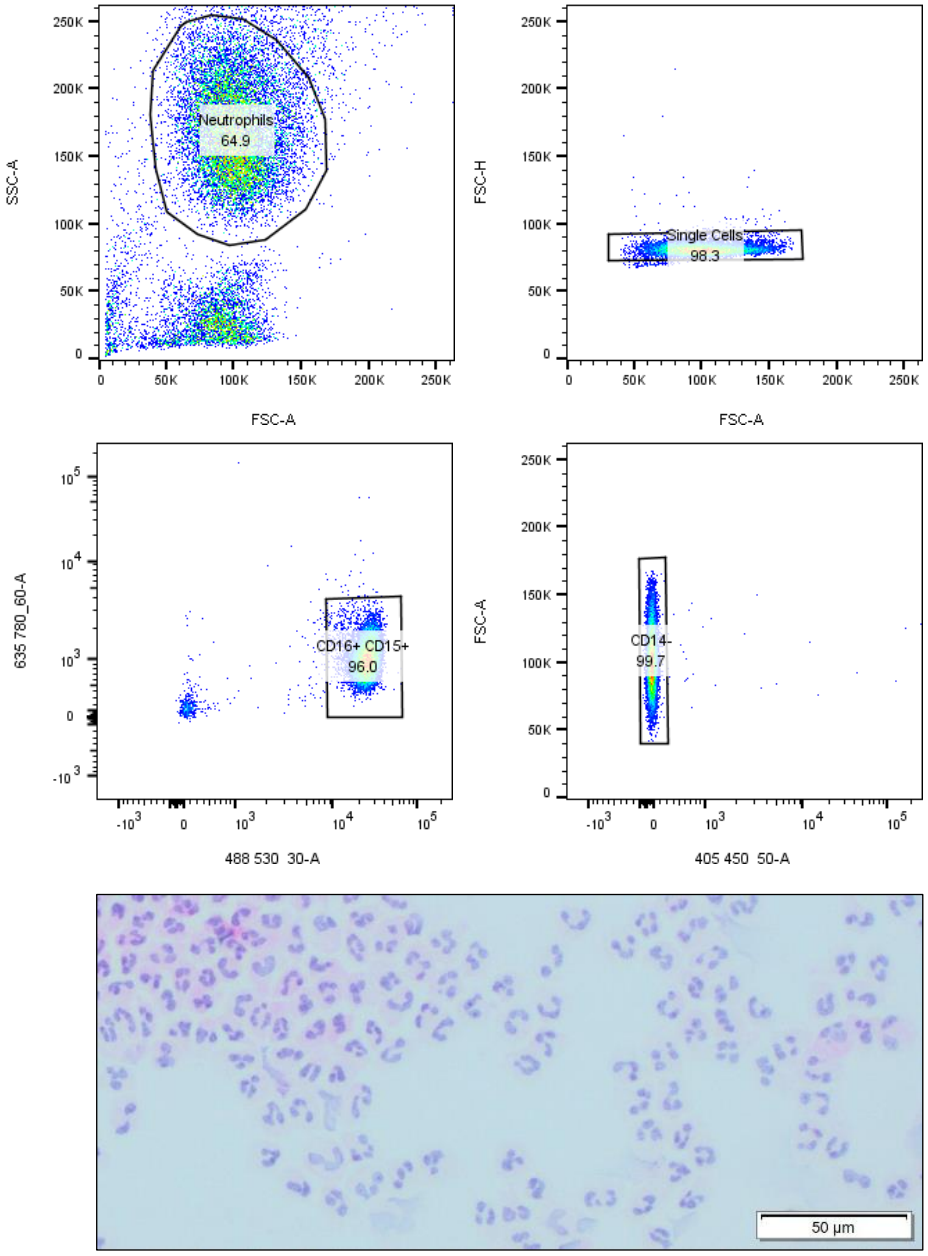

Fig. 3.3. – Human neutrophil flow cytometry and cytospin characterisations – Neutrophils were isolated from whole blood of healthy volunteers and stained for CD14, CD15 and CD16. The initial panel shows a positive stain for CD15 and CD16, with this cell population also staining negative for CD14. A small population of cells fixed

and then a Giemsa stain was performed in order to assess morphology. The cells imaged here show the typical multi-lobed nuclei that are a hallmark of neutrophils and the population shows a high level of purity (>95%).

CFSE+ neutrophils can be detected in the perfusate of human lungs during EVLP

Lung pairs perfused ex vivo were infused with a bolus of CFSE-labelled neutrophils following 30 min of stable normothermic perfusion. Following infusion, perfusate samples acquired over 120 minutes of perfusion were then measured for neutrophils using flow cytometry. Cells from donor 3 were infused but not detectable on the flow cytometer due to an error in the CFSE labelling process. An initial spike in numbers can be seen within the first few minutes of infusion, followed by a plateauing of numbers thereafter. The number of neutrophils detected at the early time points is variable between lung donors, likely due to organ quality. We could detect cells for the duration of perfusion, namely for 120 minutes. N=4.

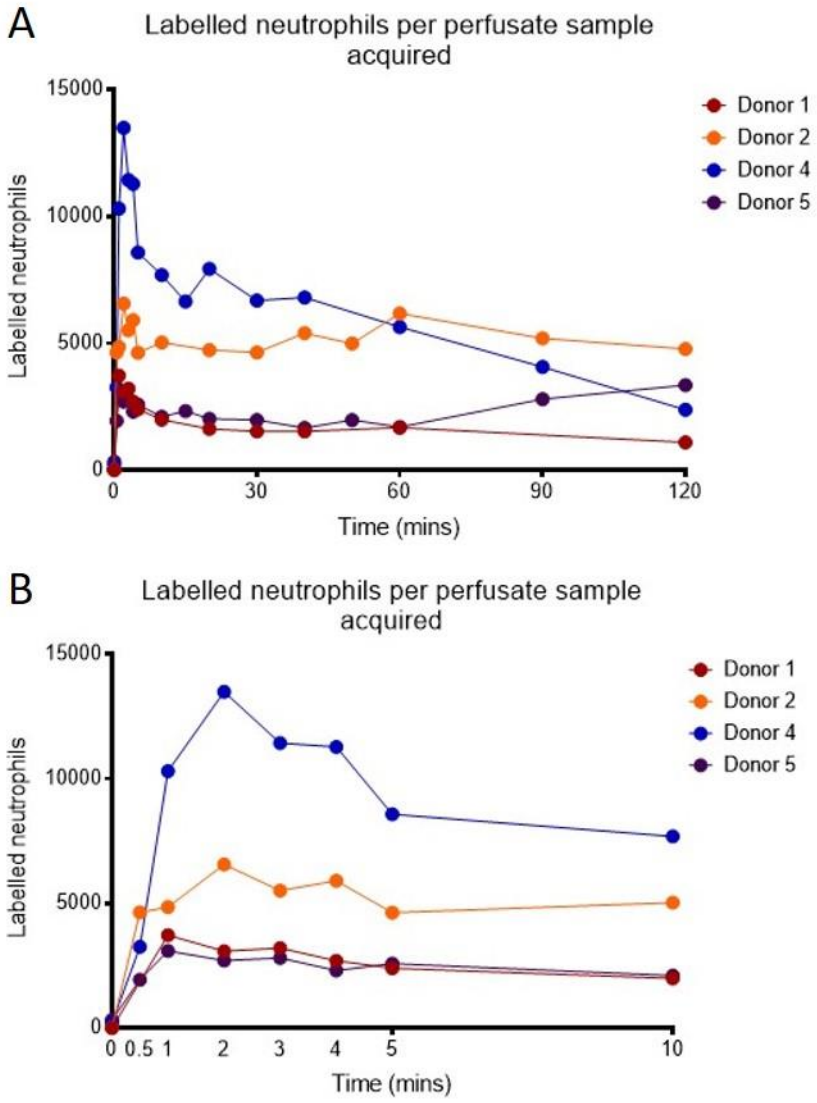

Fig. 3.4. – Neutrophil numbers in the perfusates of EVLP. Neutrophils were infused as a bolus into a perfusion circuit and then measured in regularly acquired perfusates over 120 minutes of EVLP (A). An initial peak can be seen inside 5 minutes (B) before this then reaches a plateau for the remainder of EVLP. N=4.

Weight gain significantly varies between lungs donors during EVLP

Lung pairs that underwent EVLP were weighed before and after perfusion, to assess the relative weight gain as a surrogate marker for oedema formation, which represents endothelial disruption. This information was then plotted as an absolute and percentage (%) increase. All lungs gained weight over 2 hours of EVLP, with this absolute increase statistically significant (p = 0.039) (paired t-test). A large variation in percentage increase can be observed between different donor-lungs. N=5.

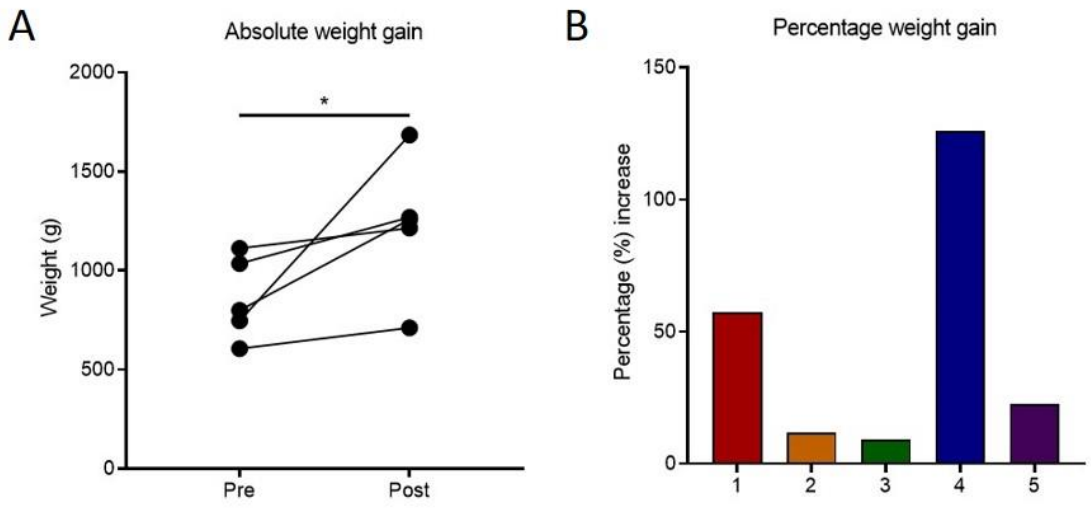

Fig. 3.5. – Weight gain of lung pairs during EVLP. Lung pairs were weighed before and after EVLP, with absolute weight gained (A) statistically significant (p = 0.039). Weight plotted as a percentage increase (B) varied significantly between donor-lungs.

Endothelial and neutrophil activation correlate with weight gain of perfused lungs *ex vivo*

Measurements of von-Willebrand factor (vWF) and neutrophil elastase (NE) were done using ELISA on perfusates acquired after 30 minutes of EVLP. Labelled neutrophils infused into the EVLP circuits were collected with a leukocyte filter at the end of EVLP and then counted using flow cytometry. All were correlated against percentage weight gain using a model of linear regression. Concentration of vWF correlated significantly ($R^2 = 0.81$, $p = 0.034$). The same was observed for NE, which also correlated with weight gain of lungs perfused *ex vivo* ($R^2 = 0.76$, $p = 0.054$). Lastly, the number of cells isolated was seen to negatively correlate with oedema formation ($R^2 = 0.65$, $p = 0.19$), though this was not statistically significant.

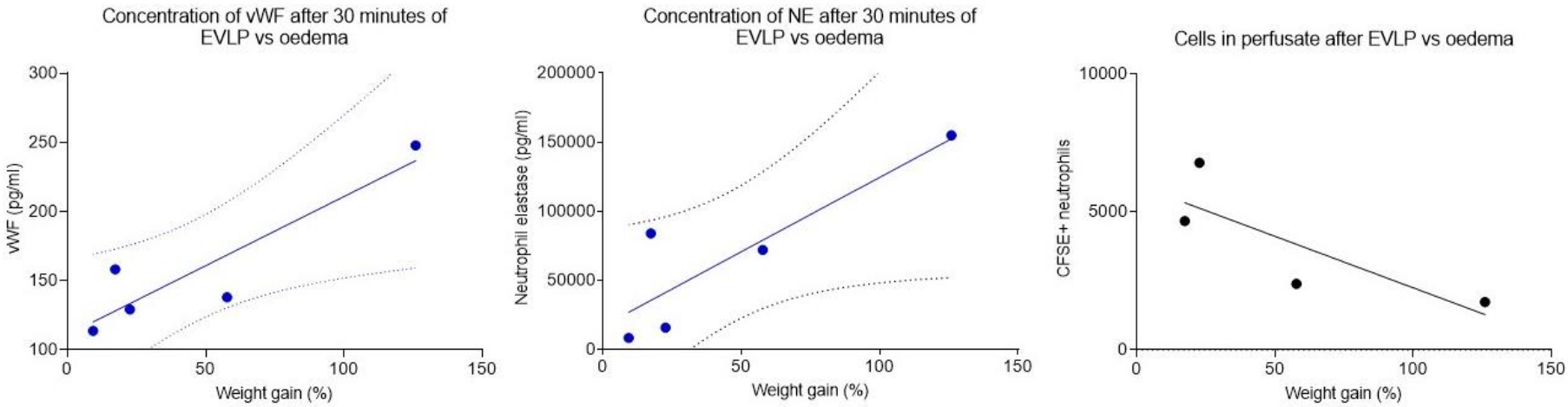

Fig. 3.6. – Weight gain correlations. Perfusates from lung pairs after 30 minutes of EVLP were measured for levels of von-Willebrand factor (vWF) and neutrophil elastase (NE). Labelled neutrophils were collected at the end of EVLP and then counted using flow cytometry. All were correlated against oedema formation in a model of linear regression, correlating positively with vWF ($R^2 = 0.81$, $p = 0.034$) and NE ($R^2 = 0.76$, $p = 0.054$) and negatively with cells in the perfusate ($R^2 = 0.65$, $p = 0.19$). N=5 for ELISA data, N=4 for cells in perfusate.

CFSE+ neutrophils can be observed in the tissue of perfused human lungs

Biopsies acquired during EVLP of a single lung were fixed in 4% PFA for 24 hours. These were then placed onto glass slides and imaged directly using a two-photon microscope to detect the presence of labelled neutrophils (green) within the tissue. Fields of view were acquired of tissue at different depths (A, B and C, respectively), shown in Fig. 3.7.

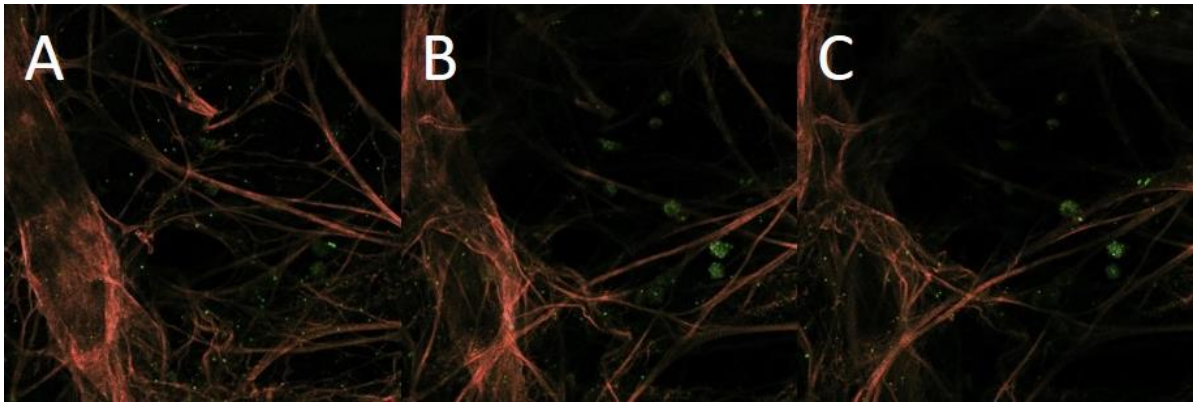

Fig. 3.7. – Different depths of PFA-fixed lung tissue with CFSE-labelled neutrophils present. Progressively deeper penetration of a PFA-fixed slice of lung tissue (A, B and C, respectively). Labelled neutrophils are visible in green.

Multi-photon images at multiple depths were also used to generate Z-stacks of neutrophils in lung tissue. Fig. 3.7 shows a 40µm thick 'slice' of lung tissue with green, CFSE+ neutrophils clearly visible within lung tissue images from donor 6.

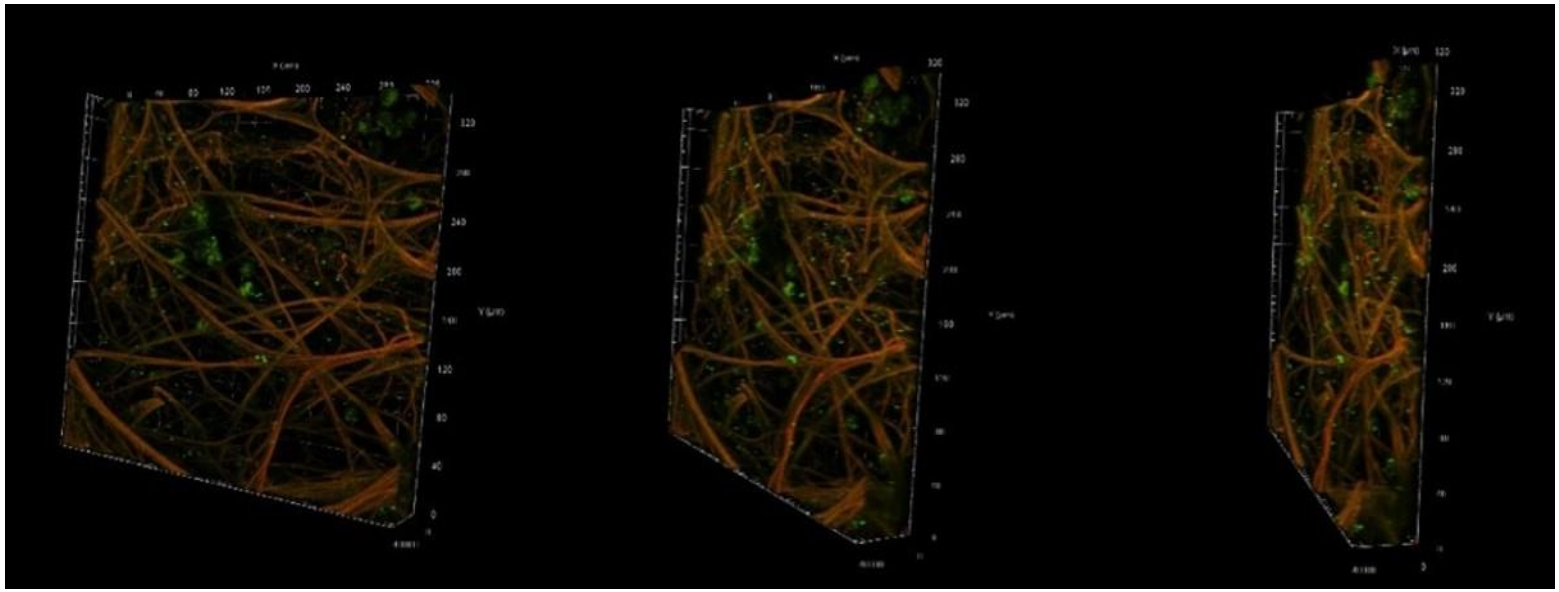

Fig. 3.8. – Rotated section of fixed lung tissue and CFSE-labelled neutrophils. 3D rotation of 40µm section of lung tissue from donor 6 – a single lung perfusion. Labelled neutrophils are visible in green.

CFSE-labelled neutrophils were measured in a split lung EVLP system

A lung pair was dissected into individual constituent lungs prior to undergoing EVLP. Individual lungs were then perfused simultaneously on separate perfusion circuits. Both were in poor condition, with only the left lung perfusing for the experimental duration of 120 minutes.

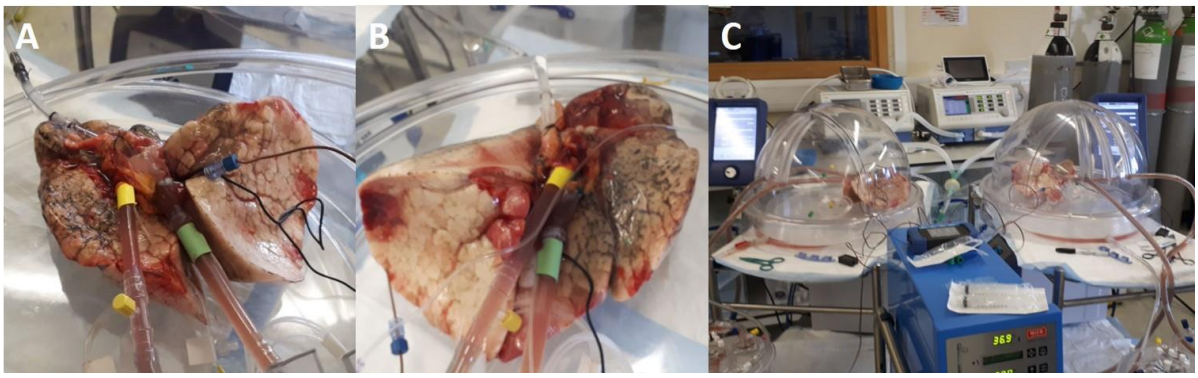

Fig. 3.9. – Paired lung perfusion model images. Lung from donor 7 were dissected and perfused simultaneously on separate EVLP circuits. Only the left lung (A) and not the right (B) received a bolus of neutrophils at 'T0.' Lungs were perfused on Medtronic circuits whilst dual-ventilated (C).

A bolus of CFSE+ neutrophils was only infused into the left lung, with perfusates then measured for cells in the same manner as previously described. No cells were observed over 120 minutes of perfusion in the lung which did not receive a bolus at the beginning of EVLP (Fig. 3.10). Fig. 3.11 shows the flow cytometry gating strategy used to quantify this, with no CFSE+ cells being observable after 30 minutes of perfusion in the right lung.

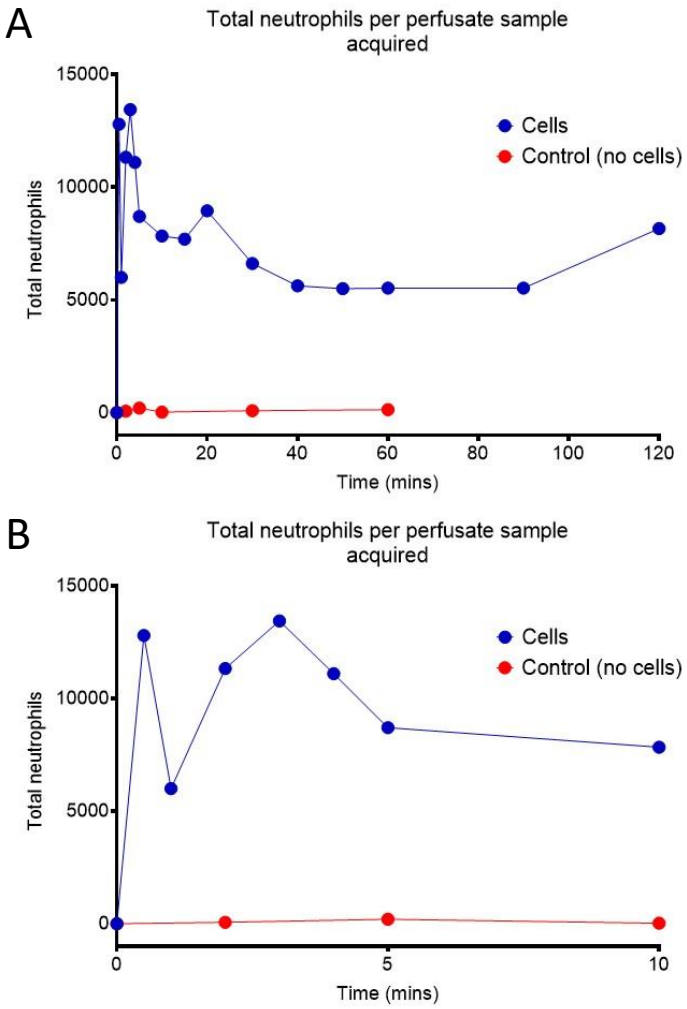

Fig. 3.10. – Neutrophil numbers for split lung perfusion. A lung pair was dissected, with individual constituent lungs then perfused on separate perfusion circuits. Only the left lung received a bolus of labelled neutrophils at 'T0.' No cells were visible during EVLP in the perfusate of the right lung for the duration of the experiment (A), with the same trend for cell numbers in perfusate visible for the left lung (B).

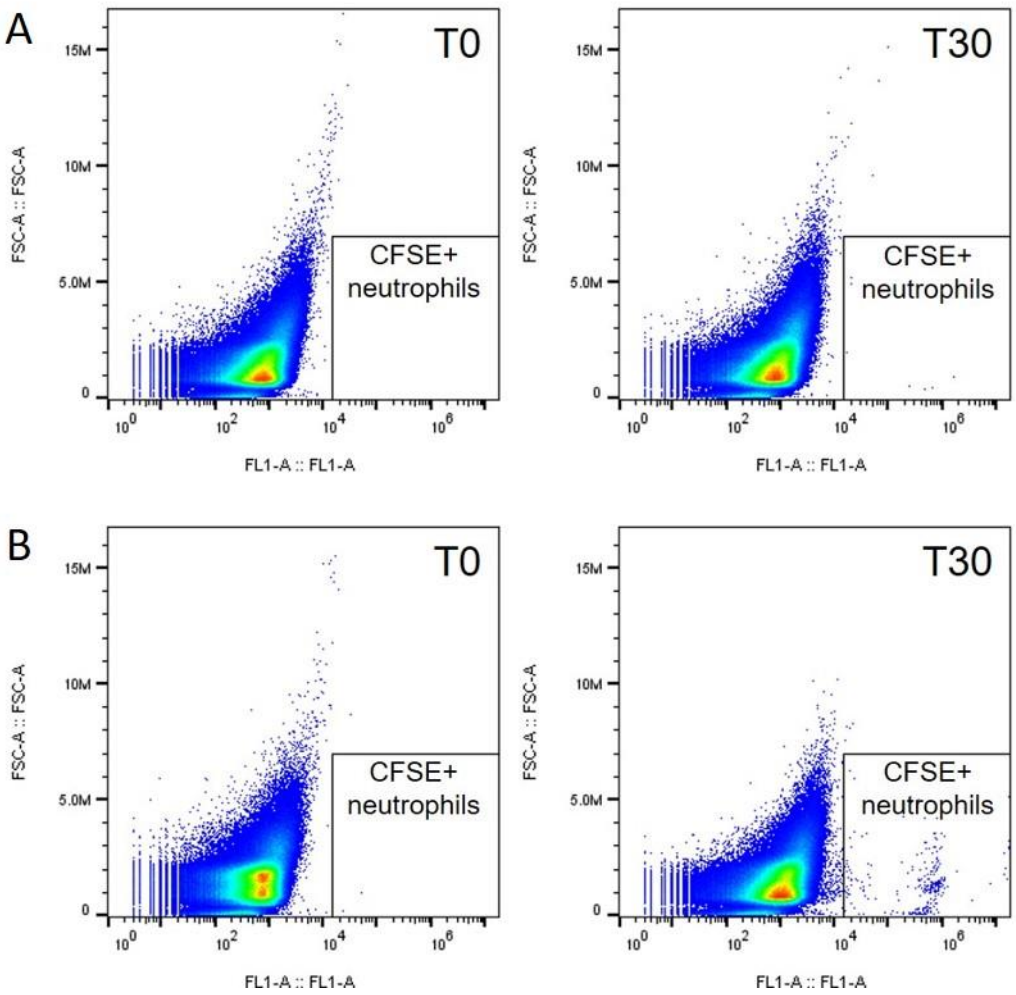

Fig. 3.11. – Flow cytometry comparisons for split lung perfusion. CFSE+ neutrophils cannot be identified at 30 minutes in the perfusate of the right lung (A), but are clearly visible in perfusate taken from the left (B) which received a bolus of neutrophils.

Discussion and concluding remarks

Discussion

EVLP offers a powerful platform to assess and recondition donor-lungs prior to transplant. Clinical and pre-clinical research has begun to identify the key mechanisms which play a role in exacerbating reperfusion injury post-transplantation, chiefly among which are the phenomena of leukocyte adhesion to the vasculature, endothelial dysfunction and an overzealous inflammatory response [76].

We aimed to develop a model whereby we could track neutrophil adherence in an *ex vivo* setting, in order to gauge whether this could be used as an output to assess donor-lung quality, rather than if the infusion had any detrimental effects on lung perfusion. We chose to isolate neutrophils, as the evidence provided understanding of IRI identifies neutrophil influx into the tissues as the key event mediating tissue disruption and is ultimately what compromises organ function. This model initially utilised EVLP of whole lung pairs before being progressed on to a human split lung model of EVLP, whereby these were dissected and perfused simultaneously, on individual perfusion circuits. We felt that simply modelling processes such as adhesion, inflammation and tissue damage on a simple, *in vitro* scale would likely limit the reliability of any observations made and fail to accurately depict the complex, multicellular environment that ultimately comprises human lung tissue.

We acquired perfusates at multiple time points following infusion of a bolus of pre-labelled human neutrophils (N=5 lung pairs). We were able to detect cells within the perfusate of these across 120 minutes of perfusion following infusion of our bolus (N=4 lung pairs). Numbers of cells varied between donor-lungs after correction for TLC. The goal of this was to ascertain neutrophil numbers rather than the infusion have any meaningful impact on lung physiology, as $1x10^7$ cells is of course an incredibly small number to infuse in the context of an entire lung pair.

All lungs followed the same dynamic trend – namely an initial spike in number, followed by a decline and then another, smaller peak, all <5 minutes following infusion. This was then followed by a general plateauing of numbers thereafter. This is likely accounted for by the natural variation in adhesion between neutrophils, i.e. some cells pass through without adhering, whereas others would likely bind as soon as making contact with lung tissue. This dynamic was variable between donor-lungs, with one explanation for this being variations in the retrieval process. Lungs are flushed upon retrieval, which aims to remove any blood and ensure there are no microthrombi remaining within the vasculature. Poor flushing would likely mean that clotting instigated by the inherently inflamed donor environment has likely blocked off vessels and resulted in poor perfusion of the lung. Variations in the degree of this phenomenon would therefore impact the number of cells detected upon the initial passes through perfused donor-lungs.

The weight of donor-lungs was measured prior to and following EVLP. These data showed an increase when plotted both as absolute values (p = 0.039) and as percentages. We chose to measure weight gain of lungs as a surrogate marker for interstitial and alveolar oedema formation. Pulmonary oedema indicates a disrupted endothelial layer within the vasculature of tissue and is indicative of a form of acute lung injury (ALI). Weight gain was highly variable between donor-lungs, indicating differences in the relative levels of tissue injury between donors.

When we used the values for percentage weight gain in a model of linear regression with vWF concentration at 120 minutes, we saw a significant correlation between the two of these (R^2 = 0.82, p = 0.034). We chose to measure vWF as it is a reliable marker of endothelial dysfunction, particularly in the context of pulmonary disease [91, 125]. These data indicate that oedema formation during EVLP was intrinsically linked to the degree of endothelial activation of these lungs. This correlation was also true for NE, though was not statistically significant (R^2 = 0.76, p = 0.054). NE is expressed by macrophages and neutrophils and excessive levels have been linked to respiratory diseases such as emphysema [126]. Our data shows that higher levels of endothelial and neutrophil activation correlate with oedema formation during EVLP, linking inflammation with an increase in damage to the tissues. We do not feel that our cohort size offers the possibility to perform comparative analysis of weight gain with donor characteristics, such as manner of donation or age etc. However, a larger cohort would provide a good means of doing this and thus, elucidating the effect of previous donor-lung injury on weight gain over the course of EVLP.

Weight gain also correlated negatively with cell numbers remaining in the perfusate following EVLP. Our explanation for this is that this higher degree of endothelial cell activation resulted in overexpression of adhesion markers, binding labelled neutrophils and resulting in fewer ‘free’ neutrophils in the perfusate. This logically would mean that more neutrophils have become adhered to or trapped within the vasculature, explaining the lower levels observed from flow cytometry. Additional fluid leaving the vasculature would facilitate higher numbers of cells to subsequently exit circulation. We accept that these observations should not be taken as read due to the low cohort size. However, we feel that these data complement each other and offer confidence in the robustness of our model taken forward.

Samples of tissue from our lungs were assessed for CFSE+ neutrophils within the tissue by multi-photon microscopy, in order to confirm that neutrophil adhesion to lung tissue had occurred. This was chosen as the technique allows penetration of solid biological material up to a depth of 1mm. We used this to identify neutrophils present within the tissue, supporting our theory that they had migrated into the tissue during EVLP. This data shows that neutrophils from our bolus have migrated into the

tissues of our lungs and offers confidence in our hypothesis as to reductions in cell numbers observed in the perfusates.

We have shown here that it is possible to use a split lung model of perfusion, whereby lung pairs are dissected into individual lungs and then perfused on separate circuits simultaneously. The concept of this was to allow lungs to be compared in real-time, whilst also controlling for inter-donor differences between lungs from. We infused neutrophils into one lung and acquired perfusates from both. As expected, CFSE+ neutrophils were not detectable in the perfusates of the lung, which did not receive a bolus of cells, giving confidence that the observations made previously were due to the bolus infused at the beginning of EVLP.

Taking this model forward, we feel that it offers a powerful, real-time testing platform for interventions and/or therapeutics. There are of course a number of examples utilising research models of EVLP, with small animal, porcine and human lungs. We feel however, that one criticism of this is failure to account for the natural variation in physiology and immunology between individuals. By adopting a method by which donor-lungs are dissected and then perfused simultaneously, these variations are controlled for. This fact is highlighted by the natural variations we saw in weight gain between our lung pair perfusions. Our model would enable paired comparisons and enable the researcher to directly compare and contrast lungs from the same donor with exposure of one lung to a treatment of interest. To our knowledge, no other pre-clinical model thus far has employed this system.

One weakness of our approach is that it does not reliably inform as to the fate of the donor neutrophils, in so far as whether these have adhered to the endothelial surface or undergone pyroptosis; a phenomenon readily done so by neutrophils during inflammation. It would be interesting to measure collected perfusate samples for the presence of pyroptosis activation-associated markers, such as high mobility group box protein-1 (HMGB-1), or to sort out labelled neutrophils and characterise receptor expression to provide insight as to the likeliness of aberrant cell death or activation.

Another interesting idea would have been to infuse peripheral blood mononuclear cells (PBMCs) rather than merely neutrophils. A large proportion of tissue damage is mediated by neutrophil infusion into the tissue, hence our interest in isolating this specific cell population. However, reperfusion injury is characterised by widespread cellular activation, including other granulocytes, monocytes and T cells. Therefore, it would have been interesting to observe the additional effects of infusing this population of cells, particularly with regard to their impact on the neutrophils, as well as bypassing some of the laboratory issues associated with neutrophil isolation.

Linking to this, it would have been interesting to examine sections of our perfusion circuit for the presence of labelled neutrophils. These are of course, a notoriously adherent, 'sticky' cell type to work with *in vitro*, so it would be unsurprising to see evidence of neutrophils on the surface of circuit tubing or trapped in parts of the oxygenator. The possibility of this occurring is of course a bias, but we feel it is a bias that is applied to all of the perfusions in our cohort. We also feel that the donor-donor variation of neutrophil activation will be controlled for in our proposed split EVLP system, as both the control and 'intervention' lung would be affected equally.

Another aspect of this model to be considered is the usage of neutrophils from non-human leukocyte antigen (HLA)-matched donors. HLA alloreactivity is of immense concern with regard to clinical practice, for example when administering blood transfusions, due to inappropriate activation of the host immune system. Due to complications with the logistics of the system, it was not possible to match this for our model. Therefore, it is therefore entirely plausible that this mechanism of activation has elicited a response from both donor neutrophils and host tissue.

Concluding remarks

We feel that the system developed here, namely a model of neutrophil adhesion coupled to a split lung system of EVLP, provides an exciting means of pre-clinical research. Modelling the effects of therapeutics and/or interventions in an *ex vivo* setting offers a much more rounded and informative system than doing so in simple *in vitro* assay formats. This work can be taken forward to provide information regarding neutrophil adhesion, endothelial dysfunction, and the relationship between these two phenomena. Moreover, coupling these observations to other aspects of EVLP such as oedema formation will enable a picture to be painted of what is a complex, multicellular environment.

CHAPTER 4

-

MODELLING THE FUNCTIONAL EFFECTS OF INTERLEUKIN-1β-MEDIATED INFLAMMATION USING EX VIVO LUNG PERFUSION

Chapter 4 – Modelling the functional effects of interleukin-1β-mediated inflammation using ex vivo lung perfusion

Introduction

One potential means of expanding the lung donor pool is through use of ex vivo lung perfusion (EVLP). This was pioneered in 2001 by Steen et al who used it to assess a single lung prior to transplantation of a 54-year old woman with COPD. Excellent function was observed immediately following reperfusion, with the 5-month follow-up also continuing to demonstrate good function in the recipient [25]. Following this early use, the emphasis of EVLP has shifted to reconditioning lungs initially deemed unsuitable for transplant, with the same group reporting this for the first time in 2007 [26]. As of 2020, two devices have achieved FDA approval for clinical use and a number of trials have been conducted; highlighting EVLP as an exciting means to safely enhance worldwide lung transplant activity.

Mitigating the early phenomena that dominate reperfusion-based injury of the lungs is of utmost importance when expanding the donor pool using technologies such as EVLP. Reperfusion injury is characterised by endothelial dysfunction, leukocyte infiltration into the graft, widespread release of reactive oxygen species (ROS) and production of pro-inflammatory cytokines. Numerous *ex vivo* models highlight the importance of the neutrophil influx in mediating this damage and in many cases, subsequent development of primary graft dysfunction (PGD) [95, 127]. Other biomarker-based studies have highlighted the relationship between neutrophilic proteins and molecules with the severity of PGD [128]. Neutrophils undoubtedly play an indispensable role in mediating tissue damage and disruption post-transplant.

The pro-inflammatory cytokine IL-1β has a number of well-established effects on mediating inflammation and apoptosis within the context of lung injury in general [129]. In a rat model of ischaemia utilised by Krishnadasan et al, IL-1β was associated with higher levels of tissue damage. Blockade of the cytokine resulted in lower production of gene transcripts associated with inflammatory processes [130]. Another study used gene-set enrichment analysis (GSEA) to assess the transcriptomic profile of bronchoalveolar lavage fluid (BALF) in PGD patients' vs healthy controls. Pathways associated with IL-1β and inflammasome signalling were significantly up regulated in individuals with PGD [110]. Undoubtedly, this cytokine plays a key role in mediating and coordinating inflammation post-lung transplantation.

Study background

Newcastle University led a UK multi-centre trial between January 2012 and October 2015; DEVELOP-UK, which aimed to establish the clinical- and cost-effectiveness of EVLP in increasing lung transplant activity. As part of this trial, a total of 53 EVLPs were run with 18 lungs proceeding to transplant [62]. As part of a wider research effort, analysis of EVLP perfusates was undertaken in order to better understand the mechanisms behind successful transplant outcome.

Fig. 4.1 shows how IL-1β level in the perfusate measured after 30 minutes of perfusion was able to stratify lungs into one of three groups. 'Declined' represents lungs perfused and not transplanted, 'non-survival' represents recipients of a lung that did not survive for a year and 'survival' represents recipients of a lung that survived for a year or more post-transplant [118]. IL-1β was able to differentiate between the latter two groups with a sensitivity and specificity of 100%, indicating enormous potential for use as a therapeutic biomarker but perhaps more significantly; representing a potential therapeutic target for modulation prior to transplantation.

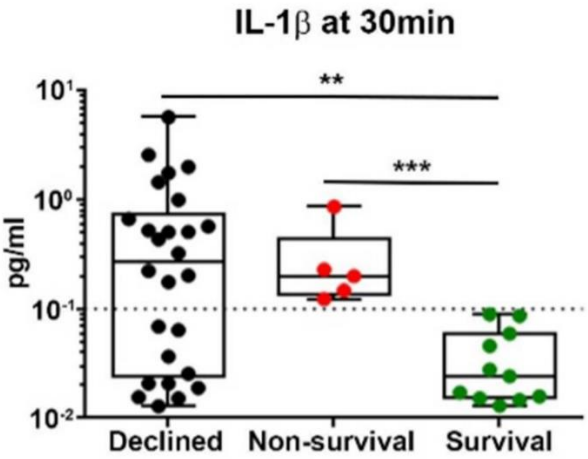

Fig 4.1 – IL-1β level relationship with 1-year patient survival. 53 EVLPs were performed as part of the DEVELOP-UK trial. Perfusate samples taken after 30 minutes of perfusion were measured for levels of IL-1β. This cytokine was able to stratify between lungs declined for transplant following EVLP 'declined,' recipients that did not survive for 1 year 'non-survival,' and recipients that survived for a year or more 'survival.' The sensitivity and specificity of IL-1β for differentiating between 1-year survival was 100% [118].

The effects of IL-1β were then further interrogated and shown to prime the endothelium more effectively for adhesion marker expression and neutrophil adhesion *in vitro* [118]. Thus, higher levels of IL-1β in lung perfusate likely facilitate an increase in recipient leukocyte adhesion and extravasation into the newly engrafted lung tissue during reperfusion. This culminates in further damage to the graft which risks loss of the graft if not addressed.

This forms the basis of the work produced here. We aimed to establish an *ex vivo* model of reperfusion injury and use this to interrogate the actions of IL-1β on neutrophil adhesion, as well as use a number of other outputs to assess any effects on lung function and viability. Finally, samples taken from lungs were analysed for levels of pro-inflammatory markers and used in a range of *in vitro* assays to assess impact of IL-1β on pulmonary endothelial cells. The pathways assessed by this work are shown in Fig. 4.2.

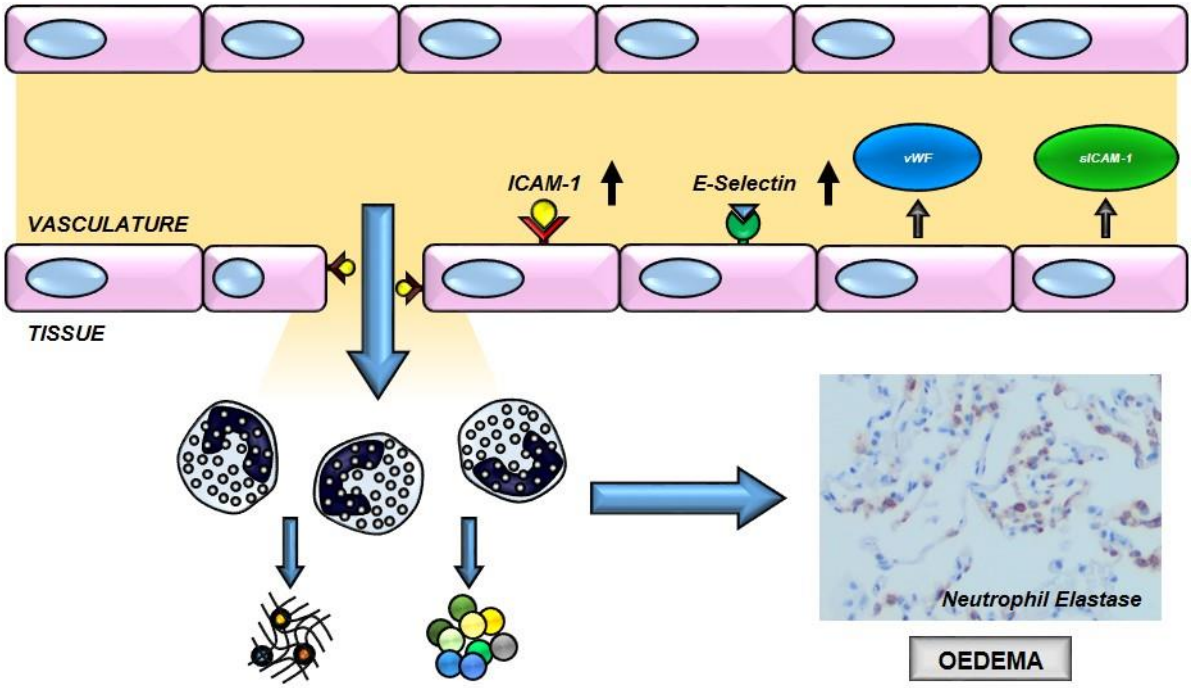

Fig. 4.2 – Predicted pathways of IL-1β activity in perfusion model – Based on the previous findings of Andreasson et al (2017); the *in vitro* functions of IL-1β have been well established. I propose that IL-1β will enhance the endothelial dysfunction, facilitate greater leukocyte trapping within the lung tissues and provoke increased oedema formation due to the disrupted vascular barriers.

Hypothesis and aims

Hypothesis

Hypothesis

We hypothesised that our model shows enhanced neutrophil trapping within lungs stimulated with IL-1β. Moreover, these lungs will display higher levels of endothelial dysfunction, which will reflect an ability to facilitate greater cell activation when samples from these lungs are used in *in vitro* assay formats.

Aims

1) Assess impact of IL-1β on neutrophil trapping and lung physiology using model developed in Chapter 3
2) Assess impact of IL-1β on pulmonary endothelial dysfunction

In order to achieve these aims, this work will consist of the following objectives: -

1) Measure neutrophil numbers in the perfusate in response to infusion of IL-1β *ex vivo*
2) Weigh lungs before and after EVLP to assess oedema formation and correlate this with markers of endothelial dysfunction
3) Use flow-based adhesion and flow cytometry to measure differences in ability of control and stimulated perfusates to stimulate endothelial dysfunction *in vitro*

Methods

Study outline

In order to ensure that neutrophil tracking could be successfully implemented in an *ex vivo* setting, the initial pilot study utilised EVLP of whole lung pairs. The in-depth results of this can be viewed in Chapter 4. Once the output of neutrophil adhesion was established, this was then taken forward and used to develop a system by which IL-1β stimulation of lungs during EVLP could be directly compared to an unstimulated control. This model is shown in Fig. 4.3. 4 lung pairs declined for transplantation were accepted through generic or specific consent pathways under NHS-BT Study 66 and then transported on ice to the Newcastle perfusion lab based at the NHS Blood Donor Centre at Barrack Road, Newcastle upon Tyne. These were then dissected into individual lungs and perfused separately and simultaneously, with one lung from each pair infused with a bolus of IL-1β prior to the infusion of labelled neutrophils and subsequent quantification of data. This experimental design allowed us to control for inter-donor differences between lungs.

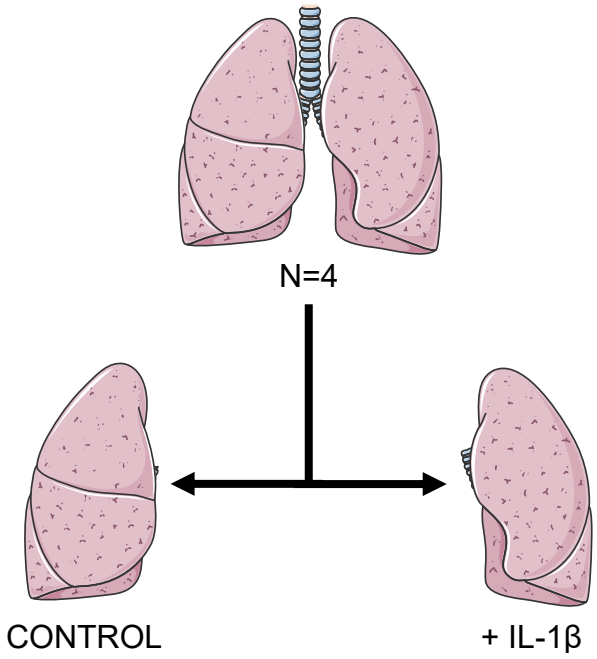

Fig. 4.3 – Study design for split lung model of IL-1β assessment – Lung pairs are split and perfused simultaneously on separate perfusion circuits. This allows for real-time, direct comparison of an intervention with a control lung. Figure created using Servier Medical art.

Set-up and perfusion

The EVLP circuits were prepared as detailed in the methods. Briefly, 2L of Steen solution circulated at 20% of cardiac output, as calculated using the ideal bodyweight formula detailed previously. The left and right lung PAs were attached in separate perfusion circuits before the flow rate was gradually

increased to 40% cardiac output (CO) over 20 minutes of perfusion. Once both lungs had reached 32°C, the airways were attached to the ventilator tubing through use of a custom-built Y-connector and then ventilation commenced. A perfusate temperature of 37°C was reached and maintained for 15 minutes before IL-1β infusion. Prior to and throughout 3 hours of EVLP, regular blood gas measurements were done to ensure that pH remained in a normal range for perfused lungs.

IL-1β addition

Sufficient human, recombinant IL-1β to achieve a 'free circuit' concentration of 1ng/ml (for 1.5L of perfusate use 1500ul of 1ng/µl IL-1β) was made up into 5ml of sterile Steen solution. This was infused as a bolus into the arterial line of the perfusion circuits at 'T-60m,' with the other receiving no IL-1β to act as a control. A sample of perfusate from the circuit was acquired and stored on ice immediately prior to infusion of the IL-1β as 'T-60m.' Further perfusate samples were acquired at '-30m,' and '-15m.'

Neutrophil tracking

Human neutrophils were isolated from whole blood of healthy volunteers and then labelled with CFSE. $4x10^7$ labelled cells were simultaneously infused into each perfusion circuit gradually over 1 minute through the arterial inlet line in the perfusion circuits. This was done by attaching the syringe of neutrophils and drawing up a small amount of perfusate before then infusing into the circuit, to ensure no air was pushed into the perfusate entering the lungs. Infusion took place at 'T0,' exactly 60 minutes after infusion of IL-1β into the circuit. Perfusates were acquired at the following time points following neutrophil infusion as detailed below (minutes):

- 0, 0.5, 1, 2, 3, 4, 5, 10, 15, 20, 30, 40, 50, 60, 90, 120

Following EVLP, the pump was shut off and donor-lungs were completely detached from the perfusion circuit. A leukocyte filter (Haemonetics) was attached to the PA and PV, with the pump then switched back on after this and left for 5 minutes. Filters were then washed anterograde to clear remaining red cells before a series of retrograde washes were performed to remove any captured leukocytes.

Weight gain

Weight gain was chosen as a surrogate marker for oedema formation. Lungs were weighed before and after perfusion and then this was plotted both as a percentage and absolute increase.

Lactate level and partial pressure of CO_2

Blood gas measurements were taken of perfusate samples during EVLP with CG4+ cartridges.

Enzyme-linked immunosorbent assay

Perfusate samples acquired at regular time points were measured for levels of soluble ICAM-1 (sICAM-1) and von-Willebrand factor (vWF) using a commercially available enzyme-linked immunosorbent assay (ELISA) for each biomarker (R&D Systems). These were prepared and then carried out according to the manufacturer's instructions. Concentration was normalised to total lung capacity (TLC) and then plotted against values for percentage weight gain from each lung.

IL-1β MSD perfusate analysis

IL-1β U-plex plates were prepared for the work according to the manufacturer's instructions. Perfusates and standards were diluted with diluent buffer in a 1:1 ratio. Final values were adjusted to total lung capacity (TLC).

Adhesion of neutrophils to pulmonary endothelial cells

Adhesion of human neutrophils to pulmonary endothelium was quantified using the Cellix© platform. Experiments were performed using human pulmonary microvascular endothelial cells (HPMECs). These were seeded onto chips, left to adhere for 20 minutes and then stimulated with neat perfusates collected from EVLPs performed as part of this study. The 120-minute time point was chosen, as this achieved the highest difference in circulating numbers between control and IL-1β-stimulated EVLPs (shown in Table 4.3). For blocking experiments, perfusates were pre-incubated for 30 minutes with an IL-1β neutralising antibody (NAb) (R&D Systems) at 4µg/ml before endothelial stimulation.

Neutrophils were isolated from blood of healthy volunteers using a Miltenyi Biotec MACSxpress® kit, chosen due to the kit negatively selecting out neutrophils from whole blood. These were then labelled with CFSE as previously outlined in Chapter 2 and re-suspended to a final density of $1x10^6$cells/ml. These were then flown over the confluent endothelial cells for 3.5 minutes, after which images were taken at 5 different fields of view for each channel. DucoCell counting software (Cellix) was then used to distinguish between neutrophils adhered to the endothelium and those under flow. An average for each channel was calculated and results were plotted using Prism 8 (GraphPad). Channels with media and media with IL-1β at 1ng/ml (Peprotech) were used as negative and positive controls, respectively.

Flow cytometry

Counting of labelled neutrophils in perfusate

Perfusates were analysed for cell numbers on the Accuri™ flow cytometer as detailed previously. Numbers were then adjusted according to total lung capacity (TLC). This is a calculation which takes into account the relative size of lungs and normalises these to enable direct comparison between donors All results were plotted using Prism 8 (GraphPad©).

Activation of pulmonary endothelial cells in vitro

This was performed as outlined in the general methods section. Briefly, HPMECs were seeded onto 12-well plates and left to adhere overnight. These cells were then incubated with EVLP perfusates from stimulated/unstimulated lungs for 4 hours. The 120-minute time point was chosen for this, as this achieved the highest difference in circulating numbers *ex vivo* between control and IL-1β-stimulated EVLPs. Cells were then removed with Accutase, washed and stained for ICAM-1 (PE), VCAM-1 (PE-Cy7) and E-Selectin (FITC) and CD31 (APC). Results were obtained using a FACS Canto II and then analysed using FlowJo software (both Becton Dickinson).

Statistical analysis

All data shown was organised using Excel software. Graphs were plotted and statistical tests were performed using Prism 8 (GraphPad).

Results

Lung donor and perfusion characteristics

Lungs declined for transplantation were enrolled in NHS-BT RINTAG-approved Study 66 entitled 'Further Evaluation of Ex Vivo Lung Perfusion to Improve Transplantation Outcomes' with REC approval number 16/NE/0230. This occurred through both generic and specific consent pathways, with the latter of these referring to hospital trusts within the North East of England. Table 4.1 highlights key donor information. Lungs used for this study were declined on the basis of poor function or bi-lateral consolidation prior to retrieval. Table 4.2 shows the ischaemic times and weight gain.

Perfusion	Donor age	Sex	Bodyweight (kg)	Height (cm)	Donation	Reason for decline
Donor 1	56	Female	80	165	DBD	Inspection
Donor 2	22	Male	65	180	DCD	Inspection
Donor 3	59	Male	95	171	DBD	Poor function
Donor 4	47	Female	50	171	DBD	Poor function

Table 4.1 – Donor data for lungs used in the split lung model

DCD – Deceased from circulatory death; DBD – Deceased from brain death

Perfusion	CIT (h, min)	+ IL-1β? (Y/N)	Weight pre	Weight post
Donor 1	10, 30	N	593.5	1040
Donor 1	10, 30	Y	408	1064.5
Donor 2	13, 40	N	666.5	1064.5
Donor 2	13, 40	Y	846	1769.5
Donor 3	17, 10	N	424.5	1059
Donor 3	17, 10	Y	557.5	1295
Donor 4	4, 37	N	366	467
Donor 4	4, 37	Y	484.5	923.5

Table 4.2 – Perfusion data for lungs used in the split lung model

H/min – Hours/minutes; CIT – cold ischaemic time; Y/N – Yes/No

Ex vivo-based assays

Circulating numbers of neutrophils *ex vivo* are lower in perfusates of lungs stimulated with IL-1β

Lung pairs declined for transplant were dissected into individual lungs and perfused simultaneously on separate EVLP circuits (N=4). Perfusate samples acquired over 120 minutes of perfusion were quantified for CFSE+ neutrophils via flow cytometry. Remaining perfusate at the end of perfusion was filtered for CFSE+ cells with a leukocyte filter, once lungs had been detached, and samples were analysed in the same way. Consistently lower numbers of circulating neutrophils are observed in lungs stimulated with IL-1β, which achieved significance at a number of time points, shown in Table 4.3 (paired t-test). This trend was apparent after 5 minutes following neutrophil addition in the EVLP circuits. Significantly fewer cells were observed in the perfusate of stimulated lungs following EVLP (p = 0.042).

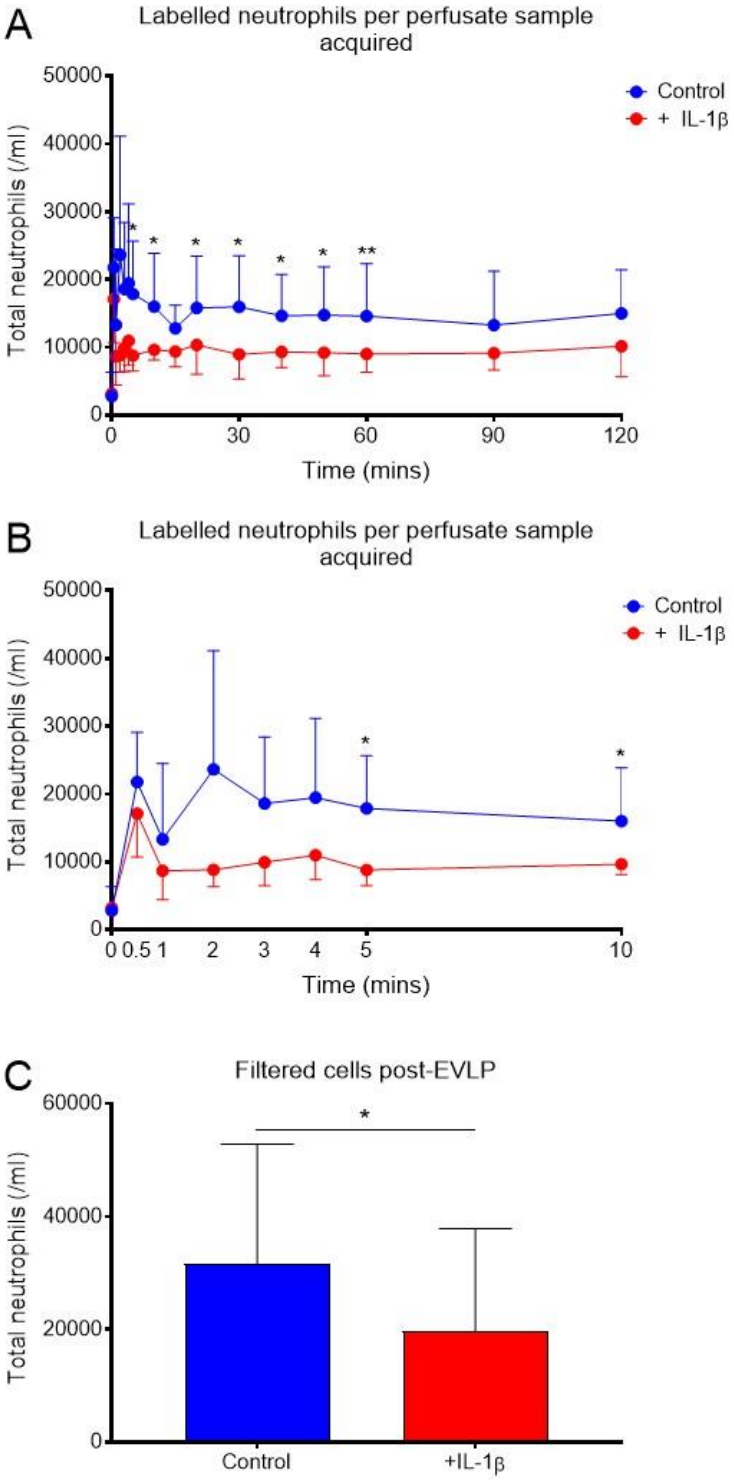

Fig. 4.4 – Labelled neutrophils in perfusate samples – Whole lungs were dissected and split into individual lungs and perfused *ex vivo*, with control (N=4) and IL-1β-stimulated (N=4). CFSE-labelled neutrophils were infused as a bolus into at 'T0,' with regular perfusate samples acquired and then analysed for FITC+ events via an Accuri™ C6 flow cytometer. Cell numbers were normalised to total lung capacity (TLC) and then plotted using Prism 8 software. These numbers are presented as total time (A) and the initial 10 minutes following cell infusion (B).

This achieved statistical significance at several time points (paired t-test). Upon completion of perfusion, lungs were detached and any remaining 'free' perfusate was filtered for labelled leukocytes before being measured for cells in the same way (C). Fewer cells remained within the perfusate as unbound cells upon completion of perfusion in IL-1β-stimulated lungs (p = 0.042). N=4.

Time (mins)	*p* value	
0.5	0.93	
1	0.37	
2	0.081	
3	0.14	
4	0.29	
5	0.013	*
10	0.018	*
15	0.012	*
20	0.28	
30	0.017	*
40	0.03	*
50	0.027	*
60	0.0036	**
90	0.58	
120	0.63	

Table 4.3 – Calculated p values for differences in circulating number between treated and untreated lung perfusions – Significance values were calculated using paired t-tests. N=4.

IL-1β stimulation facilitates greater weight gain of lungs *ex vivo*

Lungs pairs were dissected, cannulated and then weighed prior to commencing EVLP. After 180 minutes of perfusion, they were detached from the circuit and weighed again. Lungs from each pair that were stimulated with IL-1β showed a greater degree of weight gain over the course of EVLP presented as both a percentage change (p = 0.065) (A) and absolute increase (p = 0.046) (B) (paired t-test). N=4.

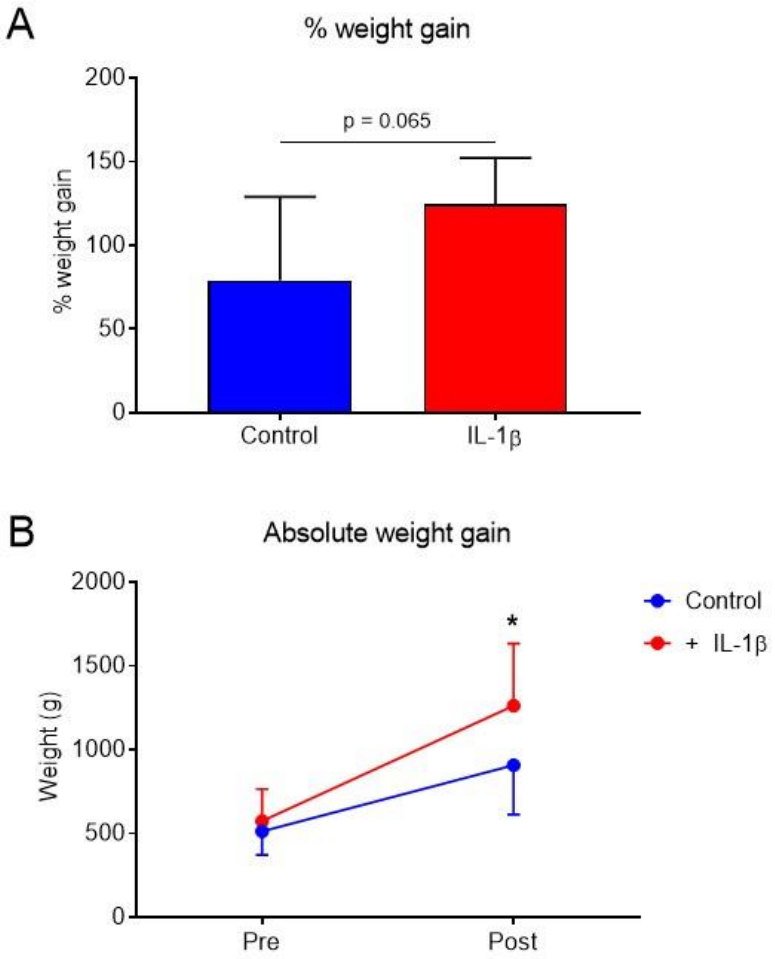

Fig. 4.5 – Oedema formation as measured by weight gain of perfused single lungs – Whole lungs were dissected and split into individual lungs and perfused *ex vivo*, with control and IL-1β-stimulated. Lung weight was measured both pre-and post-perfusion and is presented as both absolute weight gain (A) and percentage weight gain (B). Lungs stimulated with IL-1β gained more weight than control lungs when shown as both a percentage increase (p = 0.065) and absolute value (p = 0.046). N=4.

Lactate level and partial pressure of CO_2 are altered by infusion of IL-1β

Regular perfusate samples were acquired over the course of 180 minutes of EVLP. These were plotted in control and IL-1β groups. Lactate level increased in all lungs during perfusion, with this increase more noticeable in the lungs receiving a bolus of IL-1β. Partial pressure of CO_2 was consistently higher in stimulated lungs. Neither of these trends reached statistical significance. N=4.

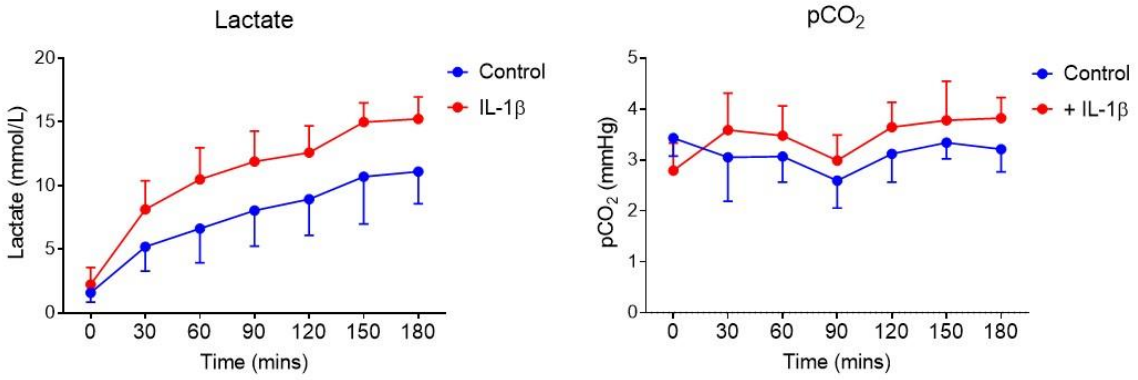

Fig. 4.6 – Lactate level and pCO_2 during EVLP – Lactate level and pCO_2 were measured during EVLP at regular time points. Lactate increased in all lungs during perfusion, with this increase greater in stimulated lungs. PCO2 was seen to be generally higher in stimulated lungs throughout EVLP. N=4.

Levels of endothelial activation markers correlate with weight gain *ex vivo*

In order to assess the relationship between endothelial activation and oedema formation *ex vivo*, perfusates acquired after 120 minutes of EVLP were measured for levels of sICAM-1 and vWF using standard ELISAs (R&D Systems). Final concentrations were normalised to TLC (pg/ml) and then compared against percentage weight gain in a linear regression model. Oedema, as illustrated by weight gain, correlated significantly with sICAM-1 ($R^2 = 0.71$, $p = 0.0043$) and vWF ($R^2 = 0.39$, $p = 0.04$).

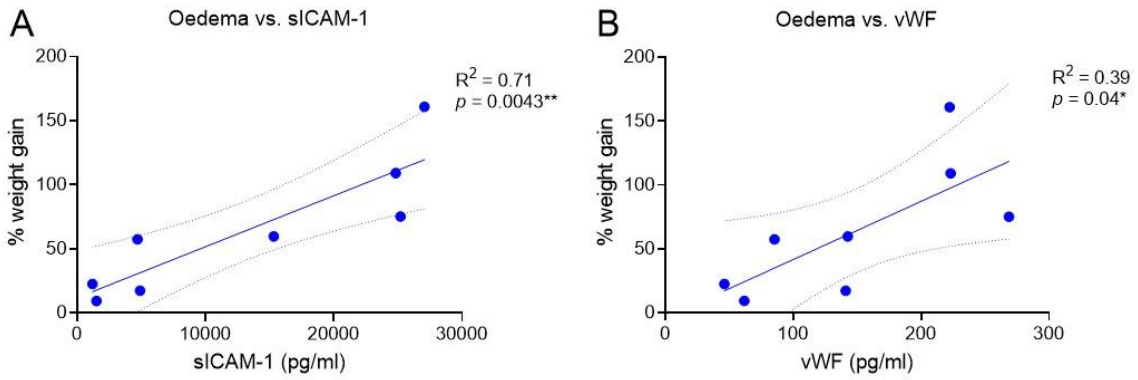

Fig. 4.7 – Levels of sICAM-1 and vWF correlate with % weight gain of lungs perfused *ex vivo* – Concentration of sICAM-1 and vWF were measured in perfusate samples taken after 120 minutes of EVLP and then adjusted to TLC (pg/ml). A linear regression model was then used to model the relationship between concentration and oedema formation *ex vivo*. Weight gain (%) correlated significantly with (A) sICAM-1 ($R^2 = 0.71$, $p = 0.0043$) and (B) vWF ($R^2 = 0.39$, $p = 0.04$) highlighting the relationship between oedema and endothelial cell activation. N=4.

IL-1β concentration varies in perfused split lungs

Lung pairs dissected and perfused separately from each split perfusion were measured for levels of IL-1β using a single-plex cytokine assay (Mesoscale Discovery). Lungs infused with IL-1β exhibited significantly greater perfusate concentrations of the cytokine as expected, with this trend consistent immediately after infusion ($p = 0.016$), 30 minutes after infusion ($p = 0.0152$) and 60 minutes after infusion ($p = 0.016$).

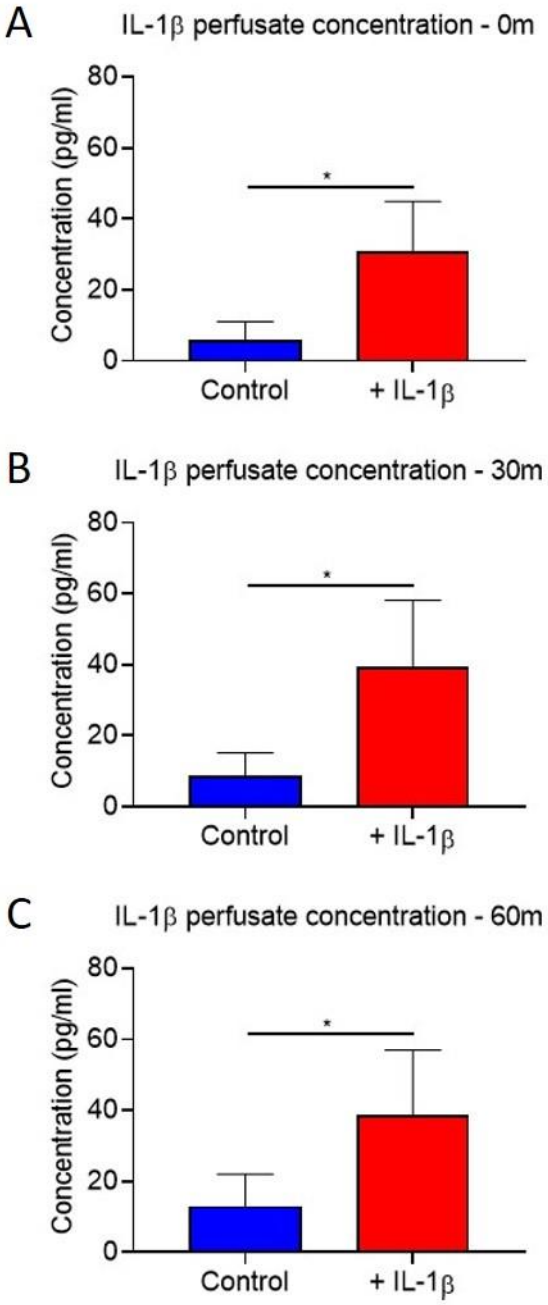

Fig. 4.8 – Perfusate concentrations of control and IL-1β-stimulated lungs – Whole lungs were dissected and split into individual lungs and perfused *ex vivo*, with control and IL-1β-stimulated cohorts perfused simultaneously. Perfusate samples acquired at regular time points were measured for levels of IL-1β using an MSD cytokine assay (Mesoscale Discovery©). Immediately following infusion (p = 0.016) (A), 30 minutes (p = 0.0152) (B) and 60 minutes (p = 0.016) (C) concentrations were significantly different between control and stimulated groups (ratio paired t-test). N=4.

In vitro-based activation assays

Perfusates from lungs stimulated with IL-1β confer greater neutrophil adhesion to conditioned endothelial cells

Lung pairs were dissected into individual lungs and then perfused separately in a split EVLP model. Perfusates taken at 120 minutes were used to stimulate HPMECs pre-coated onto specialised microfluidic chambers *in vitro* for 4 hours. Primary human neutrophils were isolated from the blood of healthy volunteers, labelled with CFSE and adhesion to stimulated HPMECs was assessed under flow. Perfusates from stimulated lungs (N=4) conferred greater adhesion of neutrophils to endothelium *in vitro* (A). When all perfusates (N=8) were pre-incubated with an IL-1β NAb at 4μg/ml for 30 minutes, this significantly down-regulated adhesion in this assay (p = 0.025).

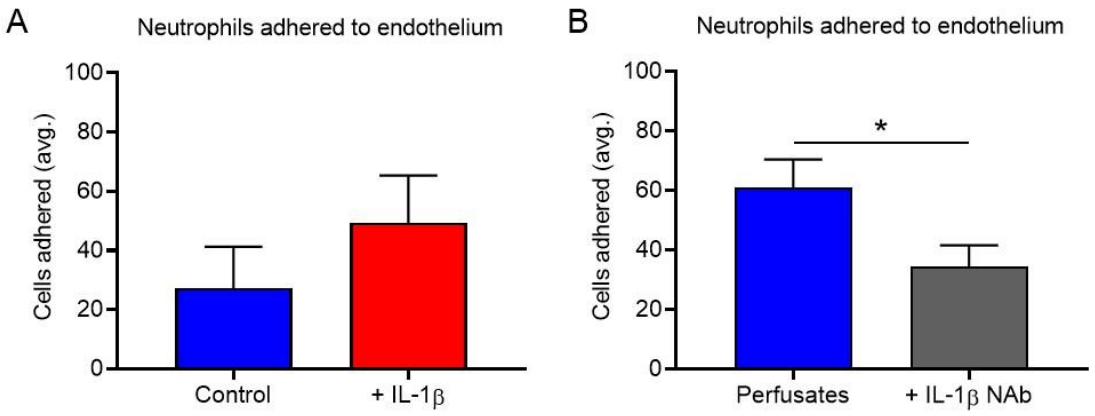

Fig. 4.9 – Adhesion of labelled neutrophils to perfusate-conditioned endothelial cells. Perfusates taken from IL-1β-stimulated lungs (N=4) were compared to control lung perfusates (N=4) for their ability to facilitate neutrophil adhesion to conditioned pulmonary endothelial cells *in vitro* (A). Samples used from IL-1β-stimulated lungs conferred a greater degree of adhesion onto endothelial cells. When all perfusates (N=8) were pre-incubated for 30 minutes with an IL-1β neutralizing antibody (NAb) (B), this reduced adhesion significantly (p = 0.025). Stimulated vs. unstimulated experiments n=2 repeats. Blocking experiments were n=1 repeats.

Adhesion marker expression of conditioned endothelial cells *in vitro*

Lung pairs were dissected into individual lungs and then perfused separately in a split EVLP model. Perfusates taken at 120 minutes were used to stimulate HPMECs pre-coated onto 24-well plates *in vitro* for 4 hours. Once stimulation was completed, HPMECs were stained for E-Selectin, ICAM-1 and VCAM-1 and expression was analysed via flow cytometry using a FACS Canto II (BD Biosciences). Perfusates from IL-1β-stimulated lungs (N=4) provoked a greater up-regulation of E-Selectin (p = 0.038), ICAM-1 (p = 0.071) and VCAM-1 (p = 0.069) than control lungs (N=4) (A) (paired t-test). When all perfusates (N=8) were pre-incubated with an IL-1β Nab at 4µg/ml for 30 minutes, this down-regulated expression of all three markers (B). MFI is higher in 'perfusates' for group B, as this represents the combined values for all perfusates (N=8) rather than the unstimulated group (N=4).

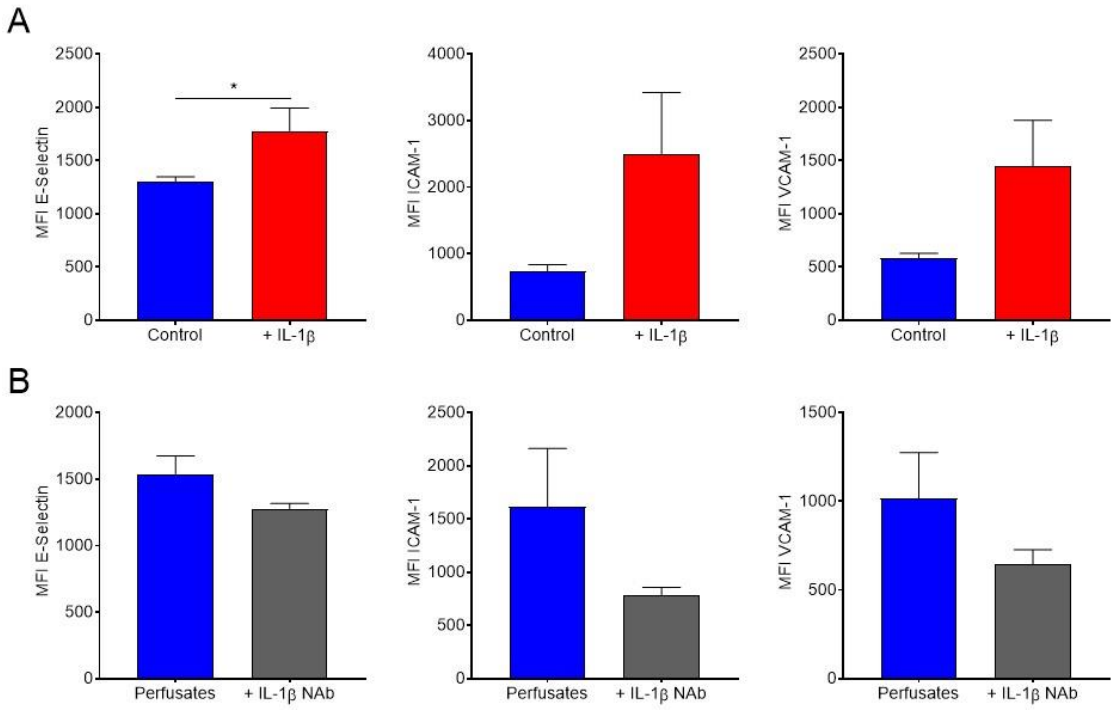

Fig. 4.10 – Expression of adhesion markers on perfusate-conditioned endothelial cells. Perfusates taken from IL-1β-stimulated lungs (N=4) were compared to control lung perfusates (N=4) for their ability to provoke expression of three different adhesion markers (A). 1. E-Selectin (p = 0.038), ICAM-1 (p = 0.071) and VCAM-1 (p = 0.069) were all up-regulated to a greater degree on the surface of pulmonary endothelial cells when stimulated lung perfusates were used. When all perfusates (N=8) were pre-incubated for 30 minutes with an IL-1β neutralizing antibody (NAb), this reduced expression of E-Selectin (13%), ICAM-1 (20%) and VCAM-1 (15%). Repeats n=3.

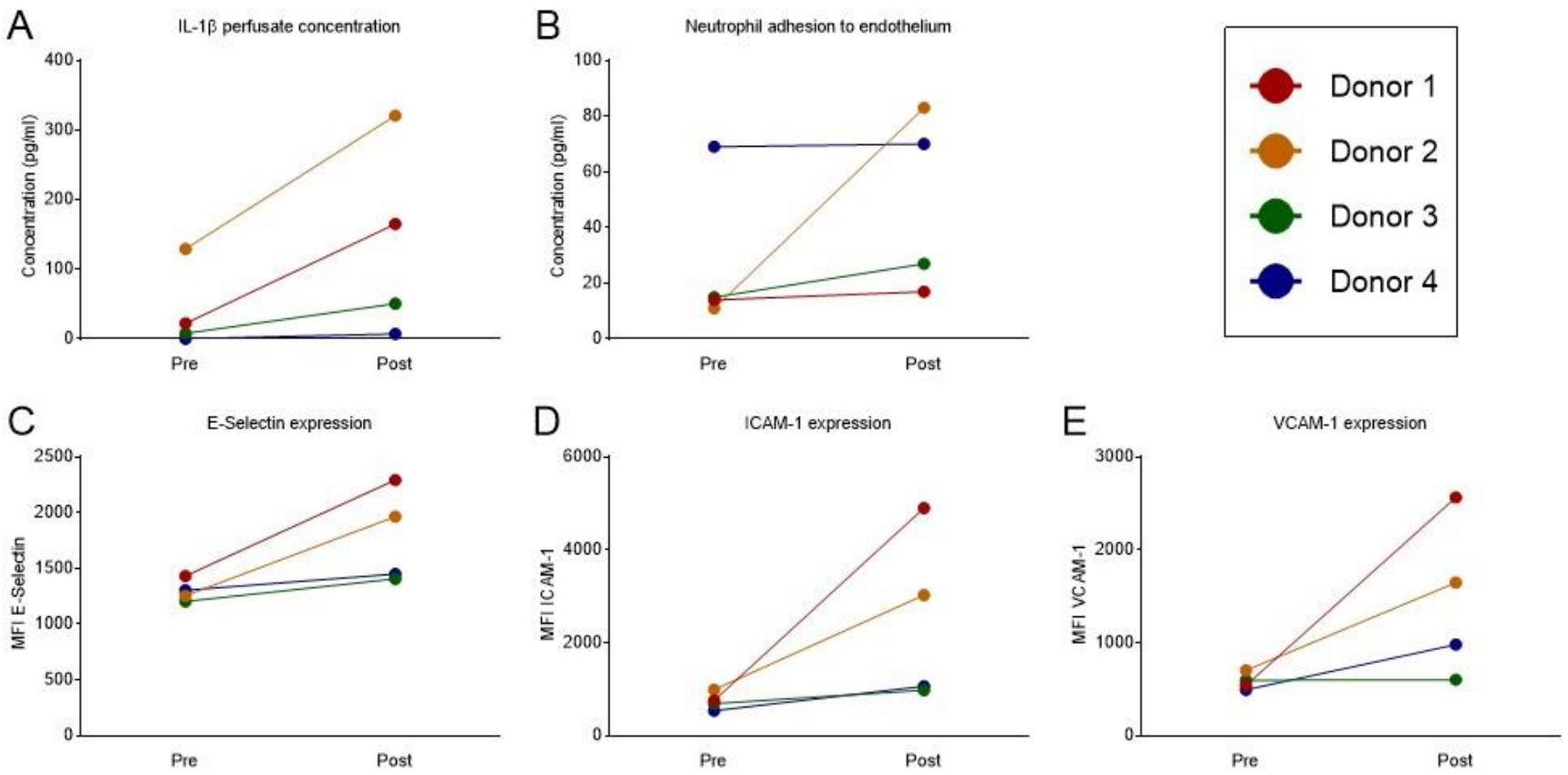

Fig. 4.11 – Relationship between IL-1β level, adhesion and adhesion marker expression *in vitro*. Perfusate IL-1β concentration (A), neutrophil adhesion (B), E-Selectin expression (C), ICAM-1 expression (D) and VCAM-1 expression (E) results shown previously in Figs. 4.8-10 are plotted out here with each point representing an individual control or stimulated lung. The data clearly highlights that other factors within the perfusate may also influence endothelial activation and that this is not solely provoked via the action of IL-1β.

Discussion and concluding remarks

Discussion

Ex vivo lung perfusion represents a potentially important means of assessing and reconditioning extended criteria donor lungs prior to a decision on transplant suitability. Whilst the physical and physiological effects of EVLP are well documented, it also has enormous potential as a platform for therapeutic intervention of an organ. Usual problems with drug delivery such as off-target effects, lack of efficacy and other issues are all abolished when an isolated *ex vivo* perfusion setting is utilised.

Compelling data from Andreasson et al highlighted IL-1β as a predictor of transplant outcome when measured during EVLP. We felt that this warranted further investigation, thus we utilised an *ex vivo* model of perfusion to assess the impact of the pro-inflammatory cytokine IL-1β on neutrophil adhesion and lung physiology. We used *in vitro* models to re-confirm these observations and validate the trends we observed. We feel that this establishes a valid and robust pre-clinical model whereby therapeutic targets can be accurately screened but patient risk is negated.

Our system used IL-1β at a final concentration of 1ng/ml, which was chosen from our previous optimisations of pulmonary endothelial activation *in vitro* (shown in Chapter 2). This was not chosen to reflect the *in vivo* scenario, which would of course be lower than this, but was done so in order to ensure a clear, observable response was elicited from cytokine infusion. This cytokine was infused as a bolus, rather than a continuous infusion throughout EVLP. This was considered easier to standardise across different donor-lung perfusions.

When levels of circulating CFSE-labelled neutrophils were measured in perfusates acquired from lung pairs, we found that lungs stimulated with IL-1β had consistently lower numbers. This was confirmed when we detached the lungs following perfusion and filtered remaining perfusate through a leukocyte filter, observing lower cell densities in our stimulated lung perfusates (p = 0.042). These data suggested that enhanced trapping of labelled neutrophils within these grafts was facilitated via the action of IL-1β on lung tissue, namely the endothelium. Whilst this provided a clear difference between control and stimulated lungs, we feel that a potential advancement of this model would be to extend the duration of IL-1β stimulation prior to infusing neutrophils into the perfusion circuits. This would likely increase the gap between the two populations and provide a clearer difference, enabling a more precise impact of therapeutic supplementation/treatment on circulating cell numbers. We accept here that the numbers of circulating neutrophils in our model fall well below those observed *in vivo* (3-5x10^6/ml). As highlighted previously in Chapter 3, the aim of this labelled cell infusion was to highlight the trends of these cells, i.e. increased adhesion to the endothelium, rather than infer any information from their activation *ex vivo*.

Weight gain of lungs was measured in order to represent a surrogate marker for oedema *ex vivo*. IL-1β infusion provoked a greater degree of oedema formation both as a percentage (p = 0.065) and absolute (p = 0.046) value compared to unstimulated lungs. This highlighted that infusion of the cytokine had triggered damage to the endothelial layer in our lungs. We then looked at how this oedema related to markers of endothelial dysfunction. We saw significant correlations between percentage weight gain and perfusate levels of both sICAM-1 (R^2 = 0.71, p = 0.0043) and vWF (R^2 = 0.39, p = 0.04) after 120 minutes of perfusion. This highlighted that endothelial dysfunction in our model is intrinsically linked with disruption of the endothelium, which facilities the loss of fluid from the vasculature and into the tissues. Both of these proteins have a number of associations with lung injury [125, 131-133], with levels of sICAM-1 also associated with worsening grades of PGD following transplantation [72]. It appears clear then, that this phenomenon of endothelial dysfunction and subsequent disruption we see provoked by IL-1β in our model, is closely linked with the success of lung transplantation.

The $PaCO_2$ and lactate level were both increased in lungs stimulated with IL-1β. A raised pCO_2 level suggests that lung ventilation has been compromised, as CO_2 is being removed from the perfusion circuit with less efficiency. Lactate level is a well-established marker of tissue damage, as local inflammatory response to extracellular pathogens such as bacteria triggers a significant drop in pH, due to immune cell response and hypoxia from vessel constriction. The steadily increasing $PaCO_2$ and lactate concentration within our system are therefore likely indicative of increased hypoxia, associated with vessel blockage and subsequent, localised immunological activation. The single ventilator used for both lungs likely also contributed to the increased rate of lactate production, as the airflow will preferentially ventilate the area of least resistance, increasing the gap in acidosis between stimulated and unstimulated lungs further. Inflammasome activation has also been linked to lower pH in terms of inflammatory disease, hence this likely served to further strengthen the IL-1β signal in our stimulated lungs, as these generally required more THAM to maintain a stable pH during EVLP.

Perfusate concentration of IL-1β in stimulated lungs was consistently higher than control lungs across our time points. What was interesting to observe however, was a variance in concentration difference between lungs from each paired perfusion. It would be interesting to look at tissue concentrations of IL-1β, as these may reflect a correlation with observed perfusate concentrations in our system.

We utilised an *in vitro* flow assay to assess the effect of EVLP perfusates on mediating neutrophil adhesion to endothelial cells and validate the *ex vivo* observations from our model. We saw an increase in adhesion when perfusates from IL-1β-stimulated lungs were used in this system relative to their controls. The same effect was observed when we used flow cytometry to observe effects on

HPMEC adhesion marker expression (E-Selectin $p = 0.038$, ICAM-1 $p = 0.071$, VCAM-1 $p = 0.069$). When all perfusates were pre-incubated with an IL-1β NAb before use in these assays, this down-regulated adhesion ($p = 0.025$) and down-regulated expression of adhesion markers, in particular E-Selectin ($p = 0.067$) on the surface of endothelial cells. Whilst we did not see a down-regulation as clearly as seen by Andreasson et al (2017), it is possible that this is owing to our cohort being more inherently inflamed and damaged by the additional trauma of dissection prior to perfusion [118]. Thus, levels of other pro-inflammatory markers are likely far higher in our lungs meaning that blockade of one cytokine would have less of an impact in lungs used clinically. This idea is further supported by the results shown in Fig. 4.11 – clearly IL-1β is not the sole mediator of endothelial activation in our cohort. Our work provides experimental evidence for down-regulation of adhesion markers directly leading to a decrease in leukocyte adhesion to endothelium lining the vessels of newly engrafted tissue.

Adherence of neutrophils and other leukocytes to the endothelium is a hallmark of reperfusion injury with IL-1β a well-established facilitator of adhesion marker expression on endothelial cells. Our data here suggests that the actions of this cytokine serve to prime the microenvironment towards a more pro-injurious phenotype. Moreover, when we inhibited the actions of IL-1β *in vitro*, we saw a decrease in adhesion and expression of receptors associated with this event. Thus, we would hypothesise that addition of an IL-1β NAb or IL-1 receptor antagonist (IL-1Ra) within our perfusion circuit would prevent infiltration and activation of neutrophils, protecting against damage and subsequent oedema formation. Experimental mouse models have clearly demonstrated that prevention of neutrophil entry into the tissues during reperfusion abolishes much of the associated tissue damage, hence targeting this event is of utmost importance when considering transplantation [127, 128, 134].

The production of IL-1β in the tissues generally occurs exclusively in response to infection, via PRR recognition largely on macrophages and other immunological cells. The large immune component present in the lungs likely accounts as the main source of this cytokine, among others which also play an effect such as IL-8 [76]. It would be interesting to use another approach such as RNAScope® to localise the source of IL-1β in our model, as concurrently down-regulating expression of this cytokine as well as another therapeutic target against the cell type(s) largely responsible for production could help to offer a more tailored and efficacious down-regulation of inflammation prior to transplantation.

IL-1β has many well-documented roles as an acute phase protein, one of which is the activation and propagation of immunological activation pathways. A key aspect of neutrophil biology to consider is that cell death is a key part of their normally functioning inflammatory response, resulting in the generation of ROS, NETs and other key inflammatory mediators which serve to further recruit cells to the site of activation *in vivo*. It would be informative to examine the concentration of cell death

markers in the perfusate, as this would be able to elicit more information as to the fate of the neutrophils, i.e. whether they have adhered or undergone apoptosis/pyroptosis. Part of the basis for infusing IL-1β as a bolus was to ensure that the majority had been absorbed into the tissue prior to the addition of neutrophils in order to minimise cell death, however, it is likely that this would have been provoked to some degree.

One aspect that would be interesting to look at in more detail would be the levels of inflammation within each lung. Whilst we looked at levels of endothelial dysfunction, which of course ties in with this, IL-1β has such a wide range of immunological and inflammatory effects, so it would be prudent to have looked in more detail on a larger range of cell types within the lung, rather than merely the endothelium. The neutrophils that have been infused in represent a tiny proportion of the total immune compartment within an individual lung, thus assessment of activity of these would have been logical to examine. The relationship of the neutrophil with other immune cells will be altered by the presence or absence of IL-1β, meaning that this wider assessment would likely provide more insight into these interactions.

A weakness of the *in vitro* adhesion/receptor expression assays is the lack of any IgG control for the IL-1β NAb when this was used within these systems. Whilst we of course compared the results of these to appropriate negative and positive controls, the isotype control would provide more insight into the non-specific Ig receptor binding of the NAb and enable more accurate interpretation of the real reduction in binding conferred by the antibody.

It would be interesting to replicate our model or similar in a porcine transplantation system, with more long-term outcomes available. Levels of IL-1β in the Andreasson cohort of 'non-survival' lungs were not markedly higher than the 'survival' cohort, demonstrating how sensitive lung tissue is to the actions of this cytokine [118]. Recipients of a lung are often extremely ill and thus minute changes in IL-1β concentration may be sufficient to have a significant effect on graft survival. If differences between cohorts are only shown to be significant in longer-term outcomes, a way of incorporating these into further modelling would be prudent.

Concluding remarks

IL-1β can contribute towards various pro-inflammatory processes prior to and during EVLP. We believe that blocking endogenous IL-1β, either via antibody or small molecule during EVLP prior to transplantation could help to produce a more anti-inflammatory and tolerant phenotype upon reperfusion of the graft. This could help to increase the lung donor pool and reduce the number of

detrimental post-transplant outcomes for patients, improving availability of suitable organs required for transplantation.

CHAPTER 5

-

INTERROGATING THE IMPACT OF IL-1β ON THE RNA PROFILE OF DONOR LUNGS PERFUSED *EX VIVO*

Chapter 5 – Interrogating the impact of IL-1β on the RNA profile of donor-lungs perfused *ex vivo*

Introduction

Lung transplantation is in many cases, the only viable treatment option for clinical lung disease. However, there remains a shortfall for utilisation of suitable donor-lungs, largely due to concerns of using organs from marginal donors. End-stage lung diseases are extremely severe in nature, meaning that every year a number of people are removed from the organ waiting list due to falling seriously ill. Despite this, fewer than 20% of potential lungs are utilised, highlighting that there is pressing need to address this disparity [17].

Ex vivo lung perfusion (EVLP) provides a means of addressing this significant shortfall. One of the promising avenues for EVLP is use as a treatment delivery platform, with organs in an *ex vivo* setting ideally positioned to receive therapeutics in concentrations not possible *in vivo* due to toxicity or off-targeting. This idea has been implemented by many groups already. Researchers based in Toronto transfected lungs with an adenoviral vector containing IL-10 and showed that this improved oxygenation and reduced airway resistance, whilst also improving the inflammatory cytokine profile of these lungs [53].

A wealth of information regarding the viability and function of lungs can be extrapolated using modern methods of RNA-Sequencing (RNA-Seq). Interrogation of diseases such as pulmonary fibrosis provide a wealth of information regarding the key cell types and molecular entities involved within pathological progression [135, 136]. Research groups have applied this technology to EVLP already, investigating the effect(s) of perfusion on the transcriptome. Ferdinand et al (2019) investigated the RNA profile of 6 transplantable donor lungs and compared these to 4 lungs deemed unsuitable for use [137]. The authors identified that lungs utilised in transplant had lesser activation of innate immune pathways such as NF-κB, as well as unearthing potential biomarkers such as CHIT1, which could potentially act as predictive of transplant success.

Another group based at the University of Pittsburgh examined the changes to RNA profile when lungs were treated with an anti-inflammatory small molecular entity, BC1215, after undergoing exposure to lipopolysaccharide (LPS) treatment during EVLP. The authors note that as well as improved oxygenation and reduction of cytokine levels in bronchoalveolar lavage fluid (BALF), the transcriptomic profile of these lungs was greatly altered in comparison to untreated lungs, with reduction in genes involved in NF-κB signalling pathways [138]. This highlights the wealth of information on drug or treatment efficacy that can be gathered from RNA interrogation of lungs during EVLP.

Study background

As previously established in Chapter 4, IL-1β supplementation of lungs during EVLP stimulated greater endothelial activation and dysfunction. This facilitated an enhancement in oedema formation as well as leukocyte adhesion, shown in both *ex vivo* and *in vitro* settings. It was concluded that assessing the impact of IL-1β on gene expression during EVLP would also be prudent and reveal a number of novel and interesting targets, as has been shown to be possible in literature cited within the introduction.

We chose an immunologically targeted approach, rather than global RNA assessment of tissues from our perfused lungs. We felt that this offered an ideal compromise between simple, benchtop methods such as PCR, versus large-scale RNA-Seq, whilst offering insight into the mechanisms affected by increasing the level of IL-1β in our system. This work was performed in collaboration with Maria Mavridou (MRes student) who assisted in the isolation and purification of RNA from tissue, Jamie Macdonald (Immunology and Inflammation group technician) who performed the Nanostring procedures and Venetia Bigley, who assisted with the planning and preparation stages of this work.

Hypothesis and aims

Hypothesis

Hypothesis

IL-1β drives transcriptomic changes of lung tissue during EVLP that predispose towards a heightened inflammatory microenvironment. Lungs with heightened levels of IL-1β in the perfusate have increased expression of pro-inflammatory genes that enhance immunologically significant pathways including those that may influence leukocyte adhesion, endothelial dysfunction, cytokine production and cell death pathways.

Aims

1) Investigate whether IL-1β stimulation of lungs *ex vivo* had the expected biological and cellular effects
2) Validate observations with alternative assay formats

In order to achieve these aims, this work will consist of the following objectives: -

1) Isolate RNA from biopsied tissue in our split lung perfusion model and analyse levels of immunologically relevant genes within these
2) Compare levels of RNA in our stimulated lungs relative to their corresponding controls
3) Perform PCR on a selection of genes of interest as highlighted from Nanostring analysis*

*Due to COVID-19 coronavirus pandemic, objective 3 was not able to be addressed within the time available

Methods

Set-up and perfusion

The EVLP circuits were prepared as detailed in the methods. Briefly, 2L of Steen solution was circulated at 20% of cardiac output (CO), as calculated using the ideal bodyweight formula. The left and right lungs were dissected apart, and their respective PA trunks were cannulated in separate perfusion circuits, before the flow rate was gradually increased to 40% CO over 20 minutes of perfusion. Upon reaching a temperature of 32°C, ventilation was commenced. A perfusate temperature of 37°C was reached and maintained for 15 minutes before IL-1β infusion. Throughout EVLP, regular blood gases measurements were taken to ensure that various parameters remained in a normal range for perfused lungs.

Tissue acquisition and storage

Biopsies were acquired for analysis upon completion of EVLP. The experimental protocol for this is outlined in detail in Chapter 4. Briefly, biopsies were acquired by dissecting down the centre of lung lobes and then cutting out sections of tissue. These were immediately placed in RNAlater, kept at 4°C for 24 hours and then at -80°C for long-term storage thereafter.

RNA isolation and quantification

Tissue samples collected from EVLP were stored in RNAlater© at -80°C until required for analysis. 20µg sections were dissected and then homogenised using a Tissue Lyser II for 2 minutes in RLT Plus buffer with stainless steel beads (Qiagen). RNA was isolated using the RNeasy Mini Plus Kit (Qiagen) as per the manufacturer's instructions. Purified RNA was analysed using a Nanodrop One for A280/260 and A260/230 ratios before being quantified for RNA concentration precisely using a Qubit high sensitivity RNA assay. The RNA obtained from the IL-1β-stimulated lung from donor 1 required concentrating prior to Nanostring. Upon thawing of the RNA, 2µl of RNaseOUT recombinant ribonuclease inhibitor (40U/µl, Invitrogen) was added to prevent degradation and concentrated using the DNA 120 SpeedVac system (ThermoFisher Scientific) for 20 minutes. The pellet was then re-suspended in RNase Free water prior to analysis.

Nanostring analysis

Nanostring technology was chosen as the methodology to perform our targeted RNA analysis. Analysis of RNA was performed using an nCounter® FLEX analysis system (Newcastle Human Dendritic Cell Laboratory) with the nCounter® Human immunology v2 Panel. Accessed with the following link:

https://www.nanostring.com/products/gene-expression-panels/gene-expression-panels-overview/ncounter-inflammation-panels?jumpto=SUPPORT

Oedema formation

The weight of lungs was measured before and after EVLP, to act as a surrogate marker for oedema formation. The increase was then plotted as a percentage increase and used in a linear regression model against absolute counts of RNA for genes of interest.

Data analysis

Results from the Nanostring were collated and processed using nSolver software (NanoString). The immunology panel contained 6 positive controls, 8 negative controls and 15 internal reference genes. These were all used for various types of data normalisation and quality control. Each lung pair was analysed separately and then these results were collated together to provide combined fold change values and absolute RNA counts. All data shown was organised using Excel software. Graphs were plotted and ratio paired t-tests were calculated using Prism 8 (GraphPad).

Results

Lung donor information

Clinically declined donor-lungs were utilised as part of this study. Table 5.1 shows the characteristics of donor-lungs used within this study. Donors 1 and 2 were both declined on the basis of bi-lateral damage, whist 3 and 4 showed poor function prior to organ retrieval. Donors 1, 3 and 4 were donated following brain death (DBD), with donor 2 from an individual who donated following circulatory death (DCD).

Perfusion	Donor age	Sex	Bodyweight (kg)	Height (cm)	Donation	Reason for decline
1	56	Female	80	165	DBD	Inspection
2	22	Male	65	180	DCD	Inspection
3	59	Male	95	171	DBD	Poor function
4	47	Female	50	171	DBD	Poor function

Table 5.1 – Donor data for lungs used in the split lung model

DCD – Deceased from circulatory death; DBD – Deceased from brain death

RNA concentration – Qubit

RNA from lung biopsies was isolated and purified for Nanostring analysis. As the sample for the IL-1β-stimulated lung from donor 1 was low (<10ng/ml), this was concentrated prior to use in our targeted RNA analysis. Final RNA values are shown in Table 5.2.

Sample ID	RNA (ng/ml)
1 - Control	38.2
2 - Control	94
3 - Control	24.7
4 - Control	33
1 - IL-1β*	19.4
2 - IL-1β	104
3 - IL-1β	21.3
4 - IL-1β	23.2

Table 5.2 – Qubit RNA concentrations of tissue biopsies acquired during EVLP. Concentrations were obtained using a Qubit High Sensitivity RNA assay to ensure that equal quantities of RNA were used in Nanostring for each sample.

*RNA required concentrating prior to final value being obtained

Differential gene regulation of lungs *ex vivo* via the action of IL-1β

Fig. 5.1 shows a volcano plot of 594 differentially regulated genes by infusion of IL-1β into all four of our lung pairs. Each grey dot on the line represents an individual control lung gene measured by Nanostring analysis, with the red dots representing genes significantly altered in terms of expression (paired T-test). LILRB1 was significantly up-regulated (p = 0.038) in lungs stimulated with IL-1β. ATG5 (p = 0.030), C3 (p = 0.017), ICAM2 (p = 0.034), MAPK1 (p = 0.068), MSR1 (p = 0.056) and PSMB7 (p = 0.022) were significantly down-regulated in these lungs.

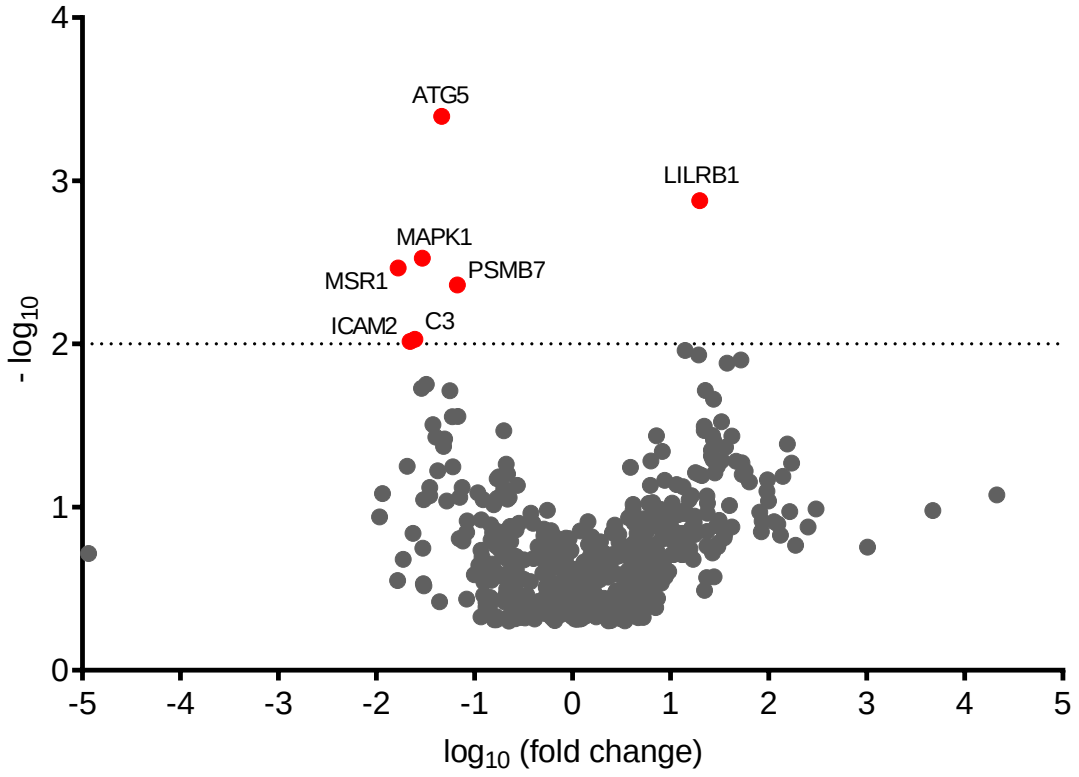

Fig. 5.1 – Volcano plot of gene fold changes in stimulated lungs. Lungs were perfused in pairs with one lung from each infused with IL-1β to a final concentration of 1ng/ml. Fold changes were calculated for each individual pair and then an average was used from N=4 perfusions. Each dot represents a gene relative in expression to the corresponding control lung gene, with a fold-change of 2 set as a cut-off for meaningful change in expression. LILRB1 was significantly up-regulated (p = 0.038) in lungs stimulated with IL-1β. Conversely, ATG5 (p = 0.030), C3 (p = 0.017), ICAM2 (p = 0.034), MAPK1 (p = 0.068), MSR1 (p = 0.056) and PSMB7 (p = 0.022) were down-regulated.

Gene	*P* value	Significance	Increase/decrease	Function(s)
LILRB1	0.038	*	Increase	Immune inhibition, control of autoreactivity
ATG5	0.030	*	Decrease	Autophagy, apoptosis, inhibition of cell cycle
C3	0.017	*	Decrease	Complement activation, opsonisation, immune cell activation
ICAM2	0.034	*	Decrease	Cell adhesion
MAPK1	0.068		Decrease	Intracellular signalling molecule
MSR1	0.056		Decrease	Scavenger receptor, LDL binding
PSMB7	0.022	*	Decrease	Proteasome subunit, protein degradation

Table. 5.3 – Expression of genes altered by IL-1β stimulation. Genes involved in a variety of cellular functions and processes were altered by way of IL-1β during EVLP of donor-lungs. LILRB1 was significantly up-regulated (p = 0.038), whilst expression of ATG5 (p = 0.030), C3 (p = 0.017), ICAM2 (p = 0.034) and PSMB7 (p = 0.022) were significantly down-regulated. Down-regulation of MAPK1 and MSR1 did not achieve statistical significance. Functions altered by this list of candidates vary greatly and include aspects involving immune regulation, adhesion, protein processing and control of cellular life cycle.

Fig 5.2 highlights some of the alterations in gene expression driven by IL-1β. Genes involved within pathways such as adhesion, migration, apoptosis and immunity are generally increased in stimulated lungs from our paired perfusions.

Expression of adhesion marker genes is increased by IL-1β stimulation

The effect of IL-1β on expression of adhesion marker genes was investigated in the tissue of lungs perfused *ex vivo*. Expression of Intercellular adhesion molecule 1 (ICAM1) was significantly increased in lungs stimulated with IL-1β (p = 0.021), with expression of E-selectin (SELE) also increased (p = 0.059). Vascular cell adhesion molecule 1 (VCAM1) expression was not altered. For ICAM1 and SELE, the change is seen most noticeably in one lung pair, with the others increasing in expression to a much lesser extent.

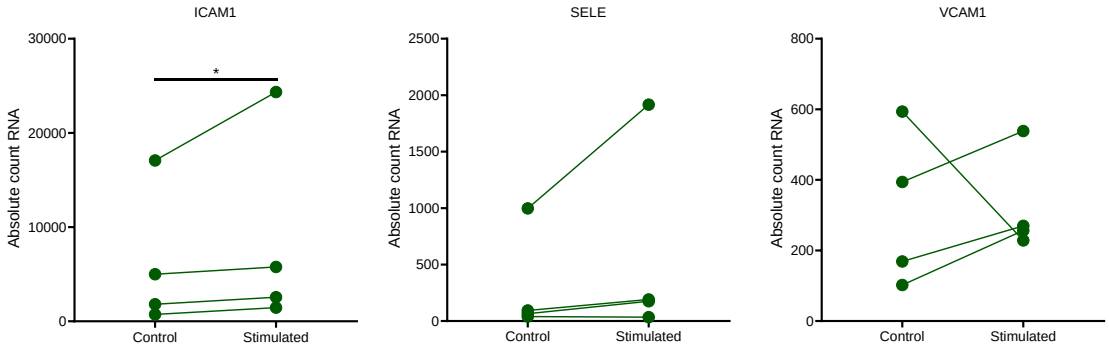

Fig. 5.2 – Adhesion marker gene expression in control and stimulated lungs. Nanostring analysis was performed on a panel which included the genes ICAM1, SELE and VCAM1 which encode the adhesion markers ICAM-1, E-Selectin and VCAM-1, respectively. ICAM1 gene expression was significantly up-regulated in stimulated lungs from each pair (ratio paired t-test, p = 0.021). SELE expression was also up-regulated by IL-1β (ratio paired t-test, p = 0.059) whilst VCAM1 expression was not altered in these lungs. N=4.

Cluster of differentiation 44 (CD44), ICAM2, ICAM4, ICAM5 and Platelet endothelial cell adhesion molecule (PECAM1) were all investigated in the same manner. CD44 and ICAM4 were significantly up-regulated by IL-1β stimulation (p = 0.032, p = 0.039, respectively) whilst up-regulation of ICAM5 did not reach statistical significance. Conversely, ICAM2 levels were down-regulated in stimulated lungs (p = 0.034), with levels of PECAM1 not following any particular trend.

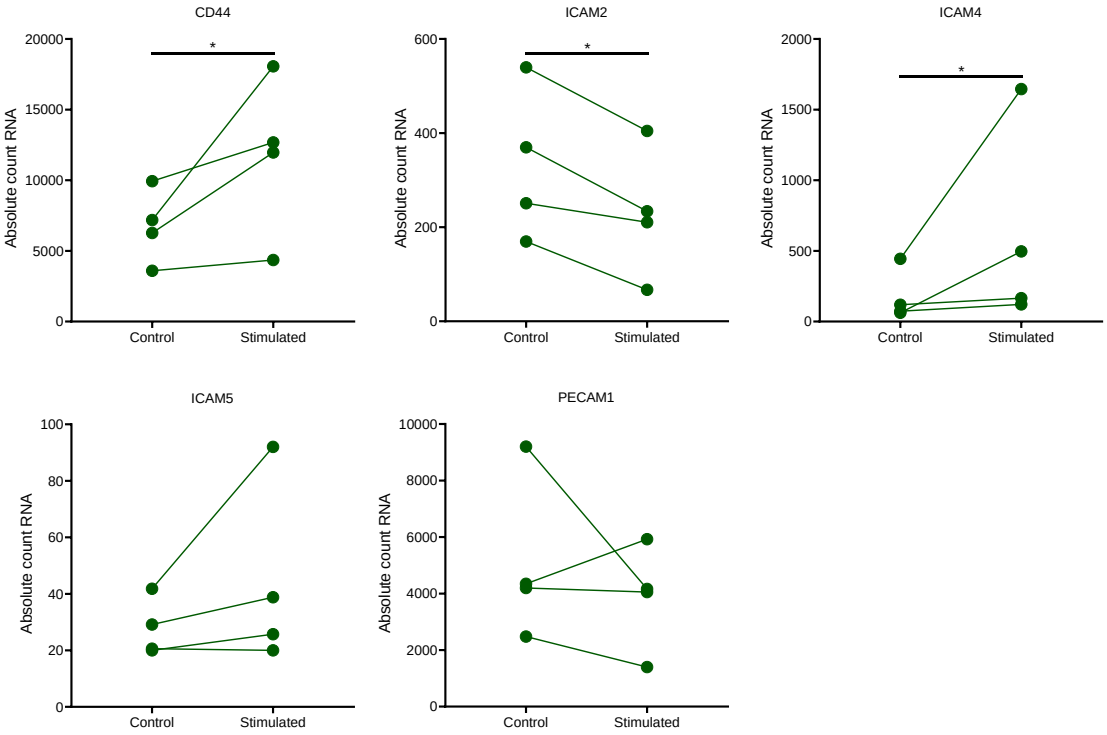

Fig. 5.3 – Adhesion marker gene expression. The effects of IL-1β were investigated during EVLP. Expression of CD44 (p = 0.0316) and ICAM4 (0.0392) was significantly up-regulated by IL-1β, with an increase in ICAM5 also observable. Levels of ICAM2 were significantly reduced (p = 0.0344), whilst PECAM1 did not follow any meaningful trend. N=4.

The inflammatory profile of *ex vivo*-perfused lungs is increased via IL-1β stimulation

A number of genes with important and well-established roles in pro-inflammatory responses were investigated via Nanostring in the tissues of lungs perfused *ex vivo*. CCAAT/enhancer-binding protein beta (CEBPB) and platelet-activating factor receptor (PTAFR) were significantly up-regulated by IL-1β ($p = 0.035$, $p = 0.0097$, respectively). Inhibitor of nuclear factor kappa-B kinase subunit epsilon (IKBKE) was seen to increase in all lungs, however this trend did not become significant. Interleukin-6 (IL6) and Interleukin-8 (IL8) generally seemed to increase, however these trends did not become statistically significant. In the case of both, one donor expressed notably low levels of both cytokines in both the control and stimulated lungs, likely affecting the result.

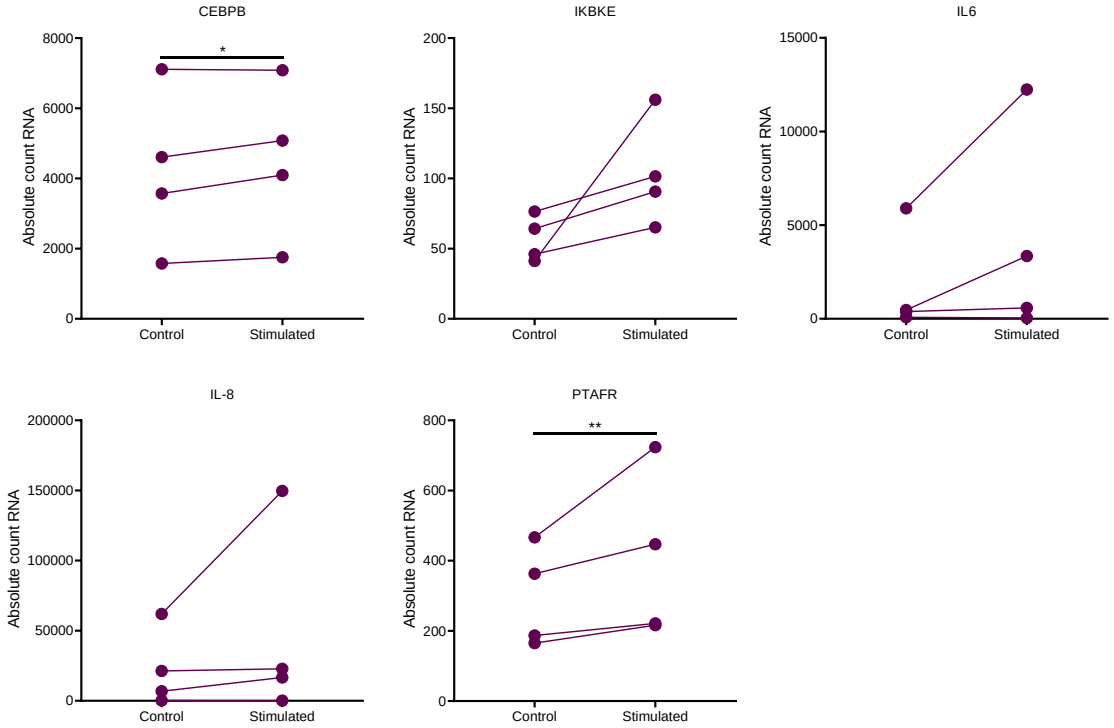

Fig. 5.4 – Inflammatory genes are up-regulated via the action of IL-1β. Levels of genes associated with the inflammatory response were measured in the tissues of perfused lungs *ex vivo*. The genes CEBPB and PTAFR were significantly up-regulated by IL-1β infusion ($p = 0.035$, $p = 0.0097$, respectively). IKBKE, IL6 and IL8 generally increased but this trend did not reach statistical significance. N=4.

IL-1β promotes transcription of genes involved in innate and adaptive immune responses

The action(s) of IL-1β on genes that play key roles in eliciting a response from the innate immune system were examined via Nanostring. The Mincle receptor (CLEC4E) and Nucleotide-binding oligomerization domain-containing protein 2 (NOD2) function as pattern recognition receptors (PRRs), with CLEC4E significantly up-regulated by infusion of IL-1β (p = 0.011). Polymeric immunoglobulin receptor (PIGR) is responsible for transcytosis of IgA and IgM to the mucosal surfaces and levels were significantly increased via IL-1β (p = 0.0108).

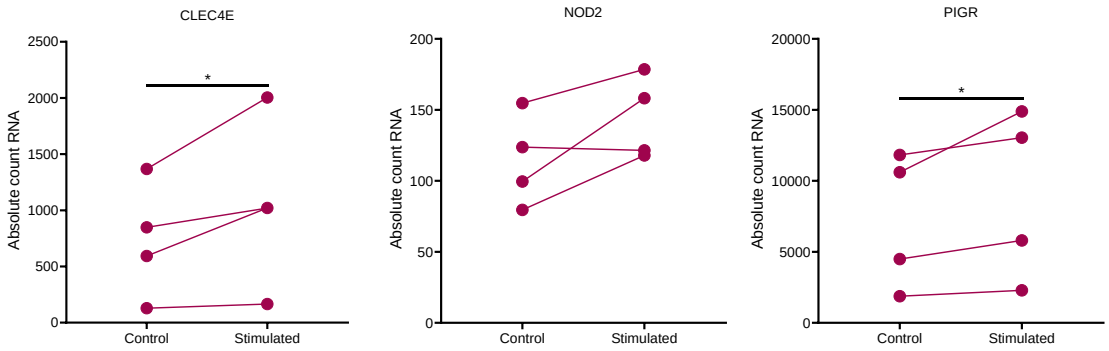

Fig. 5.5 – Expression of genes involved in innate immunity are increased via IL-1β. Levels of CLEC4E, NOD2 and PIGR were examined in tissue biopsies from lung pairs perfused *ex vivo* with or without the addition of IL-1β into the perfusion circuit. Levels of CLEC4E and PIGR increased significantly in stimulated lungs (p = 0.011, p = 0.0108, respectively) with levels of NOD2 also increasing in response to IL-1β (not significant). N=4.

IL-1β supplementation can also be seen to influence genes involved in adaptive immunity and function of lymphocytes. B-cell lymphoma 3-encoded protein (BCL3), CD274, Human leukocyte antigen-A (HLA-A) and Leukocyte immunoglobulin-like receptor subfamily B member 1 (LILRB1) all play roles in exacerbating the immune response and all were significantly up-regulated in stimulated lungs from each pair (p = 0.048, p = 0.018, p = 0.021, p = 0.038, respectively). Levels of Programmed cell death 1 ligand 2 (PDCD1LG2), a negative regulator of the immune response, were downregulated in stimulated lungs, but this did not reach significance.

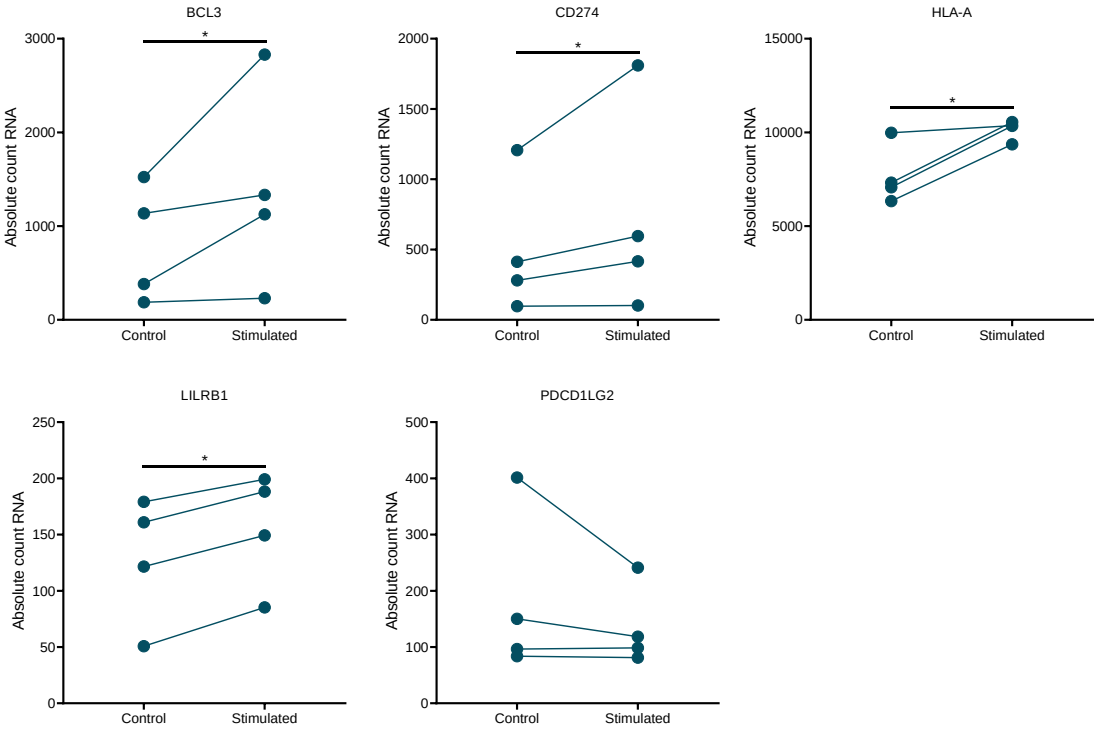

Fig. 5.6 – Levels of genes involved within the adaptive immune response. BCL3, CD274, HLA-A and LILRB1 all play key roles within adaptive immune responses and are significantly up-regulated in response to IL-1β infusion during EVLP (p = 0.048, p = 0.018, p = 0.021 and p = 0.038, respectively). PDCD1LG2 was down-regulated in stimulated lungs. N=4.

Apoptosis

IL-1β has a number of well-recognised effects on amplifying apoptotic and cell death pathways. Levels of ATG5 and BH3 interacting-domain death agonist (BID) were significantly decreased in lungs stimulated with IL-1β ($p = 0.03$, $p = 0.025$, respectively). ATG5 acts as a protective gene, encouraging autophagy and normal, healthy degradation of cells. BID is a pro-apoptotic factor. Perforin (PRF1) was significantly up-regulated by IL-1β ($p = 0.0475$) as was Granzyme B (GZMB). These two act in synergy to induce cell death by the action of CD8+ T / NK cells. CD82 and Promyelocytic leukemia protein (PML) were also up-regulated, both having pro-apoptotic functions. Levels of Caspase 3 (CASP3) were not altered by IL-1β addition into the circuit.

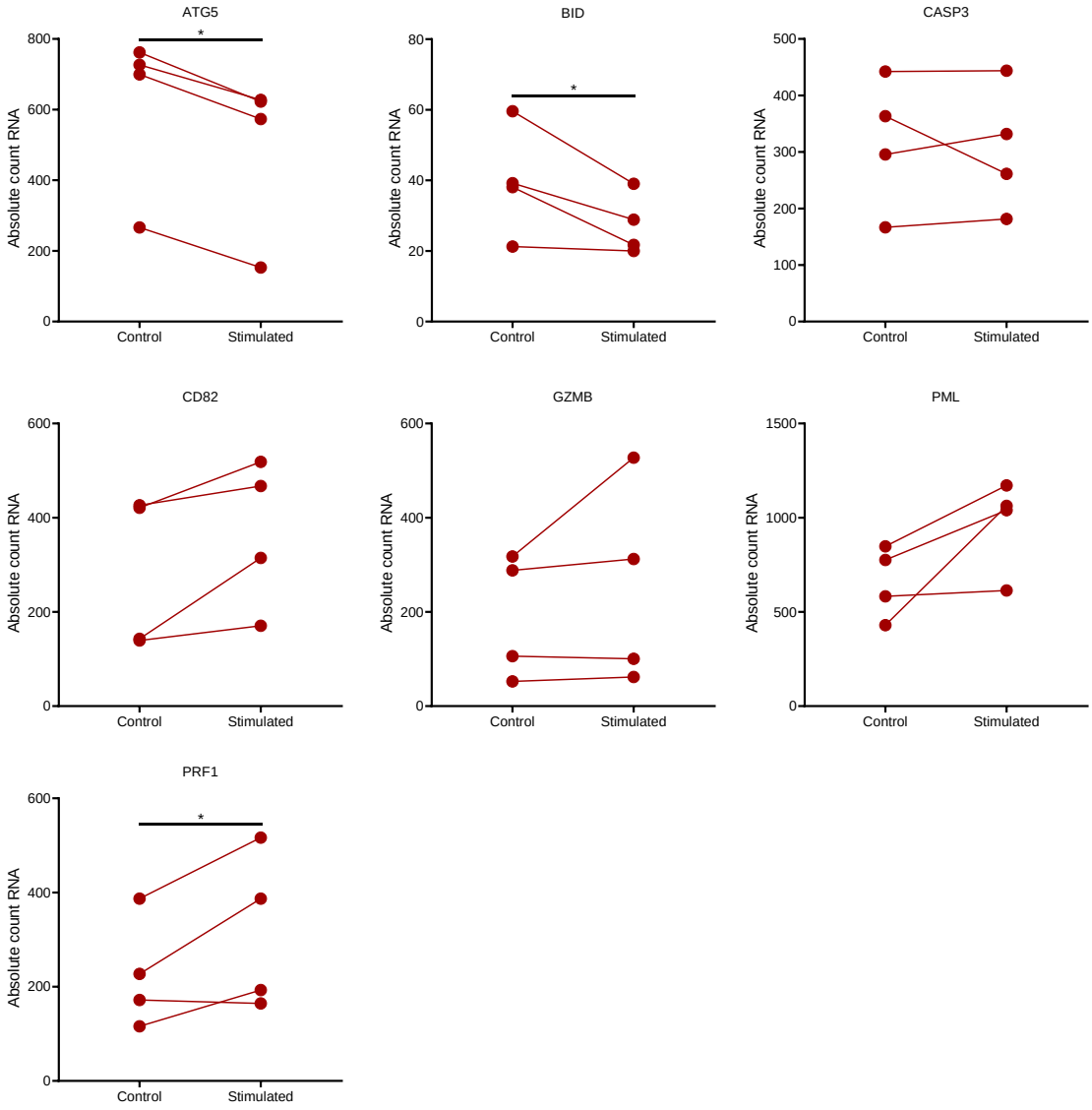

Fig. 5.7 – Apoptotic mechanism response to IL-1β stimulation. Apoptosis-associated genes were altered via infusion of IL-1β. ATG5 and BID were significantly down-regulated (p = 0.03, p = 0.025, respectively). PRF1 was significantly up-regulated (p = 0.0475), along with CD82, GZMB and PML (not significant). Levels of CASP3 were not altered by cytokine stimulation. N=4.

TNF signalling pathway-associated molecules are up-regulated in response to IL-1β

Key genes involved in Tumour necrosis factor (TNF) signalling pathways were investigated in the tissue of lungs perfused *ex vivo* either with or without IL-1β stimulation. A number of genes were significantly increased in response to IL-1β, namely Tumour necrosis factor receptor superfamily member 1B (TNFRSF1B) (p = 0.036), Tumour necrosis factor receptor superfamily, member 4 (TNFRSF4) (p = 0.0032), TNF receptor-associated factor 1 (TRAF1) (p = 0.02), TNF receptor-associated factor 1 (TRAF2) (p = 0.032) and Lipopolysaccharide-induced tumour necrosis factor-alpha factor (LITAF) (p = 0.017). Levels of TNF were also increased; however this did not reach statistical significance.

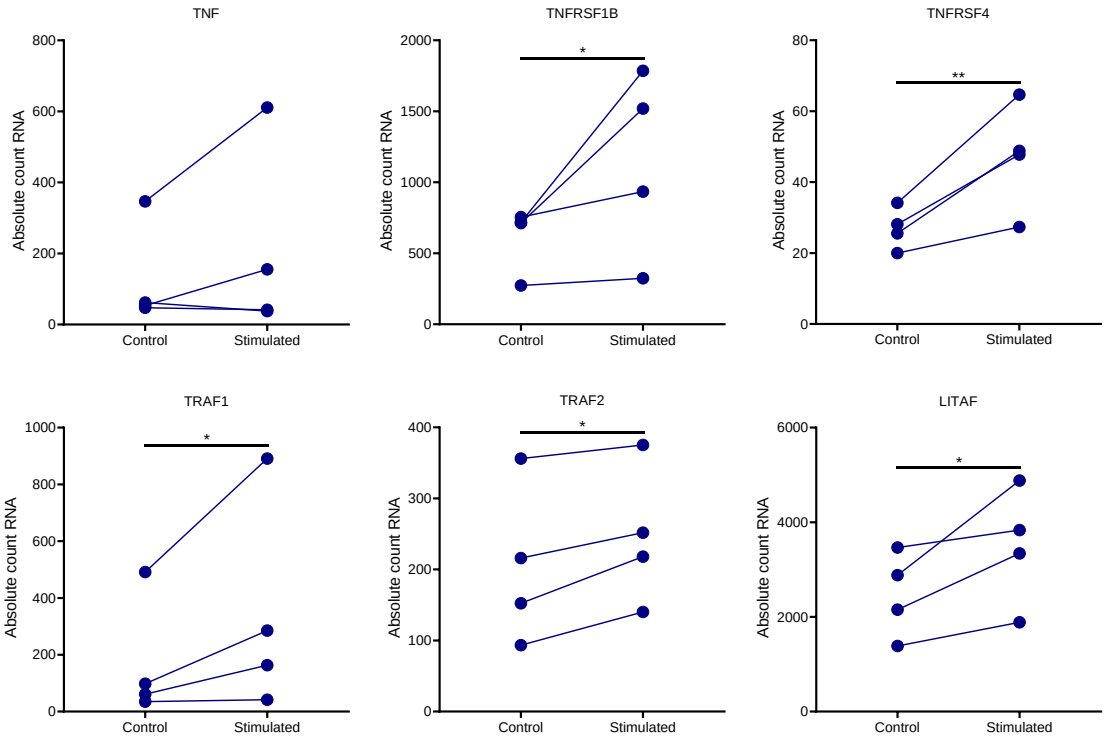

Fig. 5.8 – TNF pathway gene expression in control and stimulated lungs. Nanostring analysis was performed on a panel which included genes involved in the TNFα pathway. Expression of TNFRSF1B (p = 0.036), TNFRSF4 (p = 0.003), TRAF1 (p = 0.02), TRAF2 (p = 0.031) and LITAF (p = 0.0169) were significantly up-regulated by infusion of IL-1β into the perfusion circuit. TNF was also up regulated but did not reach significance. N=4.

Levels of T-cell-associated genes are increased in response to IL-1β stimulation

The gene panel measured in our analysis contained a plethora of genes associated with the T-cell response. Up-regulation of CD2 (p = 0.042), CD247 (p = 0.0294), CD3E (p = 0.0115), CD40LG (p = 0.0473), CD6 (p = 0.0144), CD7 (p = 0.0169) and Transcription factor 7 (TCF7) (p = 0.0475) was observed, all of which play key roles in stimulating and maintaining T-cell responses. RNA levels of Interleukin-2 receptor subunit beta (IL2RB) increased (p = 0.0482) whilst conversely, levels of the IL-4 receptor gene were decreased (p = 0.012).

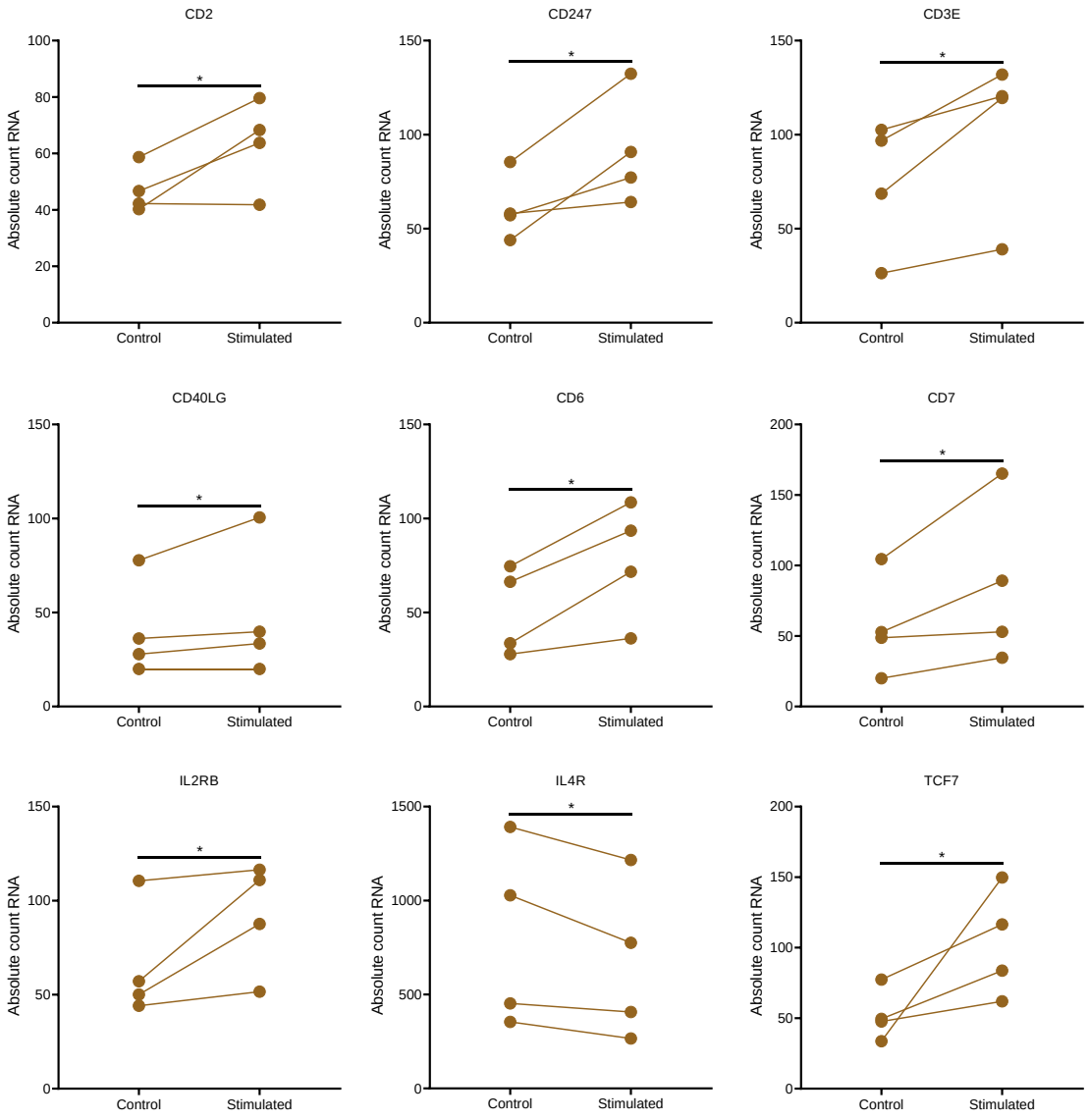

Fig. 5.9 – T cell-associated pathway gene expression in control and stimulated lungs. Nanostring analysis was performed on a panel which included genes involved in T cell activation and signalling. Significant up-regulation of CD2 (p = 0.042), CD247 (p = 0.0294), CD3E (p = 0.0115), CD40LG (p = 0.0473), CD6 (p = 0.0144), CD7 (p = 0.0169) and Transcription factor 7 (TCF7) (p = 0.0475) was observed. IL4R levels were significantly decreased (p = 0.012), whilst levels of IL2RB were increased (p = 0.0482). N=4.

Proteasome-associated subunit genes are decreased by IL-1β

Components of the proteasome, which processes unwanted or damaged proteins, were investigated as part of our analysis. Proteasome subunit beta type-5, 7 and 8 (PSMB5, PSMB7 and PSMB8) were all significantly down-regulated in stimulated lungs (p = 0.037, p = 0.022 and p = 0.015, respectively).

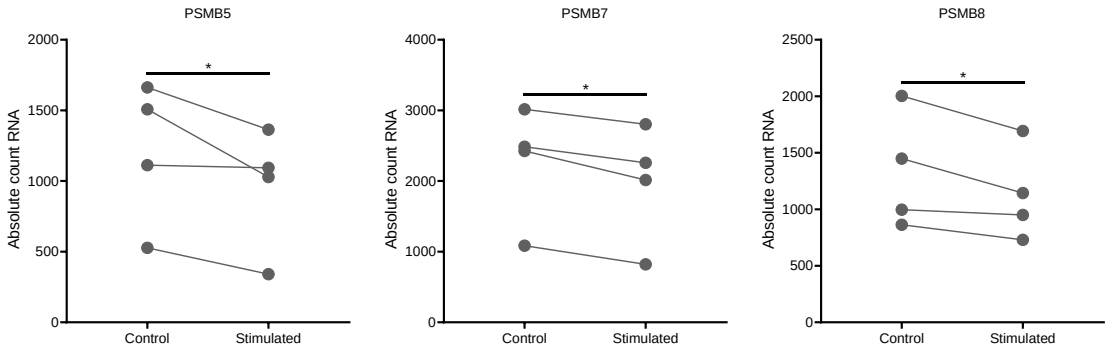

Fig. 5.10 – Proteasome subunit genes are down regulated via the actions of IL-1β into the EVLP circuit. Levels of genes encoding subunits of the 20S proteasome were measured in perfusate of lungs with or without IL-1β stimulation. PSMB5, PSMB7 and PSMB8 were all down-regulated in lungs that received a bolus of cytokine compared to the corresponding control lungs (p = 0.037, p = 0.022 and p = 0.015, respectively). N=4.

Complement pathway-associated genes are down-regulated by IL-1β

IL-1β infusion appears to down-regulate genes encoding members of the complement cascade. Levels of C3 were significantly downregulated in stimulated lungs (p = 0.0165), as well as levels of C1QB (not significant). C3 – complement component 3, plays important roles in mediating inflammatory responses, whilst C1QB encodes a component of the C1 complex, which initiates the classical complement pathway. Levels of CD46, encoding complement regulatory factor protein, were decreased in lungs from the stimulated cohort.

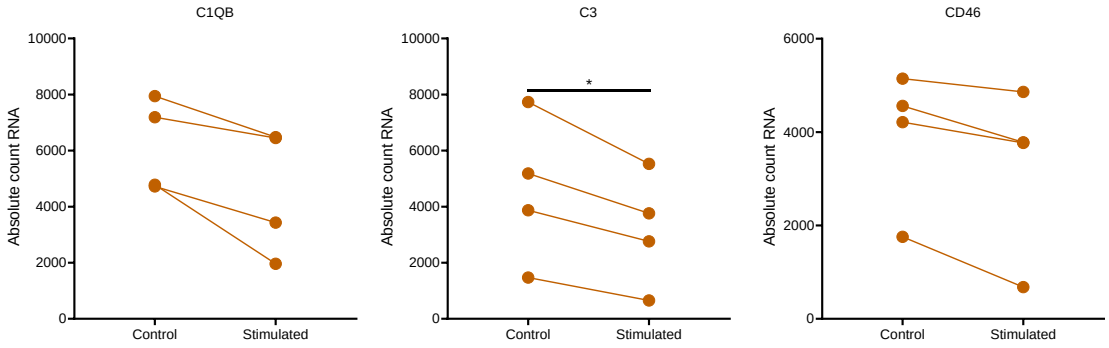

Fig. 5.11 – Complement gene regulation by IL-1β. Alterations in levels of complement system components are associated with post-transplant morbidities. Levels of C3 were significantly down-regulated in lungs stimulated with IL-1β from our paired perfusions (p = 0.017). C1QB and CD46 were both also down-regulated, but these were not significant. N=4.

Discussion and concluding remarks

Discussion

Analysing the RNA profile of tissues and organs represents a huge resource of information for transplant research. As has been shown previously, tangible differences in organ viability and health can be determined from this type of analysis [136, 137, 139]. Therefore, we used a targeted RNA profiling approach within our split lung model to assess the differential expression patterns provoked by IL-1β on immunologically associated genes in the tissue of lungs that underwent EVLP. As can be seen in Table 5.1, the panel we chose covers a wide range of different processes such as inflammation, apoptosis and innate/adaptive immunity. Therefore, it was decided that this approach investigated a sufficiently wide range of genetic pathways whilst compromising on the technical complexity that is associated with RNA-Seq methods.

When all genes were plotted as fold change against *p* value, four candidates emerged as significantly down-regulated – ATG5, C3, ICAM2 and PSMB7, with one – LILRB1 significantly up-regulated. The gene candidates here have involvement in a wide variety of cellular pathways including prevention of cell damage, complement activation, cell adhesion and immune regulation. This highlights the wide-ranging effects that IL-1β infusion has had during EVLP on a number of different immunological and cellular processes in our model.

Due to the results shown in Chapter 4, namely that ICAM-1, E-Selectin and VCAM-1 expression were provoked by perfusates *in vitro*, we felt it prudent to investigate the effect of IL-1β on transcription of genes associated with cellular adhesion. We found that expression of ICAM1 and SELE genes were up regulated in stimulated lungs from each paired perfusion ($p = 0.021$, $p = 0.059$, respectively). Both ICAM-1 and E-Selectin play key roles in mediating leukocyte adhesion to the endothelium, and heightened levels of both form a key role in the pathophysiology of a number of vascular and immunological diseases. It should be noted that for both genes however, that one pair clearly affected the overall change, as expression in this donor pair was significantly increased relative to the three other pairs in the cohort. IL-1β is a known stimulator of increasing surface levels of these adhesion markers, with our data supporting this. Moreover, expression of CD44, ICAM4 and ICAM5 also increased in stimulated lungs, whilst conversely, ICAM2 levels decreased and PECAM did not follow a meaningful trend. This would suggest difficulty concluding that all genes involved in leukocyte adhesion have been increased by IL-1β supplementation and thus expansion of the cohort could provide more conclusive results here.

Inflammation is a hallmark of IRI and subsequent PGD development, with a wide range of immune cell types shown to have involvement. The inflammatory profile of lungs that received a bolus of IL-1β was enhanced relative to the control lungs from our pairs, with significant up-regulation of CEBPB and

PTAFR (p = 0.035, p = 0.0097, respectively) in these lungs. CEBPB has been shown to mediate an acute inflammatory response, stimulating production of key cytokines such as IL-6 and TNFα, whilst PTAFR encodes the receptor for platelet-activating factor (PAF). Abnormal production of this protein can be life-threatening and is associated with traumatic injury and septic shock. These data suggest therefore, provocation of a more inflammation-favouring phenotype in these lungs. We also saw trends of increasing levels of IL6 and IL8, but these failed to reach significance. There were markedly different levels of these genes between donors and we are of the opinion that a larger sample size could unearth a significant trend of up-regulation of the latter of these in particular. IL-8, produced by the IL8 gene, is well-documented as a predictor of lung transplant outcome and so further investigation of this in future work would be prudent [76].

Levels of key genes associated in innate and adaptive immune pathways were also up-regulated in our IL-1β-stimulated lungs. Levels of pattern-recognition receptor genes CLEC4E and NOD2 were increased. PIGR, encoding the Polymeric immunoglobulin receptor, mediates the movement of IgA and IgM antibodies from the basal to mucosal surfaces. We identified that IL-1β stimulation produced an increase in levels of this gene [140]. These increases suggest an innate system becoming more primed to detect and respond to foreign material, which would enhance an undesirable response to cells from the donor-lung. When we looked at adaptive immunity-associated genes, we saw an increase in the production of HLA-A. HLA typing is crucial to immune recognition of 'self,' therefore heightened production of this gene may heighten the immune response from the recipient immune system following reperfusion of the graft. Interestingly, we also saw an up-regulation of inhibitory genes such as CD274 and LILRB1, which protect against unwanted, overzealous immune responses. These mechanisms may be a protective auto-reaction to heightened pro-inflammatory cytokine levels, as present in our system.

A cohort of TNF pathway-related genes were investigated as part of our study, with previous data from Andreasson et al highlighted that the TNFα signal could be predictive of 1-year patient survival [118]. TNF did not show significant up-regulation, which we found very surprising, given the strength of its predictivity of 1-year patient survival. We did, however, observe that several other pathway-related genes did. TRAF1 and TRAF2; both anti-apoptotic factors were increased in our cohort. Levels of LITAF, which potently activates monocytic cell lineages, were increased in lungs we stimulated with IL-1β. Overall, genes associated with TNF activity are up-regulated via the infusion of IL-1β *ex vivo*, which, given the associations made by Andreasson et al previously with 1-year mortality following transplant, suggest that these pathways contribute negatively towards graft survival. The fact that TNF itself was not found to be of significance in our cohort could indicate that our analysis has missed

some of the crucial signal due to analysis of RNA, rather than combining this with additional analysis of protein level.

Whilst IL-1β has many well-defined roles in promoting and exacerbating apoptotic pathways, a lot of our data here suggests that lungs stimulated with the cytokine during EVLP down-regulate many pro-apoptotic genes. Genes such as BCL3 can be seen in the literature to promote lymphocyte survival and are even implicated in the progression of numerous different cancers. If one considers data shown in Fig. 5.9, namely increased production of co-stimulatory T-cell genes as well as an increase/decrease in IL2RB/IL4R, respectively, the picture is one of an enhanced Th1 phenotype being established. This is corroborated further by raised levels of cytotoxic mediators such as GZMB and PRF1, which encode Granzyme B and Perforin, respectively – the main effector molecules of CD8+ T-cells which predominate a Th1 immune response. This combination of simultaneously enhancing leukocyte activation and persistence within the tissues likely contributes towards worse long-term outcomes in individuals with higher concentrations of IL-1β, as seen in the 1-year mortality data by Andreasson et al (2017) [118].

In the case of lung transplantation, the early events immediately following engraftment accurately predict the longer-term outcomes. Primary graft dysfunction (PGD) is a significant cause of poor short- and long-term outcomes for transplant recipients [66]. All grades of PGD were found in a 2008 study for example, to be independent predictors of Bronchiolitis Obliterans (BOS) in transplant recipients [139]. By promoting early signals that initiate activation of T-cells, it is entirely plausible that this mechanism plays the role by which increasing IL-1β levels reduce recipient survival due to persistent immune activation at the site of the engrafted tissue.

We observed significant decreases in levels of genes encoding subunits of the 20S proteasome, namely PSMB5, PSMB7 and PSMB8, in stimulated lungs. The proteasome performs important regulatory processes within the cell, ensuring that improperly produced or dysfunctional proteins are degraded and recycled, as well as playing key roles in MHC class I antigen preparation. Improper proteasome function has also been associated with a number of autoimmune diseases such as Systemic Lupus Erythematosus (SLE).

Whilst we see a down-regulation of complement-activating protein production in our perfusions, we also see a similar trend with CD46. Suzuki et al (2013), note that in a study of BOS patients, CD46 down-regulation was seen to be more prevalent in individuals with the disease, suggesting that a lack of complement regulation enhanced disease progression [141]. The decrease in protective signals from cells mediated by IL-1β would suggest higher susceptibility to the damage provoked by immune responses that may be activated by engraftment of tissue into the recipient. It is interesting to note

that the overall expression of complement genes is decreased however, due to the importance of the role that the complement pathway plays in IRI development and progression. C3 is a well characterised 'anaphylatoxin' that potently attracts leukocytes, whilst C1QB forms a component of the initial complex involved in progression of the classical pathway. The observations here therefore warrant further investigation due to the importance of complement in mediating tissue damage during IRI, and the seemingly conflicting results in terms of how these relate to IL-1β stimulation, as complement has the ability to stimulate production of IL-1β and vice-versa.

Changes in RNA level do not necessarily reflect a resulting change in expression of protein, meaning that it is difficult to interpret the significance of many of the results without complementary protein expression data. With this in mind, an aspect of the original work plan included some validation of our results using alternative assay formats. Unfortunately, given when the EVLP work was concluded relative to the COVID-19 pandemic, this has not been possible given time constraints. The original plan utilised PCR, as well as immunofluorescent (IF) staining to assess some key pathways that we observed as being affected, such as ICAM1 production. This would have been insightful to undertake, as there are obviously a plethora of post-translational modifications and mechanisms that can switch off protein expression, which our analysis here does not offer any real insight into. The feasibility of this will be looked at in the near future prior to the reopening of laboratories within the medical school at Newcastle University.

Concluding remarks

IL-1β stimulation of lungs undergoing EVLP facilitated an increase in levels of RNA for genes involved in a number of different cellular processes. Cellular adhesion, apoptosis, innate/adaptive immunity, TNF signalling, and T-cell activation were all up-regulated via the actions of the cytokine. Down-regulation of a number of cytoprotective and normal regulatory genes was also observed, indicating a reduction in normal immune homeostasis. Together, these results suggested early adhesion events and inflammation facilitates down-regulation of anti-inflammatory and pro-apoptotic signals, enabling activation and persistence of lymphocyte responses. The data here could suggest pathways of interest to explore, but due to the small sample size and the discovery nature of the work, it is difficult to draw definitive conclusions regarding the absolute effects of IL-1β on the RNA profile of perfused lungs.

CHAPTER 6

-

DISCUSSION, CONCLUSIONS AND FUTURE DIRECTIONS

Chapter 6 – Discussion and conclusions

Discussion

The advent of clinical EVLP in the 21st century has opened a realm of possibilities regarding the future of lung transplantation. Widespread application of perfusion could increase donor-lung availability, reduce waiting list mortality and improve quality of life for individuals who have likely struggled with day-to-day activities beforehand. However, decision making on use of organs in transplantation still relies on physiological outputs and generalised criteria.

Research has highlighted that biomarkers measured during the perfusion process prior to transplantation can offer insight into the viability and health of an organ. Differences in IL-1β level measured after just 30 minutes of EVLP can accurately predict 1-year patient mortality, highlighting the potency of which IL-1β coordinates and orchestrates damage to the donor graft [118]. We chose to investigate the roles of IL-1β during EVLP and exacerbate some of the mechanisms of injury facilitated by higher levels of this cytokine.

The original hypothesis of our work was that IL-1β stimulation *ex vivo* would provoke increasing levels of leukocyte adhesion, endothelial dysfunction and an increased inflammatory profile in the tissue of stimulated lungs. In order to do this, we established a pre-clinical model whereby we could measure real-time levels of neutrophils in a split lung model of perfusion, whilst acquiring transcriptomic data from biopsied tissue post-EVLP.

When we infused IL-1β into one lung from each pair in our paired split lung model, we identified lower circulating numbers of neutrophils within the perfusate, indicating a higher degree of trapping within the graft. This also produced a higher degree of weight gain, plotted as both percentage and absolute increases over the course of perfusion. This observation correlated strongly with endothelial activation, as shown by release of ICAM-1 and vWF into the perfusate. Activation of the endothelium *ex vivo* was then replicated using functional assays *in vitro*, whereby cultured cells expressed higher levels of adhesion markers and facilitated greater neutrophil adhesion when stimulated with perfusates from IL-1β-infused lungs. Biopsies from these lungs also showed an altered RNA transcriptome, with lungs showing higher levels of genes involved in adhesion, inflammation, TNF signalling, innate/adaptive immunity and T cell activation. This suggests that not only are acute, inflammatory changes stimulated via IL-1β infusion, but also that mechanisms enabling a sustained immune response to donor tissue are able to persist. Therefore, whilst most of the focus of our study is on the relationship between leukocytes and the endothelium, the data also helps to underline other consequences of injury to lung tissue.

As part of our work we focused here on neutrophils and their interaction with the endothelium. During IRI following transplantation, the influx and activation of neutrophils is the major mediator of inflammation and subsequent tissue damage, as indicated by both pre-clinical modelling of IRI. As previously discussed, this influx occurs after accumulation of cytokines and DAMPs within the donor-lung, priming the recipient neutrophils to effectively extravasate out of circulation and into the tissues. One study for example, used a pre-clinical mouse model of PGD and established that NETs could be detected, with level of these correlating with tissue damage [74]. As has been mentioned previously, one failure of the work here was not to clearly establish the fates of the neutrophils that we infused into our circuit during EVLP. Neutrophil activation results in increased phagocytosis, degranulation and NETosis, ultimately resulting in increased rate of cell death. Moreover, more analysis of the lung tissue and quantification of any known neutrophil stimuli present would have provided more insight into the microenvironment that the neutrophils were encountering upon infusion and thus given more clues as to their likely fate, be it activation or NETosis.

Whilst our model did not reflect a reperfusion model of transplantation, in that it was not assessing the impact of neutrophil influx on inflammation within the lungs, it would have been interesting to look for the presence of neutrophil stimulatory molecules within homogenised tissues from our split lung cohort. We would propose looking for potent chemoattractants such as ATP and IL-8, as well as examining protein levels of NETs and other molecular entities associated with neutrophil degranulation. These data could provide more insight into the environment that the neutrophil would likely enter upon reperfusion injury, with the lung tissue having been exposed to IL-1β beforehand. This approach could be combined with a porcine model of complete organ reperfusion to give a much more detailed picture of how potent the effects of IL-1β are on not only mediating infiltration of neutrophils, but also their subsequent activation once into the local microenvironment.

The role of IL-1 pathways in the context of lung injury is well established, with increased activation of the pathway and its associated mediators related to increased severity of diseases such as IPF [117, 142]. Minimisation of this pathway during EVLP prior to transplantation would therefore appear to be of key importance in maintaining an immunological homeostasis between the donor graft and recipient, which is nicely demonstrated by Andreasson et al [118]. We feel that our data adds to this narrative, as IL-1β served to facilitate cellular dysfunction in our study. When we blocked IL-1β in perfusate samples *in vitro*, activation conferred on these cells was abolished. Whilst we accept that levels of endogenous cytokine in the perfusate during EVLP do not usually reach the levels seen in our stimulated lung cohort, the data shown by Andreasson et al highlights how sensitive the lung environment is to subtle changes in IL-1β concentration. This demonstrates that our observations have likely occurred post-transplant in these lungs, but on a much smaller, gradual timescale.

Our model utilised human donor-lungs to model the events following transplant reperfusion of the graft. Whilst these results are easier to relate to the clinical situation, it perhaps lacks the post-transplant events of a mouse or porcine model of transplantation. These models can provide additional information regarding lung function following surgery, which our system is unable to do [53]. However, we feel the advantage of using human tissues and samples in the work depicted here lies in the fact that these have been subjected to complex, peri-transplant damage arising from events such brain-death cytokine storm and mechanical stress caused by ICU ventilation over the course of the donation process. This makes the results easier to relate to the *in vivo* microenvironment and thus the clinical scenario of transplantation.

One shortcoming of the work is the lack of validations for the RNA analysis performed in Chapter 5. Moving forward, completion of these PCRs and immunofluorescence assays will be a priority, with a view to publication of this work in the future.

Overall, I feel that the observations compel me to suggest measurement of IL-1β during EVLP would provide a reliable biomarker of post-transplant success to aid decision-making around organ suitability. This approach could be coupled to a strategy of therapeutic blockade of IL-1β, though this blockade needs validation *ex vivo* rather than just the *in vitro* system used here to confirm these observations. Over the course of just 3 hours, a notable difference between lungs that received a bolus of IL-1β compared to control lungs was observed. We feel that application of an IL-1β NAb or IL-1Ra therapeutic during EVLP could potentially dampen down inflammation provoked by ischaemia or the retrieval process, particularly given that these could be administered at higher doses than possible *in vivo*. As previously stated however, these observations required confirmation on a larger cohort. This would ultimately help to diminish the resultant effects of reperfusion injury following transplantation. The clinical significances of this could be twofold. Firstly, transplanted lungs could have improved function immediately following transplant, resulting in shorter ICU stays and higher rates of survival. Secondly, a higher number of donor-lungs could be made available for transplant, reducing waiting list mortality.

Conclusions

The work shown in this thesis can be divided into 3 main conclusions, with the findings of each summarised below:

1) Neutrophils were measured in real-time in the perfusate of lungs during EVLP. This was initially done in whole lung pairs before being moved into individual lungs into a novel, paired split-lung perfusion model. This system controlled for inter-donor differences between lungs and offered an effective opportunity to test the impact of interventions during EVLP. We also established a number of outputs that could be used to assess differences between perfusions.
2) The functional effects of IL-1β supplementation were investigated in both *ex vivo* and *in vitro* assay formats. Lungs from our split perfusion model that received a bolus of IL-1β exhibited greater neutrophil trapping during EVLP, higher levels of lactate and higher levels of endothelial damage markers. Perfusates from these lungs also facilitated enhanced adhesion of neutrophils to endothelial cells *in vitro*, enabled by increasing the expression of adhesion markers on the surface of the latter. These effects were diminished via blockade of IL-1β *in vitro*. These results indicate that *ex vivo* blockade of IL-1β, either through administration of an antibody or small molecule antagonist could reduce endothelial damage and subsequent neutrophil sequestration in engrafted tissues.
3) The RNA transcriptome of lungs was altered by infusion of IL-1β during EVLP. Pathways associated with leukocyte adhesion, inflammation, immune activation, TNF signalling and T-cell activation were markedly increased in stimulated lungs relative to their corresponding control lungs. Expression of genes involved in protective mechanisms such as ubiquitin degradation and complement regulation were downregulated in our treated lungs. These data highlighted the large transcriptional changes stimulated by IL-1β.

Strengths of studies

This project was performed as part of a wider research programme that has excellent access to human organs and tissues for pre-clinical studies. My study examines the genetic and protein changes stimulated on lungs by IL-1β when perfused in an *ex vivo* setting. This enables the complex underpinnings of cellular and immunological processes to be far more accurately mapped than in the case of simpler, *in vitro* experiments.

For our comparative perfusions, these utilised a split lung model of perfusion, whereby lung pairs were dissected and perfused simultaneously on separate perfusion circuits. This model controls for inter-genetic and physiological differences, ensuring that comparison of cell adhesion, production of cytokines and RNA profiles are more informative. Traditional perfusion-based studies use separate organs according to treatment group; therefore, we feel the split lung model used here offers a novel way to approach testing of interventions during perfusion, enabling improved throughput for therapeutic screening.

The neutrophil tracking model gave us a real-time pattern of cell adhesion to the vasculature during EVLP. Continued measurement of cell numbers in the perfusates meant that comparison of adhesion was consistently measured over 2 hours of EVLP rather than at a single time point, an approach which would be less informative than our approach. Any observation made regarding cell adhesion with our *ex vivo* work was re-confirmed by additional *in vitro* assays. As our observations complemented one another, we feel that this robustness of investigation adds validity to any conclusions drawn.

For the RNA profiling work depicted in Chapter 5 of this thesis, Nanostring technology was selected. This strategy does not use any amplification stages for the RNA of interest, unlike PCR or next-generation sequencing-based methods. It also tolerates degraded or low-quality RNA much more effectively and has an overall lower preparation time. Whilst our RNA was generally of a high quality, we feel that the reliability of this approach offers further validation to the results that we obtained from our analysis.

Limitations of studies

The most significant weakness to our work here is the low sample size. We used 4 donor-lungs as part of assays to investigate the functions of IL-1β during EVLP. The original aim for this work was to utilise 5 lung pairs, but unfortunately this was not possible due to time restrictions and shortage of research donor-lungs. This owed to the fact that our study was in direct competition with others, with previous EVLP and excessively long ischaemic time also being chosen as exclusion criteria. This of course then subsequently impacted on availability of perfusates and tissue for *in vitro* functional assays and RNA analysis, respectively.

During our model optimisations in Chapter 3, and indeed the later work investigating IL-1β, we used freshly isolated human primary neutrophils. Whilst our approach utilised a negative selection method – i.e. less immunogenic than a traditional density centrifugation approach, it is entirely possible that neutrophils from different donors activated to a greater or lesser degree for different EVLPs. Moving forwards with our model, we would put aside a small sample to assess for activation following perfusion. This would enable us to highlight any EVLP for which neutrophil activation status was particularly heightened. Along with this, we did not investigate into the definitive fate of neutrophils, other than confirming we could see them in the tissue. This could be looked into more in future work.

Regarding the work depicted in Chapters 4 and 5, the concluding statements remark that blockade of IL-1β *ex vivo* could potentially improve lung function during EVLP and subsequent transplantation. This was something that we did for our functional *in vitro* assays but were unable to extend to our *ex vivo* system. Being able to use samples collected from perfusions in which we had both infused IL-1β and blocked endogenous levels of the cytokine would have been more informative than simply the former.

The stimulation time with IL-1β during EVLP was for 3 hours prior to obtaining and storing samples for RNA analysis. This is a relatively short activation time and means that gene expression is likely lower than if we were to have increased the duration of stimulation. Future studies would aim to increase this where possible, as significant oedema often meant that it would have been unlikely that we would have been able to extend perfusion times much beyond this.

The cytokine blockade assays in Chapter 4 for our microfluidic flow assays did not use an appropriate IgG control. Whilst the assay did have negative controls in, we would look to add these in to give a true indication of any non-specific Fc receptor binding and blockade caused by addition of an IgG into the model.

Profiling of lungs in Chapter 5 was done of tissue RNA levels only. This meant that we did not observe whether alterations in transcriptomic activity had any subsequent effects at the protein level. For our RNA analysis, we chose an RNA profiling method, rather than sequencing. This would have provided a

much wider scope of genes to examine rather than the panel of 594 assessed with the Nanostring technology.

The work in Chapter 5 examined RNA from tissue biopsies of four lung pairs as part of a split lung model of perfusion. As can be seen in many genes here, one lung-pair often did not follow the trend of the others, significantly altering the final result. Thus, a larger cohort size would enhance the robustness of our data. Analysis of genes was also performed from a single tissue biopsy from each perfused lung. This means that a large amount of information has been ascertained for each individual organ from a single site, whereas gene expression is likely markedly different across different regions of the lungs we perfused.

Regarding our perfusion set-up, we designed tubing to allow simultaneous oxygenation of both lungs from one ventilator. We felt that this approach meant that whilst we were more accurately mimicking the *in vivo* scenario of reperfusion, as our model aimed to. However, the air from our ventilator will favour the area of least resistance, meaning that more oxygen may be preferentially delivered to a lung with more compliance, relative to the other. This means that the higher pressures exhibited on the airways in lungs with greater oedema likely further exacerbated the difference in oxygenation between lungs with differing function. Gradual build-up of CO_2 would result in hypoxia and eventual acidosis, which as discussed previously links with over-activation of the inflammasome and the pathways being investigated as part of this work. Moving this approach forward therefore, we would aim to ventilate lungs in split pairs separately, to ensure that both received the same level of ventilation *ex vivo*.

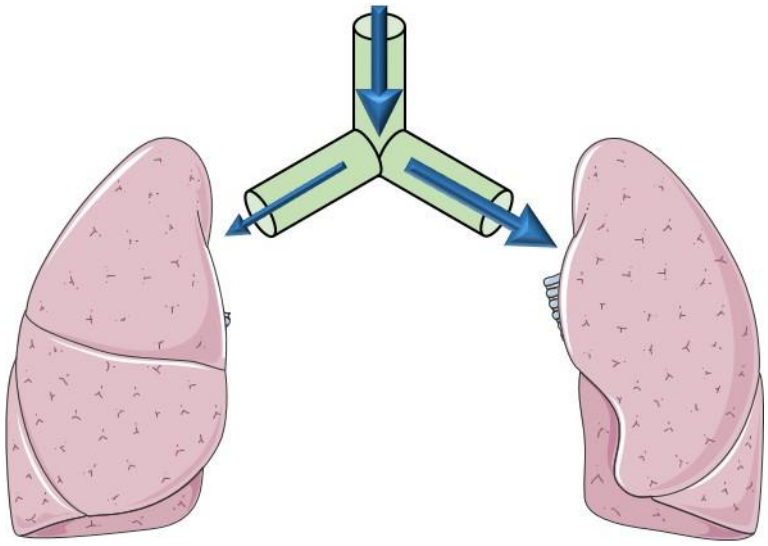

Fig. 6.1. – Split lung ventilation strategy. Air delivered from the ventilator will favour the path of least resistance, meaning that the lung with inherently worse function will gradually receive less and less oxygenation.

Future directions

The role of IL-1β in EVLP

The work here highlights the range of functions elicited by the pro-inflammatory cytokine IL-1β in EVLP. The *in vitro* data suggests that blockade of IL-1β would be beneficial during EVLP. This thought underpins how we believe this work could be progressed on:

1) Repeat work performed in Chapters 4 and 5 using split lung model with a neutralising antibody (NAb) or small molecular antagonist to block either endogenous IL-1β or IL-1R. We would hypothesise the opposite observations to IL-1β stimulation, namely increased cell numbers *ex vivo*, reduced oedema formation and reduced activation of endothelium *in vitro*
2) Repeat targeted RNA analysis on tissues from these lungs to observe, hypothetically, reductions in genes associated with pro-inflammatory pathways, adhesion marker expression and lymphocyte activation

Longer-term, it is hoped that this research could progress onto two key clinical developments:

1) Testing of IL-1β signature in EVLP perfusate and using this information to aid peri-transplant decision making
2) A clinical trial whereby a cohort of lungs are treated with an anti-IL-1β therapy during EVLP and compared to an untreated cohort

Future developments for EVLP research

Real-time cytokine measurement during perfusion

The work performed as part of this thesis and by previously by Dr Anders Andreasson highlights the importance of IL-1β concentration during EVLP. The question remains of how to utilise this information moving forward in a clinical sense. Newcastle University, in collaboration with MyCartis, have developed a rapid cytokine testing platform which enables IL-1β concentration to be produced in <30 minutes. This uses a similar experimental approach to ELISA or MSD formats, by measuring absorbance relative to pre-made standards.

As many of the current criteria for judging lung transplant suitability have come under scrutiny in recent years. This additional information could therefore prove invaluable to surgical teams when making a decision on transplantation. We have already performed testing of IL-1β in real-time during a research EVLP with extremely promising results.

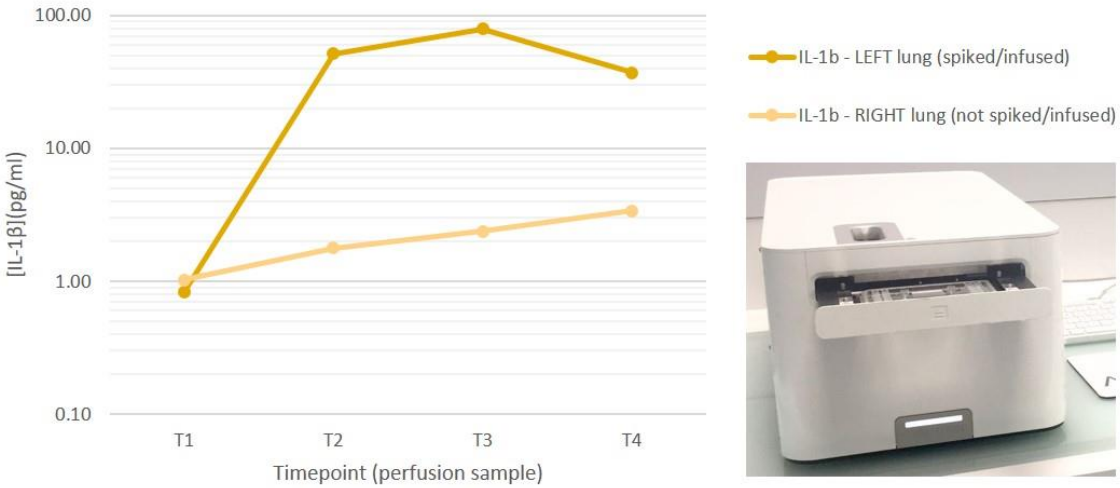

Fig. 6.2. – MyCartis™ Evaluation® platform – real-time cytokine testing. The Evaluation platform enables rapid, accurate testing of IL-1β concentration during EVLP. During a split lung EVLP (not in Chapter 4/5 cohort) we could detect differences in IL-1β in real-time. This would provide additional information to transplant centres on the suitability of donor-lung(s) for transplant.

Lobar model of EVLP

Joseph Barsby completed an MRes project as part of our wider research group in 2019. The focus of this work was to develop and use a lobar model of EVLP that moved one step further than a split lung perfusion model, enabling multiple treatments or doses to be simultaneously run with tissues from the same donor. Porcine lungs were retrieved as by-products from food production, this being as close

to a clinical protocol as possible. These were then dissected into constituent lobes and perfused simultaneously.

The project ran into difficulty due to poor quality of porcine donor-lungs. However, the concept of lobar perfusion would allow additional treatments and comparisons between identical donor tissue to be made, advancing on from the model employed in Chapters 4 and 5 of this thesis. Further investigation into this approach is warranted.

Fig. 6.3. – Porcine lobar perfusion. Two porcine lobes are perfused simultaneously using roller pumps with Medtronic lung platforms.

Thermal imaging

One potential way to gain information about the perfusion of lungs is by examining how effectively they are warmed during EVLP. Fig. 6.4 shows an example of one of our split lung perfusions. Darker regions indicate a lower temperature and would indicate that warmed perfusate solution has not effectively reached these regions of the lung, indicating the presence of micro thrombi due to poor flushing upon retrieval. This is one way that additional information can be gleaned from one of our research perfusions. This of course would need standardising, as we found that images taken of one lung show a large degree of variation in temperature, depending on the area photographed. Perhaps a set series of positions could be used for this.

We also felt that it would be prudent to have a way of comparing the tissue relative to material or liquid of a known temperature. Imaging pre-warmed perfusate could therefore ensure greater accuracy for reporting relative temperature of lung tissue *ex vivo*. Further development of this method will be published in the future.

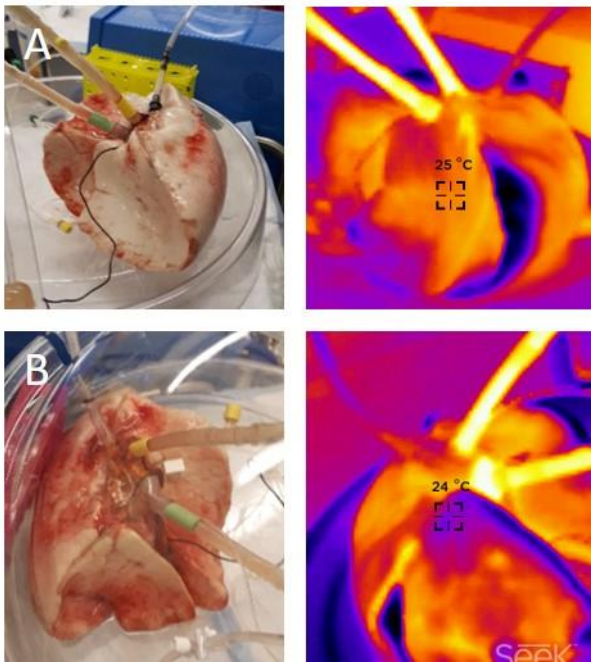

Fig. 6.4. – Thermal images of a split lung pair. Thermal images are shown of (A) IL-1β-stimulated and (B) control lungs from Donor 1 in our split lung approach. Darker, black regions indicate poor perfusion to the periphery of the lungs. No significant differences in temperature were observed when we used this approach in our model. However, this could be taken forward if refined and standardised.

Ongoing ex vivo perfusion-based research at Newcastle University

Sphingosine-1-phosphate supplementation in EVLP

Miss Jenny Gilmour is investigating sphingosine-1-phosphate (S1P) as a therapeutic intervention during EVLP. The project aims to test modulation of S1P and its receptors in a number of functional assays *in vitro* with pulmonary endothelial cells and in an *ex vivo* porcine system. This will also involve collaborative work with the Lund group in Sweden to test various S1P agonists in porcine perfusion. It is hypothesised that these could reduce endothelial permeability and improve reduce lung damage during EVLP and during subsequent transplantation.

Cell-based therapy delivery during EVLP

Miss Chelsea Griffiths is investigating amniotic epithelial cells and whether these could be used as a therapy during EVLP. Her PhD project has involved isolating these cells from placental tissue and investigating their functions, as well as those of exosomes produced by these cells. She has already shown that these cells can down-regulate an inflammatory signature in macrophages *in vitro*. It is postulated that these effects may translate to EVLP, and could have general, wide-ranging immunomodulatory properties. This would make these cells or their exosomes an effective pre-transplant therapeutic for marginal lungs.

Investigating biomarkers of heart function during perfusion

Dr Lu Wang is investigating hypothermic oxygenated perfusion of hearts and whether this can safely preserve contractile function for up to 12 hours, through reduction of mitochondrial dysfunction, inflammation and cardiomyocyte death. Human hearts, declined for transplantation, are retrieved in standard fashion and preserved by either hypothermic oxygenated perfusion or static cold storage, before being reanimated on the modified Langendorff system at 37°C for 4 hours for functional analysis. Tissues and perfusate samples collected before and after reperfusion will be compared to look for markers that correlate with hearts' contractile function post-preservation. The promising markers identified will be studied in the samples collected from patients who undergo clinical heart transplantation, in order to investigate their clinical relevance.

Concluding remarks

EVLP now offers an effective means of increasing the lung donor pool. Over the last 20 years since its first clinical use, continued refinement and development mean that more grafts are being preserved *ex vivo* than ever before. However, there remains a high proportion of mortality on the waiting list for a suitable donor-lung, meaning that there is still an unmet need in the world of transplantation. Much of the work performed here and indeed elsewhere, highlights the importance of understanding the molecular and cellular mechanisms that underpin EVLP so that we may address the clinical questions that remain today. It is truly an exciting time for transplantation.

Reference list

1. Hardy, J.D., et al., *Lung Homotransplantation in Man: Report of the Initial Case.* JAMA, 1963. **186**(12): p. 1065-1074.
2. *Unilateral Lung Transplantation for Pulmonary Fibrosis.* New England Journal of Medicine, 1986. **314**(18): p. 1140-1145.
3. McGregor, C.G., et al., *Early results of single lung transplantation in patients with end-stage pulmonary fibrosis.* J Thorac Cardiovasc Surg, 1989. **98**(3): p. 350-4.
4. Reitz, B.A., J.L. Pennock, and N.E. Shumway, *Simplified operative method for heart and lung transplantation.* J Surg Res, 1981. **31**(1): p. 1-5.
5. Goldberg, M., et al., *A comparison between cyclosporin A and methylprednisolone plus azathioprine on bronchial healing following canine lung autotransplantation.* J Thorac Cardiovasc Surg, 1983. **85**(6): p. 821-6.
6. *NHS-BT - Donation after brainstem death*. 2020 07/08/2020]; Available from: https://www.odt.nhs.uk/deceased-donation/best-practice-guidance/donation-after-brainstem-death/.
7. Romano, R., et al., *Inflammatory response following DCD and DBD lung transplantation.* European Respiratory Journal, 2016. **48**(suppl 60): p. OA3333.
8. Inci, I., *Donors after cardiocirculatory death and lung transplantation.* Journal of Thoracic Disease, 2017. **9**(8): p. 2660-2669.
9. Mohty, M., *Mechanisms of action of antithymocyte globulin: T-cell depletion and beyond.* Leukemia, 2007. **21**(7): p. 1387-1394.
10. Ivulich, S., et al., *The Evolution of Lung Transplant Immunosuppression.* Drugs, 2018. **78**(10): p. 965-982.
11. Furuya, Y., et al., *The Impact of Alemtuzumab and Basiliximab Induction on Patient Survival and Time to Bronchiolitis Obliterans Syndrome in Double Lung Transplantation Recipients.* Am J Transplant, 2016. **16**(8): p. 2334-41.
12. Jaksch, P., et al., *Antithymocyte globulin induction therapy improves survival in lung transplantation for cystic fibrosis.* Transpl Int, 2013. **26**(1): p. 34-41.
13. Lima, O., et al., *Effects of methylprednisolone and azathioprine on bronchial healing following lung autotransplantation.* The Journal of Thoracic and Cardiovascular Surgery, 1981. **82**(2): p. 211-215.
14. Fan, Y., Y.B. Xiao, and Y.G. Weng, *Tacrolimus versus cyclosporine for adult lung transplant recipients: a meta-analysis.* Transplant Proc, 2009. **41**(5): p. 1821-4.
15. Penninga, L., et al., *Tacrolimus versus cyclosporin as primary immunosuppression for lung transplant recipients.* Cochrane Database Syst Rev, 2013(5): p. Cd008817.
16. Transplant, N.B.a. *Transplant activity report*. 2019; Available from: https://www.organdonation.nhs.uk/helping-you-to-decide/about-organ-donation/statistics-about-organ-donation/transplant-activity-report/.
17. *NHS-BT Transplant activity report*. 2019 [cited 2020; Available from: https://www.organdonation.nhs.uk/helping-you-to-decide/about-organ-donation/statistics-about-organ-donation/transplant-activity-report/.
18. De Vleeschauwer, S.I., et al., *Medium-term outcome after lung transplantation is comparable between brain-dead and cardiac-dead donors.* J Heart Lung Transplant, 2011. **30**(9): p. 975-81.
19. De Vleeschauwer, S., et al., *Early outcome after lung transplantation from non-heart-beating donors is comparable to heart-beating donors.* J Heart Lung Transplant, 2009. **28**(4): p. 380-7.
20. De Oliveira, N.C., et al., *Lung transplantation with donation after cardiac death donors: long-term follow-up in a single center.* J Thorac Cardiovasc Surg, 2010. **139**(5): p. 1306-15.
21. Van De Wauwer, C., et al., *The use of non-heart-beating lung donors category III can increase the donor pool.* Eur J Cardiothorac Surg, 2011. **39**(6): p. e175-80; discussion e180.

22. *Increasing Lung Transplant Availability Using Normothermic Ex Vivo Lung Perfusion (EVLP) at a Dedicated EVLP Facility*. 2018 28/01/20]; Available from: https://clinicaltrials.gov/ct2/show/NCT03641677.
23. Sommer, W., et al., *Extended criteria donor lungs and clinical outcome: results of an alternative allocation algorithm.* J Heart Lung Transplant, 2013. **32**(11): p. 1065-72.
24. MacGowan, G.A., et al., *Effects of drug abuse, smoking and alcohol on donor hearts and lungs.* Transpl Int, 2019. **32**(10): p. 1019-1027.
25. Steen, S., et al., *Transplantation of lungs from a non-heart-beating donor.* The Lancet, 2001. **357**(9259): p. 825-829.
26. Steen, S., et al., *First Human Transplantation of a Nonacceptable Donor Lung After Reconditioning Ex Vivo.* The Annals of Thoracic Surgery, 2007. **83**(6): p. 2191-2194.
27. Cypel, M., et al., *Experience with the first 50 ex vivo lung perfusions in clinical transplantation.* J Thorac Cardiovasc Surg, 2012. **144**(5): p. 1200-6.
28. Dark, J.H., et al., *323 Successful Transplantation of Unusable Donor Lungs Using Ex-Vivo Lung Perfusion: The Newcastle Experience.* The Journal of Heart and Lung Transplantation, 2012. **31**(4): p. S115.
29. Fildes, J.E., et al., *Clinical Outcome of Patients Transplanted with Marginal Donor Lungs via Ex Vivo Lung Perfusion Compared to Standard Lung Transplantation.* Transplantation, 2015. **99**(5): p. 1078-83.
30. Fang, A., et al., *Elevated Pulmonary Artery Pressure Is a Risk Factor for Primary Graft Dysfunction Following Lung Transplantation for Idiopathic Pulmonary Fibrosis.* Chest, 2011. **139**(4): p. 782-787.
31. Resnick, N. and M.A. Gimbrone, Jr., *Hemodynamic forces are complex regulators of endothelial gene expression.* Faseb j, 1995. **9**(10): p. 874-82.
32. Jain, S.V., et al., *The role of high airway pressure and dynamic strain on ventilator-induced lung injury in a heterogeneous acute lung injury model.* Intensive care medicine experimental, 2017. **5**(1): p. 25-25.
33. Beitler, J.R., A. Malhotra, and B.T. Thompson, *Ventilator-induced Lung Injury.* Clinics in chest medicine, 2016. **37**(4): p. 633-646.
34. Andreasson, A.S.I., J.H. Dark, and A.J. Fisher, *Ex vivo lung perfusion in clinical lung transplantation—State of the art.* European Journal of Cardio-Thoracic Surgery, 2014. **46**(5): p. 779-788.
35. Steen, S., et al., *Transplantation of lungs from non–heart-beating donors after functional assessment ex vivo.* The Annals of Thoracic Surgery, 2003. **76**(1): p. 244-252.
36. Cypel, M., et al., *Technique for Prolonged Normothermic Ex Vivo Lung Perfusion.* The Journal of Heart and Lung Transplantation, 2008. **27**(12): p. 1319-1325.
37. Warnecke, G., et al., *Normothermic perfusion of donor lungs for preservation and assessment with the Organ Care System Lung before bilateral transplantation: a pilot study of 12 patients.* The Lancet, 2012. **380**(9856): p. 1851-1858.
38. Cypel, M., et al., *Normothermic ex vivo lung perfusion in clinical lung transplantation.* N Engl J Med, 2011. **364**(15): p. 1431-40.
39. Sanchez, P.G., et al., *The NOVEL Lung Trial One-Year Outcomes.* The Journal of Heart and Lung Transplantation, 2014. **33**(4): p. S71-S72.
40. Warnecke, G., et al., *Normothermic ex-vivo preservation with the portable Organ Care System Lung device for bilateral lung transplantation (INSPIRE): a randomised, open-label, non-inferiority, phase 3 study.* The Lancet Respiratory Medicine, 2018. **6**(5): p. 357-367.
41. Loor, G., et al., *Results of the OCS Lung EXPAND International Trial Using Portable Normothermic OCS Lung Perfusion System (OCS) to Recruit and Evaluate Extended Criteria Donor (ECD) Lungs.* The Journal of Heart and Lung Transplantation, 2018. **37**(4): p. S147.

42. Aboelnazar, N.S., et al., *Negative pressure ventilation decreases inflammation and lung edema during normothermic ex-vivo lung perfusion.* The Journal of Heart and Lung Transplantation, 2018. **37**(4): p. 520-530.
43. Steinmeyer, J., et al., *Cellular and acellular ex vivo lung perfusion preserve functional lung ultrastructure in a large animal model: a stereological study.* RESPIRATORY RESEARCH, 2018. **19**(1): p. 238.
44. Yeung, J.C., et al., *Physiologic assessment of the ex vivo donor lung for transplantation.* The Journal of Heart and Lung Transplantation, 2012. **31**(10): p. 1120-1126.
45. Aboelnazar, N., et al., *Improved Outcomes with Negative Pressure Ventilation (NPV) during Normothermic Ex Vivo Lung Perfusion.* Transplantation, 2017. **101**(5S-3).
46. Nelson, K., et al., *Determination of Optimum Ventilation Strategy for Ex-Vivo Lung Perfusion: Comparing Negative and Positive Pressure Ventilation.* The Journal of Heart and Lung Transplantation, 2015. **34**(4): p. S270.
47. Ricard, J.D., D. Dreyfuss, and G. Saumon, *Ventilator-induced lung injury.* European Respiratory Journal, 2003. **22**(42 suppl): p. 2s.
48. *The University of Alberta Negative Pressure Ventilation Ex-Vivo Lung Perfusion (NPV-EVLP) Trial (UA NPV-EVLP)*. 2017; Available from: https://clinicaltrials.gov/ct2/show/NCT03293043.
49. *Clinical trial of Ex-Vivo Organ Support System results in 12 successful lung transplants*. 2019; Available from: https://www.globenewswire.com/news-release/2019/11/07/1943431/0/en/UNIVERSITY-HOSPITAL-FOUNDATION-FUND-RECIPIENTS-POISED-TO-REVOLUTIONIZE-ORGAN-TRANSPLANTS.html.
50. Ingemansson, R., et al., *Clinical Transplantation of Initially Rejected Donor Lungs After Reconditioning Ex Vivo.* The Annals of Thoracic Surgery, 2009. **87**(1): p. 255-260.
51. Stone, J.P., et al., *Altered Immunogenicity of Donor Lungs via Removal of Passenger Leukocytes Using Ex Vivo Lung Perfusion.* American Journal of Transplantation, 2016. **16**(1): p. 33-43.
52. Stone, J.P., et al., *Ex Vivo Normothermic Perfusion Induces Donor-Derived Leukocyte Mobilization and Removal Prior to Renal Transplantation.* Kidney international reports, 2016. **1**(4): p. 230-239.
53. Cypel, M., et al., *Functional Repair of Human Donor Lungs by IL-10 Gene Therapy.* Science Translational Medicine, 2009. **1**(4): p. 4ra9.
54. Weathington, N.M., et al., *Ex vivo lung perfusion as a human platform for preclinical small molecule testing.* JCI insight, 2018. **3**(19): p. e95515.
55. Andreasson, A., et al., *The effect of ex vivo lung perfusion on microbial load in human donor lungs.* The Journal of Heart and Lung Transplantation, 2014. **33**(9): p. 910-916.
56. Chaparro, C., et al., *Causes of death in lung transplant recipients.* J Heart Lung Transplant, 1994. **13**(5): p. 758-66.
57. Nosotti, M., P. Tarsia, and L.C. Morlacchi, *Infections after lung transplantation.* Journal of thoracic disease, 2018. **10**(6): p. 3849-3868.
58. Mariscal, A., et al., *Pig lung transplant survival model.* Nature Protocols, 2018. **13**(8): p. 1814-1828.
59. Yeung, J.C., et al., *Ex vivo adenoviral vector gene delivery results in decreased vector-associated inflammation pre- and post-lung transplantation in the pig.* Mol Ther, 2012. **20**(6): p. 1204-11.
60. Emaminia, A., et al., *Adenosine A(2)A agonist improves lung function during ex vivo lung perfusion.* Ann Thorac Surg, 2011. **92**(5): p. 1840-6.
61. *Increasing Lung Transplant Availability Using Normothermic Ex Vivo Lung Perfusion (EVLP) at a Dedicated EVLP Facility*. 2018; Available from: https://clinicaltrials.gov/ct2/show/NCT03641677.
62. Fisher, A., et al., *An observational study of Donor Ex Vivo Lung Perfusion in UK lung transplantation: DEVELOP-UK.* Health Technol Assess, 2016. **20**(85).

63. Gilmour, J., et al., *Normothermic machine perfusion of donor-lungs ex-vivo: promoting clinical adoption.* Curr Opin Organ Transplant, 2020. **25**(3): p. 285-292.
64. Whitson, B.A., et al., *Primary graft dysfunction and long-term pulmonary function after lung transplantation.* J Heart Lung Transplant, 2007. **26**(10): p. 1004-11.
65. Huang, H.J., et al., *Late primary graft dysfunction after lung transplantation and bronchiolitis obliterans syndrome.* American journal of transplantation : official journal of the American Society of Transplantation and the American Society of Transplant Surgeons, 2008. **8**(11): p. 2454-2462.
66. Morrison, M.I., T.L. Pither, and A.J. Fisher, *Pathophysiology and classification of primary graft dysfunction after lung transplantation.* Journal of Thoracic Disease, 2017. **9**(10): p. 4084-4097.
67. de Perrot, M., et al., *Ischemia-reperfusion-induced lung injury.* Am J Respir Crit Care Med, 2003. **167**(4): p. 490-511.
68. Dhaliwal, K., et al., *Monocytes control second-phase neutrophil emigration in established lipopolysaccharide-induced murine lung injury.* Am J Respir Crit Care Med, 2012. **186**(6): p. 514-24.
69. Christie, J.D., et al., *Association of protein C and type 1 plasminogen activator inhibitor with primary graft dysfunction.* Am J Respir Crit Care Med, 2007. **175**(1): p. 69-74.
70. Christie, J.D., et al., *Plasma Levels of Receptor for Advanced Glycation End Products, Blood Transfusion, and Risk of Primary Graft Dysfunction.* American Journal of Respiratory and Critical Care Medicine, 2009. **180**(10): p. 1010-1015.
71. Shah, R.J., et al., *A panel of lung injury biomarkers enhances the definition of primary graft dysfunction (PGD) after lung transplantation.* The Journal of heart and lung transplantation : the official publication of the International Society for Heart Transplantation, 2012. **31**(9): p. 942-949.
72. Covarrubias, M., et al., *Plasma intercellular adhesion molecule-1 and von Willebrand factor in primary graft dysfunction after lung transplantation.* Am J Transplant, 2007. **7**(11): p. 2573-8.
73. Krieglstein, C.F. and D.N. Granger, *Adhesion molecules and their role in vascular disease*.* American Journal of Hypertension, 2001. **14**(S3): p. 44S-54S.
74. Sayah, D.M., et al., *Neutrophil Extracellular Traps Are Pathogenic in Primary Graft Dysfunction after Lung Transplantation.* American Journal of Respiratory and Critical Care Medicine, 2015. **191**(4): p. 455-463.
75. De Perrot, M., et al., *Interleukin-8 release during early reperfusion predicts graft function in human lung transplantation.* Am J Respir Crit Care Med, 2002. **165**(2): p. 211-5.
76. Fisher, A.J., et al., *Elevated levels of interleukin-8 in donor lungs is associated with early graft failure after lung transplantation.* Am J Respir Crit Care Med, 2001. **163**(1): p. 259-65.
77. Machuca, T.N., et al., *Protein expression profiling predicts graft performance in clinical ex vivo lung perfusion.* Ann Surg, 2015. **261**(3): p. 591-7.
78. Tecchio, C., A. Micheletti, and M.A. Cassatella, *Neutrophil-derived cytokines: facts beyond expression.* Frontiers in immunology, 2014. **5**: p. 508-508.
79. Ishii, T., et al., *Neutrophil Elastase Contributes to Acute Lung Injury Induced by Bilateral Nephrectomy.* The American Journal of Pathology, 2010. **177**(4): p. 1665-1673.
80. Liu, G.Q., et al., *Src Phosphorylation of Endothelial Cell Surface Intercellular Adhesion Molecule-1 Mediates Neutrophil Adhesion and Contributes to the Mechanism of Lung Inflammation.* Arteriosclerosis Thrombosis and Vascular Biology, 2011. **31**(6): p. 1342-U242.
81. Lomas-Neira, J., et al., *Neutrophil-endothelial interactions mediate angiopoietin-2-associated pulmonary endothelial cell dysfunction in indirect acute lung injury in mice.* Am J Respir Cell Mol Biol, 2014. **50**(1): p. 193-200.
82. Mercer, P.F., et al., *Proteinase-activated receptor-1, CCL2, and CCL7 regulate acute neutrophilic lung inflammation.* Am J Respir Cell Mol Biol, 2014. **50**(1): p. 144-57.
83. Novitzky, D., et al., *Pathophysiology of pulmonary edema following experimental brain death in the chacma baboon.* Ann Thorac Surg, 1987. **43**(3): p. 288-94.

84. Shimamura, T., et al., *Protective role of nitric oxide in ischemia and reperfusion injury of the liver.* Journal of the American College of Surgeons, 1999. **188**(1): p. 43-52.
85. Tousoulis, D., et al., *The role of nitric oxide on endothelial function.* Curr Vasc Pharmacol, 2012. **10**(1): p. 4-18.
86. Fang, A., et al., *Elevated pulmonary artery pressure is a risk factor for primary graft dysfunction following lung transplantation for idiopathic pulmonary fibrosis.* Chest, 2011. **139**(4): p. 782-787.
87. Yu, H., et al., *Interleukin-8 Regulates Endothelial Permeability by Down-regulation of Tight Junction but not Dependent on Integrins Induced Focal Adhesions.* International Journal of Biological Sciences, 2013. **9**(9): p. 966-979.
88. Simms, H.H. and R. D'Amico, *Increased PMN CD11b/CD18 expression following post-traumatic ARDS.* Journal of Surgical Research, 1991. **50**(4): p. 362-367.
89. Ross, G.D. and V. Větvicka, *CR3 (CD11b, CD18): a phagocyte and NK cell membrane receptor with multiple ligand specificities and functions.* Clinical and experimental immunology, 1993. **92**(2): p. 181-184.
90. Nomellini, V., et al., *Dysregulation of Neutrophil CXCR2 and Pulmonary Endothelial ICAM-1 Promotes Age-Related Pulmonary Inflammation.* Aging and Disease, 2012. **3**(3): p. 234-247.
91. Horvath, B., et al., *Measurement of von Willebrand factor as the marker of endothelial dysfunction in vascular diseases.* Experimental and clinical cardiology, 2004. **9**(1): p. 31-34.
92. Tsushima, Y., et al., *The depletion of donor macrophages reduces ischaemia-reperfusion injury after mouse lung transplantation.* Eur J Cardiothorac Surg, 2014. **45**(4): p. 703-9.
93. Zhao, M., et al., *Alveolar macrophage activation is a key initiation signal for acute lung ischemia-reperfusion injury.* Am J Physiol Lung Cell Mol Physiol, 2006. **291**(5): p. L1018-26.
94. Tsushima, Y., et al., *The depletion of donor macrophages reduces ischaemia-reperfusion injury after mouse lung transplantation†.* European Journal of Cardio-Thoracic Surgery, 2013. **45**(4): p. 703-709.
95. Dhaliwal, K., et al., *Monocytes control second-phase neutrophil emigration in established lipopolysaccharide-induced murine lung injury.* American journal of respiratory and critical care medicine, 2012. **186**(6): p. 514-524.
96. Tatham, K.C., et al., *Retention and Activation of Donor Vascular Monocytes in Transplanted Lungs Suggests a Central Role in Primary Graft Dysfunction*, in *C34. IMMUNE REGULATION OF TRANSPLANT REJECTION*. 2016, American Thoracic Society. p. A4890-A4890.
97. Shah, R.J., et al., *Plasma monocyte chemotactic protein-1 levels at 24 hours are a biomarker of primary graft dysfunction after lung transplantation.* Translational research : the journal of laboratory and clinical medicine, 2012. **160**(6): p. 435-442.
98. Frick, A.E., et al., *Early protein expression profile in bronchoalveolar lavage fluid and clinical outcomes in primary graft dysfunction after lung transplantation.* Eur J Cardiothorac Surg, 2020.
99. Yang, Z., et al., *CD4+ T lymphocytes mediate acute pulmonary ischemia–reperfusion injury.* The Journal of Thoracic and Cardiovascular Surgery, 2009. **137**(3): p. 695-702.
100. Hoffman, S.A., et al., *Plasma cytokines and chemokines in primary graft dysfunction post-lung transplantation.* American journal of transplantation : official journal of the American Society of Transplantation and the American Society of Transplant Surgeons, 2009. **9**(2): p. 389-396.
101. Bobadilla, J.L., et al., *Th-17, Monokines, Collagen Type V, and Primary Graft Dysfunction in Lung Transplantation.* American Journal of Respiratory and Critical Care Medicine, 2008. **177**(6): p. 660-668.
102. Iwata, T., et al., *Anti-Type V Collagen Humoral Immunity in Lung Transplant Primary Graft Dysfunction.* Journal of immunology (Baltimore, Md. : 1950), 2008. **181**(8): p. 5738-5747.
103. Burlingham, W.J., et al., *IL-17–dependent cellular immunity to collagen type V predisposes to obliterative bronchiolitis in human lung transplants.* The Journal of Clinical Investigation, 2007. **117**(11): p. 3498-3506.

104. Li, L., et al., *NKT Cell Activation Mediates Neutrophil IFN-γ Production and Renal Ischemia-Reperfusion Injury.* The Journal of Immunology, 2007. **178**(9): p. 5899.
105. Sharma, A.K., et al., *Receptor for advanced glycation end products (RAGE) on iNKT cells mediates lung ischemia-reperfusion injury.* Am J Transplant, 2013. **13**(9): p. 2255-67.
106. Rieger, J.M., A.R. Shah, and J.M. Gidday, *Ischemia-reperfusion injury of retinal endothelium by cyclooxygenase- and xanthine oxidase-derived superoxide.* Exp Eye Res, 2002. **74**(4): p. 493-501.
107. Matsushima, S., H. Tsutsui, and J. Sadoshima, *Physiological and pathological functions of NADPH oxidases during myocardial ischemia-reperfusion.* Trends Cardiovasc Med, 2014. **24**(5): p. 202-5.
108. Zhang, J., et al., *ROS and ROS-Mediated Cellular Signaling.* Oxidative Medicine and Cellular Longevity, 2016. **2016**: p. 4350965.
109. Habas, K. and L. Shang, *Alterations in intercellular adhesion molecule 1 (ICAM-1) and vascular cell adhesion molecule 1 (VCAM-1) in human endothelial cells.* Tissue and Cell, 2018. **54**: p. 139-143.
110. Cantu, E., et al., *Gene set enrichment analysis identifies key innate immune pathways in primary graft dysfunction after lung transplantation.* Am J Transplant, 2013. **13**(7): p. 1898-904.
111. Losa García, J.E., et al., *Evaluation of inflammatory cytokine secretion by human alveolar macrophages.* Mediators of Inflammation, 1999. **8**(1): p. 43-51.
112. Zhang, Y., et al., *Enhanced IL-1 beta and tumor necrosis factor-alpha release and messenger RNA expression in macrophages from idiopathic pulmonary fibrosis or after asbestos exposure.* J Immunol, 1993. **150**(9): p. 4188-96.
113. Barlo, N.P., et al., *Genetic variability in the IL1RN gene and the balance between interleukin (IL)-1 receptor agonist and IL-1β in idiopathic pulmonary fibrosis.* Clin Exp Immunol, 2011. **166**(3): p. 346-51.
114. Patella, M., et al., *Role of cytokine profile in the differential diagnosis between acute lung rejection and pulmonary infections after lung transplantation†.* Eur J Cardiothorac Surg, 2015. **47**(6): p. 1031-6.
115. Kolb, M., et al., *Transient expression of IL-1beta induces acute lung injury and chronic repair leading to pulmonary fibrosis.* The Journal of clinical investigation, 2001. **107**(12): p. 1529-1536.
116. Ganter, M.T., et al., *Interleukin-1beta causes acute lung injury via alphavbeta5 and alphavbeta6 integrin-dependent mechanisms.* Circulation research, 2008. **102**(7): p. 804-812.
117. Gasse, P., et al., *IL-1R1/MyD88 signaling and the inflammasome are essential in pulmonary inflammation and fibrosis in mice.* J Clin Invest, 2007. **117**(12): p. 3786-99.
118. Andreasson, A.S.I., et al., *The role of interleukin-1β as a predictive biomarker and potential therapeutic target during clinical ex vivo lung perfusion.* The Journal of heart and lung transplantation : the official publication of the International Society for Heart Transplantation, 2017. **36**(9): p. 985-995.
119. Fisher, A., et al., *An observational study of Donor Ex Vivo Lung Perfusion in UK lung transplantation: DEVELOP-UK.* Health Technol Assess, 2016. **20**(85): p. 1-276.
120. Schindelin, J., et al., *Fiji: an open-source platform for biological-image analysis.* Nature Methods, 2012. **9**(7): p. 676-682.
121. Tsushima, Y., et al., *The depletion of donor macrophages reduces ischaemia-reperfusion injury after mouse lung transplantation.* European Journal of Cardio-Thoracic Surgery, 2014. **45**(4): p. 703-709.
122. Yang, Z., et al., *CD4+ T Lymphocytes Mediate Acute Pulmonary Ischemia-Reperfusion Injury.* The Journal of thoracic and cardiovascular surgery, 2009. **137**(3): p. 695-702.

123. Zheng, Z., et al., *Donor pulmonary intravascular nonclassical monocytes recruit recipient neutrophils and mediate primary lung allograft dysfunction.* Science Translational Medicine, 2017. **9**(394).
124. Cantu, E., et al., *Gene set enrichment analysis identifies key innate immune pathways in primary graft dysfunction after lung transplantation.* American journal of transplantation : official journal of the American Society of Transplantation and the American Society of Transplant Surgeons, 2013. **13**(7): p. 1898-1904.
125. Ware, L.B., et al., *Significance of Von Willebrand Factor in Septic and Nonseptic Patients with Acute Lung Injury.* American Journal of Respiratory and Critical Care Medicine, 2004. **170**(7): p. 766-772.
126. Shapiro, S.D., et al., *Neutrophil elastase contributes to cigarette smoke-induced emphysema in mice.* The American journal of pathology, 2003. **163**(6): p. 2329-2335.
127. Zheng, Z., et al., *Donor pulmonary intravascular nonclassical monocytes recruit recipient neutrophils and mediate primary lung allograft dysfunction.* Science Translational Medicine, 2017. **9**(394): p. eaal4508.
128. Sayah, D.M., et al., *Neutrophil Extracellular Traps Are Pathogenic in Primary Graft Dysfunction after Lung Transplantation.* American Journal of Respiratory and Critical Care Medicine, 2014. **191**(4): p. 455-463.
129. Borthwick, L.A., *The IL-1 cytokine family and its role in inflammation and fibrosis in the lung.* Seminars in immunopathology, 2016. **38**(4): p. 517-534.
130. Krishnadasan, B., et al., *The role of proinflammatory cytokines in lung ischemia-reperfusion injury.* J Thorac Cardiovasc Surg, 2003. **125**(2): p. 261-72.
131. Siemiatkowski, A., et al., *von Willebrand factor antigen as a prognostic marker in posttraumatic acute lung injury.* Haemostasis, 2000. **30**(4): p. 189-95.
132. Calfee, C.S., et al., *Soluble intercellular adhesion molecule-1 and clinical outcomes in patients with acute lung injury.* Intensive care medicine, 2009. **35**(2): p. 248-257.
133. Schmal, H., et al., *Soluble ICAM-1 Activates Lung Macrophages and Enhances Lung Injury.* The Journal of Immunology, 1998. **161**(7): p. 3685.
134. Morrone, C., *Inhibition of Neutrophil Serine Proteases by Alpha 1 Antitrypsin in Perfadex Preserves Primary Graft Functions of Transplanted Murine Donor Lungs.* The Journal of Heart and Lung Transplantation, 2018. **37**(4): p. S123.
135. Reyfman, P.A., et al., *Single-Cell Transcriptomic Analysis of Human Lung Provides Insights into the Pathobiology of Pulmonary Fibrosis.* American journal of respiratory and critical care medicine, 2019. **199**(12): p. 1517-1536.
136. Sivakumar, P., et al., *RNA sequencing of transplant-stage idiopathic pulmonary fibrosis lung reveals unique pathway regulation.* ERJ Open Research, 2019. **5**(3): p. 00117-2019.
137. Ferdinand, J.R., et al., *Transcriptional analysis identifies novel biomarkers associated with successful ex-vivo perfusion of human donor lungs.* bioRxiv, 2019: p. 612374.
138. Weathington, N.M., et al., *Ex vivo lung perfusion as a human platform for preclinical small molecule testing.* JCI Insight, 2018. **3**(19).
139. Huang, H.J., et al., *Late primary graft dysfunction after lung transplantation and bronchiolitis obliterans syndrome.* Am J Transplant, 2008. **8**(11): p. 2454-62.
140. Kaetzel, C.S., *The polymeric immunoglobulin receptor: bridging innate and adaptive immune responses at mucosal surfaces.* Immunol Rev, 2005. **206**: p. 83-99.
141. Suzuki, H., et al., *Role of complement activation in obliterative bronchiolitis post-lung transplantation.* Journal of immunology (Baltimore, Md. : 1950), 2013. **191**(8): p. 4431-4439.
142. Pauwels, N.S., et al., *Role of IL-1α and the Nlrp3/caspase-1/IL-1β axis in cigarette smoke-induced pulmonary inflammation and COPD.* Eur Respir J, 2011. **38**(5): p. 1019-28.

Appendices

Appendix 1 – MSD standard curve

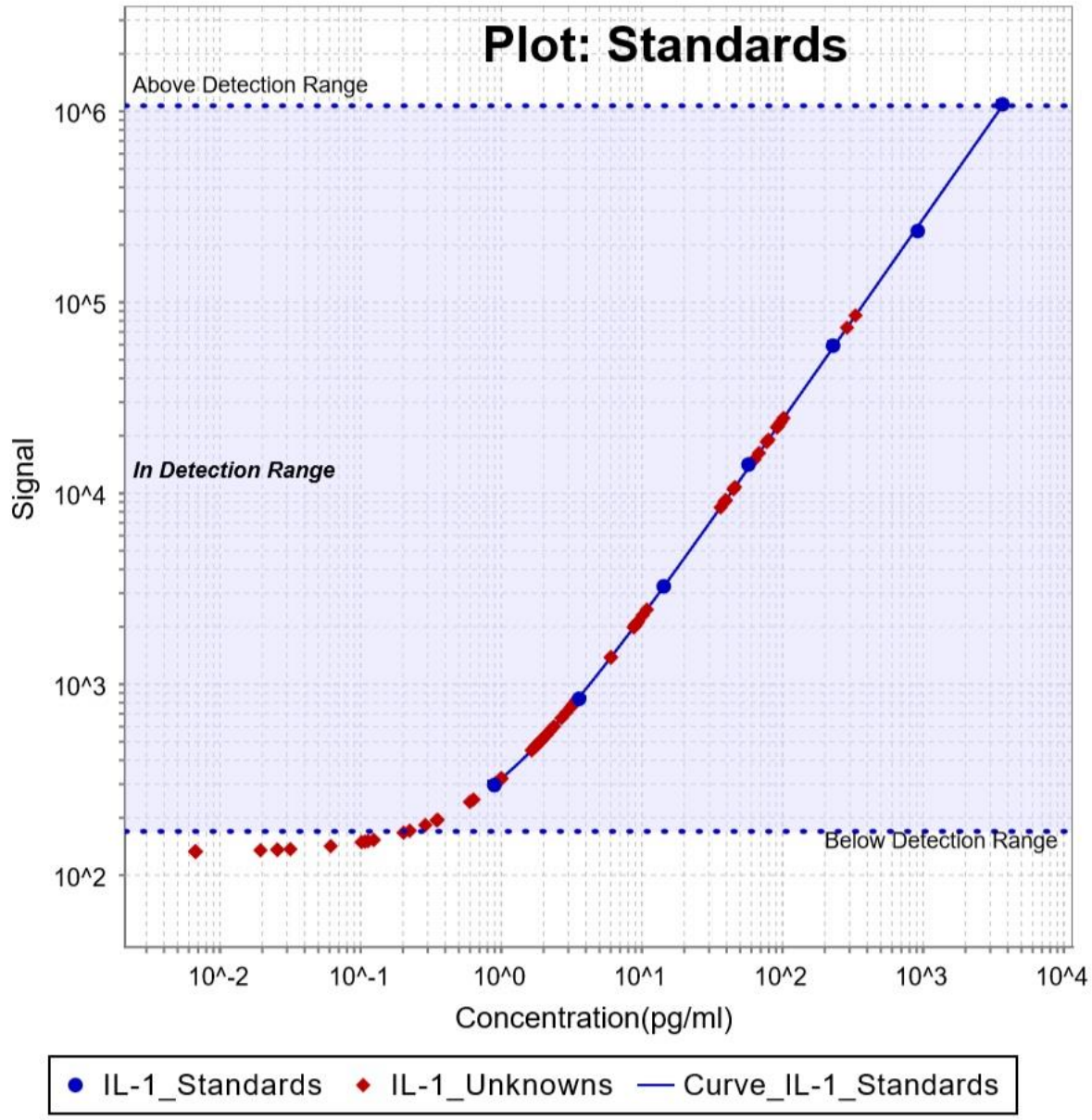

Appendix 2 – EVLP standard operating procedure (SOP)

For EVLP, a homemade version of Steen solution was made up prior to beginning experiments. The details listed below are for making up 2L:

Homemade Steen components

- 140g BSA
- 10g Dextran 40
- 2g Krebs Henseleit buffer modified
- 56ml Sodium Bicarbonate solution
- 50ml Calcium chloride
- Heparin
- Ultra Cruz 1L 0.22µm sterile filters

Instructions for making homemade Steen

- Weigh out 140g of BSA and 10g of Dextran 40 into a sterile 2L glass bottle
- Add 1600ml of ultra-pure water and add magnetic stir bar into solution
- Add 56ml of sodium bicarbonate solution
- Add 50ml of calcium chloride
- Place bottle on magnetic stirrer and set to speed 5
- Leave until components all fully dissolved into the water
- Add water until 2L
- Open up a tissue culture hood and transfer 2L bottle of unfiltered Steen and another sterile 2L glass bottle
- Place the Ultra Cruz filter on top of the sterile bottle and add the unfiltered Steen to the top of the filter
- Connect filter to the pump and switch pump on
- Allow Steen to drain through and then seal bottle and label

Ex-vivo lung perfusion for whole lung pair

Set-up of circuit

- Open two Medtronic© circuit boxes and remove the circuits
- Attach the circuits to two trolleys. Clamp the tubing between the reservoir and the pump and the tubing between the pump and the oxygenator
- Place the oxygenator by the holder to make sure the tubing and pump and aligned. Place the pump into the pump head holder then attach the oxygenator
- Place the arterial and venous tubing ends into the dome hood
- Lock the 6-prong port located on the arterial tubing into the flow holder ensuring this is orientated correctly
- Clamp smaller arterial tubing
- Clamp the small tubing emerging from the top of the oxygenator
- Check all 3-way taps in the circuit are closed
- Fill the heater/cooler unit and set to 32^{o}C
- Attach heater/cooler to oxygenator in circuit (flow into top and out of bottom)
- Switch Medtronic© consoles on

Priming of circuit

- Add 1.5L of Steen solution™ and 7500 units of heparin to each circuit
- Remove air from perfusate by removing the clamps and ensuring no air bubbles remain in the pump head and oxygenator
- Set flow rate to 0.5-1l/min and leave this circulating, ensuring perfusate is effectively draining from the hoods
- Place blood gas/ventilator/flow parameter monitoring sheets on appropriate trolleys
- Acquire sample of perfusate from each circuit for blood gas analysis. Ensure pH and CO_2 are within appropriate ranges and adjust these accordingly if required

Preparation of lungs for split perfusion model (2 people minimum)

In the case of whole lung pair perfusions, skip to bronchial and tracheal cannulation steps

- Open hospital box and remove any ice on top of the lungs
- Cut open the bags containing the lungs and pour solution inside these into the dissection bowl
- Remove lungs from the bag and place these into the dissection bowl, being careful to handle these carefully
- Leave the trachea stapled and the lungs inflated
- Locate exactly where the pulmonary artery (PA) splits into the left and right lung branches

- Cut down the front and back so that the PA opens, ensuring enough is left to cannulate both lungs
- Cut between the left and right branches to separate (bias this towards the left, as the right PA is shorter)
- Insert yellow cannulas into both PA branches and secure using 1usp tie
- Locate left and right pulmonary vein
- Insert a green cannula inside left atrium (LA)
- Cut the green LA cannula down to an appropriate size and then suture this securely in place using a 4-0 Prolene on a 20mm needle
- Repeat the previous two steps with the right half of the LA
- Dissect down the trachea until the carina is located
- Dissect around the right side of the carina
- Clamp just before the left bifurcation and cut the trachea just below. The left lung will now deflate
- Cannulate the left main bronchus by securing a cannula in place with a 1usp tie
- Remove the clamp on the right bronchus. The right lung will now deflate
- Cannulate the right main bronchus by securing a cannula in place with a 1usp tie

Perfusion procedure (1)

- Tare dissection bowl on scale
- Weigh lungs and record the starting weights of each on the relevant information sheets
- Calculate the flow rate for 20% cardiac output (CO)
- Set flow rate for each lung and attach the arterial tubing to the PA cannula (may have to adjust flow rate slightly as sometimes 20% CO may cause backflow of circulating perfusate)
- Wait until return from the venous cuff cannula is visible and then attach this to the venous tubing
- Adjust positioning of tubing and lungs on dome if necessary to achieve an appropriate arterial pressure
- Attach CO_2 tubing from gas cylinder and begin infusion into circuit. Perform a blood gas measurement
- Increase to 40% CO gradually over 15 minutes of perfusion
- Place temperature probe under the venous cuff

Priming pressure transducers

- Attach one pressure transducer to the 3-way tap on the arterial line

- Attach a 50ml syringe to a free port on the 3-way tap
- Close the tap to the pressure transducer and slowly draw up 30ml of perfusate from the circuit into the syringe
- Close the tap
- Depress the syringe and gently push perfusate into the pressure transducer balloon, ensuring that the membrane does not become overstretched
- Remove air from the balloon by drawing up with the syringe
- Repeat the previous two steps until all air has been removed and the membrane within the balloon is level
- Attach the pressure transducer to the back of the console
- Open the 3-way tap to the transducer
- Press the double arrow icon at the bottom of the console and select the 0 button next to the pressure inlet used for the transducer
- There should now be a pressure reading present on the console screen. Record this value and continue to monitor for the duration of perfusion

Perfusion procedure (2)

- When lungs reach 32°C switch on the ventilator
- Set the tidal volume and breaths per minute based on the appropriate values for lung temperature and ideal body weight of the donor
- Set PEEP to 5, Pinsp to 15, flow to 19 and O_2 to 21
- Once set, attach the bronchiole tree to the lungs
- Record various readings on the monitoring sheets
- Adjust the tidal volume and breaths per minute accordingly as the temperature increases
- Increase the heater/cooler temperature to 38°C to achieve a lung temperature of 37°C
- Once normothermia is achieved, clamp leukocyte filters on each circuit
- Acquire blood gases regularly to ensure measurements are within strict parameters

Sample acquisition and storage

Perfusate

- Collect 5ml of perfusate from the venous line at the appropriate time
- Centrifuge at 200g for 5 minutes
- Aliquot out perfusate into cryovials and store these on ice until transfer to freezer
- If tracking labelled cells in sample, re-suspend pellet in 1ml of FACS buffer (PBS, 2% BSA) and store on ice prior to flow cytometry analysis

- All perfusates not used in flow cytometry stored at -80°C long-term

Tissue

- Acquire first sample upon initiation of perfusion with TLC 75 tissue stapler
- Dissect biopsy into two samples and store these in Formalin and RNAlater
- Upon completion of EVLP and weighing of lungs, transfer lungs to sterile dissection area
- Dissect down centre of lobes for each lung
- Acquire biopsy with scalpel and cut in half
- Place tissue in Formalin and RNAlater
- For samples placed in Formalin, leave at room temperature for 48 hours before being embedded in paraffin (assistance from Cellular Pathology, RVI)
- For samples placed in RNAlater, leave at 4°C for 24 hours and then transfer to -80°C for long-term storage

Appendix 3 – *In vitro* SOP for EVLP experiments

IL-1β addition

- Reconstitute recombinant IL-1β to a working concentration of 1ng/µl
- Add 1500µl of IL-1β to 3500µl of perfusate solution
- Acquire perfusate sample from circuit for later analysis as 'Pre'
- Infuse IL-1β into EVLP circuit at '-60m'
- Acquire perfusate samples from circuit at '-30m' and '-15m' prior to start of neutrophil tracking model

Neutrophil isolation

The following steps were performed using a MACSXpress® Neutrophil isolation kit (Miltenyi Biotec). This was chosen due to selecting out neutrophils from whole blood quickly and negatively – i.e. without receptor binding. It was felt that this reduced the chance of cell activation prior to labelling and use in our EVLP system.

- Collect 8ml of whole blood from a healthy donor
- Add 2ml of buffer A to isolation beads
- Add 2ml of buffer B to isolation beads and mix well
- Add 4ml of isolation cocktail to a 15ml falcon tube. Transfer blood to tube gently.
- Ensure tube lid is securely closed and gently invert the tube 3 times. Leave to stand for 5 minutes
- Place the tube in the MACSXpress magnet and leave for 15 minutes with the lid unscrewed
- Carefully remove supernatant from tube and transfer into new 50ml falcon tube. Make up to 25ml with Hank's balance salt solution (HBSS)
- Re-suspend cells in HBSS and count neutrophil numbers

Neutrophil tracking assay

- Attach syringe to the arterial 3-way tap and gently pull up perfusate from the circuit to ensure no air is added into the perfusion circuit
- Infuse 20ml of a pre-determined number of CFSE-labelled neutrophils gradually over 1 minute
- Acquire 5ml of perfusate at the appropriate time points for the experiment
- Centrifuge the perfusate samples at 200g for 5 minutes
- Aliquot out perfusates into 1ml cryovials and store these at -80^{o}C for future investigations
- Re-suspend cell pellet in 1ml of FACS buffer and transfer to FACS tubes

Appendix 4 – Cellix protocol

1. Switch on the incubator for the system and wait until it reaches 37°C before starting the experiment.
2. Switch on the camera and the pump.
3. Open Cellix PC, choose Cellix user, password: **Password99**
4. Open Vena Flux Assay software
5. Press 'open protocol', go to folder D:\Cellix\Protocols\New Protocols and choose the appropriate protocol (Vena8 biochip single channel if changing channels manually).

For any step use right click to run or stop

6. Run the first step (Vena Flux Setup)
7. Run Geometry ID step
8. Setup camera image by pressing Set Image Properties on Setup VenaFlux tab. Make sure Auto White Balance is checked. If needed use buttons on microscope to control the light until you achieve the required image.
9. Next step is to washout the pump and the whole system. Wash with dH_2O first, then 70% ethanol, and then with dH_2O again, using Pump Washout step. Make sure no air bubbles remain, if there are, repeat washing.
10. Connect output wire (green) with tubing connection (wire with a needle attached in the end).
11. Use Pub Washout to wash the tubing
12. Change with medium (pre-warmed RPMI) and wash again using Pump Washout
13. Attach biochip on the black holder and then put under microscope
14. Focus on the channel you are interested in
15. Use Dispense into Chip step when attaching needle on the channel, to avoid air bubbles. Wait until a bubble of liquid can be seen at the end of the needle then insert it in the channel port.
16. Use Chip Washout step (40µl, 40dyne/cm^2) to wash the channel with medium
17. Remove excess media from the opposite well of the channel
18. Put 100µl of cell suspension (1x10^{6}cells/ml) on the same well.
19. Start Cell Assay Step, Variable flow rate dispension, with the flow settings you want for your experiment (i.e. -10 dyne/cm^2 for 10sec, -0.5 dyne/cm^2 for 5min, 2 dyne/cm^2 for 1min 45sec). The "-" means flow goes towards the opposite direction (from the well with the cells towards the well with the needle), so cells are sucked in the channel.
20. Remember to focus on the appropriate channel while running the assay. To take pictures (usually towards the end of each step), click Acquire Image and choose a folder to store your images in.

21. When changing channels, repeat steps 14-20.
22. When the experiment is over, wash the system again (including the tubing connection) with dH_2O, 70% ethanol, and dH_2O again. Remove the tubing connection and use a syringe with air to remove remaining dH_2O inside it. Close the software first then switch off the pump, camera and incubator.

Appendix 5 – Porcine neutrophil tracking *ex vivo*

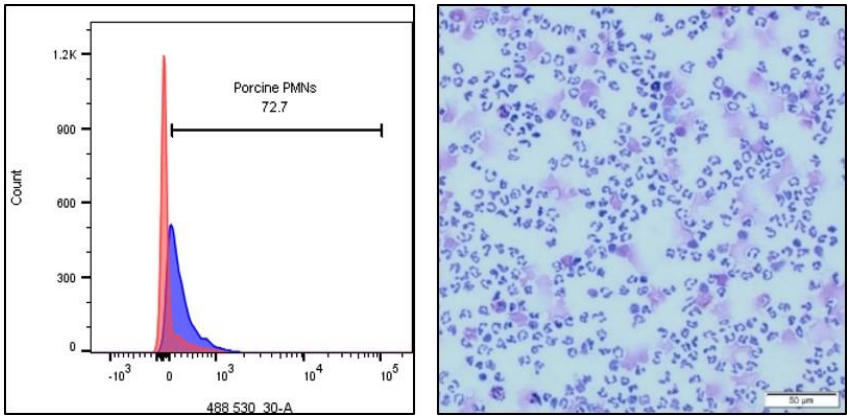

SFig. 1. – Porcine neutrophil flow cytometry and cytospin characterisations. Porcine neutrophils were isolated from whole blood and stained with a 6D10 antibody, specific for a 60kDa region on these cells. Flow cytometry shows a positive result for this stain, as well as the cytospin showing a the typical, multi-lobed nuclei of neutrophils at a high purity (>95%).

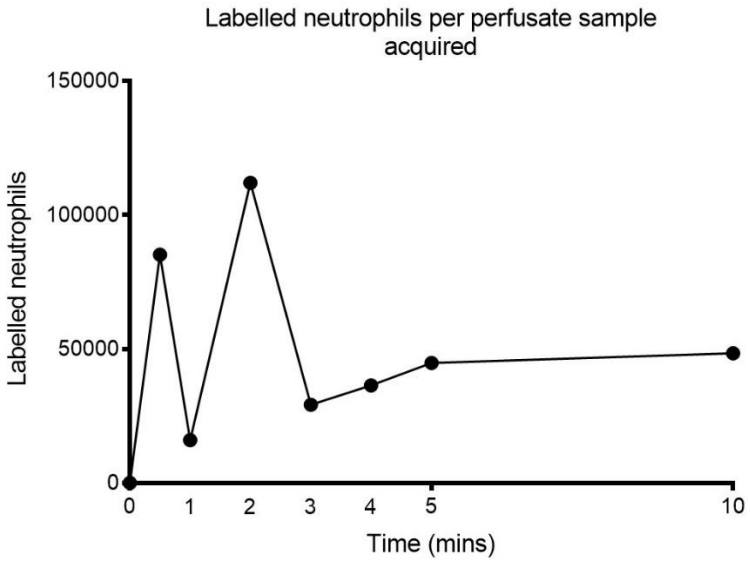

SFig. 2. – Porcine neutrophil tracking during EVLP. CFSE-labelled porcine neutrophils were infused into an EVLP circuit and then regular perfusate samples were acquired. These were measured for cells using a FACS Accurri flow cytometer. An initial spike of cell numbers can be observed <5 minutes before this flattens out thereafter. Perfusion was ceased after 20 minutes due to poor quality of the donor-lung.

Appendix 6 – Presentations and publications

Original articles

[Review] Morrison MI*, Pither TL*, Fisher AJ. Pathophysiology and classification of primary graft dysfunction after lung transplantation. *J Thorac Dis*. 2017; 9(10):4084–4097.

* indicates co-authorship

The term primary graft dysfunction (PGD) incorporates a continuum of disease severity from moderate to severe acute lung injury (ALI) within 72 h of lung transplantation. It represents the most significant obstacle to achieving good early post-transplant outcomes, but is also associated with increased incidence of bronchiolitis obliterans syndrome (BOS) subsequently. PGD is characterised histologically by diffuse alveolar damage, but is graded on clinical grounds with a combination of PaO2/FiO2 (P/F) and the presence of radiographic infiltrates, with 0 being absence of disease and 3 being severe PGD. The aetiology is multifactorial but commonly results from severe ischaemia-reperfusion injury (IRI), with tissue-resident macrophages largely responsible for stimulating a secondary 'wave' of neutrophils and lymphocytes that produce severe and widespread tissue damage. Donor history, recipient health and operative factors may all potentially contribute to the likelihood of PGD development. Work that aims to minimise the incidence of PGD in ongoing, with techniques such as *ex vivo* perfusion of donor lungs showing promise both in research and in clinical studies. This review will summarise the current clinical status of PGD before going on to discuss its pathophysiology, current therapies available and future directions for clinical management of PGD.

[Review] Gilmour J, Griffiths C, Pither T, Scott WE 3rd, Fisher AJ. Normothermic machine perfusion of donor-lungs ex-vivo: promoting clinical adoption. *Curr Opin Organ Transplant*. 2020; 25(3):285-292.

Purpose of review: Lung transplantation offers the only realistic therapeutic option for patients with end-stage lung disease. However, this is impacted by a shortfall in availability of suitable donor-lungs. Normothermic machine perfusion of donor-lungs outside the donor body also known as ex-vivo lung perfusion (EVLP) offers a potential solution through objective assessment, reconditioning and treatment of donor-lungs initially deemed unsuitable for use. This review discusses key advances and challenges in the wider clinical adoption of this technology.

Recent findings: This review will summarize key research within the following areas: recent clinical trials utilizing EVLP, logistical challenges, EVLP protocol innovations, novel assessment methods and current research into therapeutic modulation of lung function during EVLP.

Summary: Normothermic machine perfusion of donor-lungs ex-vivo offers a promising platform to assess and modulate donor-lung quality prior to transplantation. Consensus on how and when to best utilize EVLP is yet to be reached, meaning that widespread clinical adoption of the technology has not yet become a reality. Further work is needed on agreed indications, perfusion protocols and organization of services before becoming a regularly used procedure prior to lung transplantation.

[Article accepted for publication] Wang L, Thompson E, Bates L, Pither TL, Hosgood SA, Nicholson ML, Watson CJ, Wilson C, Fisher AJ, Ali S, Dark J. Flavin Mononucleotide as a Biomarker of Organ Quality – A Pilot Study. *Transplantation Direct*.

Background: Flavin mononucleotide (FMN), released from damaged mitochondrial complex-I during hypothermic liver perfusion, has been shown to be predictive of 90 day graft loss. Normothermic machine perfusion (NMP) and normothermic regional perfusion (NRP) are used for organ reconditioning and quality assessment prior to transplantation. This pilot study aimed to examine whether FMN is detectable during NMP and abdominal NRP and correlates with allograft quality measures and posttransplant results.

Methods: FMN concentrations in perfusates collected during NMP of kidneys, abdominal NRP, and ex-vivo lung perfusion, were measured using fluorescence spectrometry, and correlated to the available perfusion parameters and clinical outcomes.

Results: Among seven transplanted kidneys out of the 21 kidneys that underwent NMP, FMN levels at 1 hour were significantly higher in the allografts that developed delayed graft function and primary non-function (p=0.02). 15 livers from 23 circulatory death donors that underwent NRP were deemed suitable for transplantation. Their FMN levels at 30 minutes of NRP were significantly lower than those not procured for transplantation (p=0.01). In contrast, little FMN was released during the 8 lung perfusion.

Conclusions: This proof of concept study suggested that FMN in the perfusates of NMP and NRP, has the potential to predict quality of kidneys and livers. More work is required to validate the role of FMN as a putative biomarker to facilitate safe and reliable decision making before transplantation.

[Manuscript in preparation] Pither TL … Dark J, Scott WE, Ali S, Fisher AJ, The effects of IL-1β-mediated inflammation during ex-vivo lung perfusion (working title)

[Manuscript in preparation] Pither TL, Mavridou M, Macdonald J, Dark J, Scott WE, Ali S, Fisher AJ, IL-1β produces transcriptional changes in donor-lungs during ex-vivo lung perfusion (working title)

Project supervision

Undergraduate summer project

Ryan Lamb (2018)

Bachelor of Science (BSc) research project

Harry Clarke (2019)

Chong Pang (2019)

Master of Research (MRes) research project

Raj Maan (2019)

Maria Mavridou (2020)

Presentations

Mar-20	Oral presentation no.7 for the Medawar medal session British Transplant Society Annual Congress 2020 Belfast, U.K.
Nov-19	Oral presentation Annual Newcastle Edinburgh Cambridge Sheffield (NECS) Respiratory Meeting Cambridge, U.K.
Oct-19	Oral presentation Blood and Transplant Research Unit in Organ Donation and Transplantation (BTRU ODT) progress review Newcastle upon Tyne, U.K.
Oct-19	Oral presentation Inflammation, immunology and immunotherapy group meeting Newcastle upon Tyne, U.K.
Jun-19	Oral presentation Institute of Cellular Medicine research seminar Newcastle upon Tyne, U.K.
Jun-19	Oral presentation by supervised MRes student Immunology North East research meeting Newcastle upon Tyne, U.K.
May-19	Poster presentation – best poster prize winner Institute of Cellular Medicine Director's Day event Newcastle upon Tyne, U.K.
Apr-19	Poster presentation British Transplant Society Annual Congress 2019 Harrogate, U.K.
Mar-19	Oral presentation Inflammation, immunology and immunotherapy group meeting Newcastle upon Tyne, U.K.
Oct-18	Oral presentation Blood and Transplant Research Unit in Organ Donation and Transplantation (BTRU ODT) trainee day Newcastle upon Tyne, U.K.
Sep-18	Poster presentation Institute of Cellular Medicine Director's Day event Newcastle upon Tyne, U.K.
Dec-17	Poster presentation British Society of Immunology Annual Congress 2017 Brighton, U.K.
Oct-17	Oral presentation Blood and Transplant Research Unit in Organ Donation and Transplantation (BTRU ODT) trainee day Newcastle upon Tyne, U.K.